

Aus dem Max Planck Institut für molekulare Genetik

DISSERTATION

**IDENTIFICATION AND CHARACTERIZATION OF
SERINE/THREONINE KINASE 9 AS A CAUSATIVE GENE FOR
X-LINKED MENTAL RETARDATION**

Zur Erlangung des akademischen Grades

Doctor rerum medicarum (Dr. rer. medic.)

vorgelegt der Medizinischen Fakultät der Charité –

Universitätsmedizin Berlin

von

Jiong Tao

aus Shanghai, P. R. China

Dekane: Prof. Dr. med. Martin Paul

Gutachter: 1. Prof. Dr. H.-Hilger Ropers

2. Prof. Dr. Karl Sperling

3. Priv. –Doz. Dr. Gudrun Rappold

Datum der Promotion: January 21, 2005

CONTENTS

Abbreviations.....	6
1 Introduction.....	10
1.1. Research background.....	10
1.1.1 Mental retardation (MR): definition, prevalence and causes.....	10
1.1.2 X-linked mental retardation (XLMR): a historical overview.....	10
1.1.3 Studies in XLMR.....	11
1.1.3.1 Clinical delineation and classification of XLMR.....	11
1.1.3.2 Linkage analysis in families with XLMR.....	12
1.1.3.3 Molecular identification of XLMR genes.....	12
1.1.4 Impacts of XLMR studies.....	16
1.1.4.1 Contributions in the nosology of XLMR.....	16
1.1.4.2 Understanding the molecular and cellular basis of MR.....	18
1.1.5 Perspectives.....	22
1.2 Outline of the project.....	23
2 Materials, subjects and methods.....	24
2.1 Materials.....	24
2.1.1 Chemicals and reagents.....	24
2.1.2 Solutions and media.....	26
2.1.3 Enzymes.....	30
2.1.4 Kits.....	31
2.1.5 Vectors.....	31
2.1.6 Antibodies.....	32
2.1.7 Primers.....	32
2.1.8 Human genomic clones.....	32
2.1.9 Bacterial materials.....	32
2.1.10 Mammalian cell line.....	32
2.2 Subjects.....	33
2.3 Methods.....	33
2.3.1 DNA isolation.....	33
2.3.2 RNA isolation.....	34
2.3.3 Fluorescence <i>in situ</i> hybridization.....	34
2.3.4 Preparation of DNA probes for Southern blot hybridization.....	34
2.3.5 Isotope-labeling of probes for Southern blot hybridization.....	35
2.3.6 Southern blot hybridization.....	35
2.3.7 Genomic walking.....	36
2.3.8 RT-PCR.....	37
2.3.9 Denaturing high performance liquid chromatography (DHPL) analysis.....	38
2.3.10 Construction of bacterial, yeast and mammalian expression vectors.....	40
2.3.11 Construction of STK9 kinase-deficient mutant.....	41
2.3.12 Expression of 6 × His tagged STK9 peptides in <i>E. coli</i>	42

2.3.13	Purification of 6 × His tagged fusion proteins.....	42
2.3.14	Immunization.....	42
2.3.15	Yeast two-hybrid library screening.....	43
2.3.16	Analysis of prey inserts in yeast positive clones.....	43
2.3.17	Preparation of yeast protein extracts.....	44
2.3.18	Cell culture and DNA transfection.....	44
2.3.19	Immunofluorescence.....	44
2.3.20	SDS PAGE and Western blot analysis.....	45
3	Results.....	47
3.1	Disruption of serine/threonine kinase 9 gene (<i>STK9</i>) in a female patient with severe infantile spasms, global developmental arrest and profound mental retardation (patient 1).....	47
3.1.1	Clinical investigation of patient 1.....	48
3.1.2	Cytogenetic investigation of the translocation breakpoints.....	49
3.1.3	Molecular investigation of the translocation breakpoints.....	50
3.1.4	Truncation of <i>STK9</i> in patient 1.....	52
3.2	De novo mutations in <i>STK9</i> are associated with a severe form of atypical Rett syndrome.....	57
3.2.1	Mutation screening in the coding region of <i>STK9</i>	58
3.2.2	Patient 2 with p.C152F missense mutation.....	59
3.2.3	Patients 3 and 4 with p.R175S missense mutation.....	60
3.2.4	Sequence analysis of p.C152F and p.R175S missense mutations.....	62
3.3	Generation of a polyclonal antibody against <i>STK9</i> protein.....	65
3.3.1	Expression of 6 × His tagged <i>STK9</i> peptides in <i>E. coli</i>	65
3.3.2	Purification and concentration of 6 × His tagged <i>STK9</i> peptides.....	66
3.3.3	Evaluation of immunoreactivity of the anti- <i>STK9</i> antiserum.....	69
3.4	Screening for <i>STK9</i> interaction partners.....	73
3.4.1	Construction of a kinase-deficient mutant <i>STK9</i> -K42R.....	74
3.4.2	Yeast two-hybrid library screening.....	77
4	Discussion.....	79
4.1	Positional cloning identified <i>STK9</i> as a candidate gene for XLMR.....	79
4.2	Mutation analysis confirmed the causative role of <i>STK9</i> in MR.....	80
4.3	<i>STK9</i> alterations are likely to affect its kinase activities.....	81
4.4	<i>STK9</i> alterations are associated with a wide range of clinical features.....	82
4.5	The phenotypic spectrum associated with <i>STK9</i> alterations overlaps with that of <i>MECP2</i> mutation.....	85
4.6	Primary sequence analysis suggests that <i>STK9</i> function in a similar way as ERKs in activity-dependent synaptic plasticity.....	86
4.7	Function of the putative interaction partners of <i>STK9</i> mutant suggests a role of <i>STK9</i> signaling in synaptic plasticity.....	90
4.8	Localization of <i>STK9</i> in the centrosome suggests its potential association with the microtubule network.....	93
4.9	Abnormal synaptic plasticity may be a common cellular cause for some MR.....	94
4.10	The future.....	96

5 Summary.....	97
6 Electronic database information.....	100
7 References.....	101
8 Acknowledgement.....	115
9 Curriculum vitae.....	116
10 Publications.....	119
11 Declaration	120

ABBREVIATIONS

ABC	ATP binding cassette
ARHGEF 6	Rho GEF protein 6
AMPA	α -amino-3-hydroxy-5-methyl-4-isoxazole propionic acid
APS	Ammonium persulfate
ARX	Aristaless-related homeobox, X-linked
ATR-X	Alpha-thalassemia/mental retardation syndrome, X-linked
BAC	Bacterial artificial chromosome
BDNF	Brain-derived neurotrophic factor
BSA	Bovine serum albumin
BLAST	Basic local alignment search tool
bp	Base-pair
Cdc	Cell division cycle
CDK	Cyclin-dependent kinase
CDKL	Cyclin-dependent kinase-like
cDNA	Complementary DNA
CLS	Coffin-Lowry syndrome
CLTC	Clathrin heavy chain
CMGC	CDK family, MAPK family, GSK3 family, and Clk family
CNS	Central nervous system
CREB	Cyclic-AMP-responsive element-binding protein
Cy3	Cyanine 3
DAPI	4',6-Diamidino-2-phenylindole
DCX	Doublecortin
DEPC	Diethylpyrocarbonate
DHPLC	Denaturing high performance liquid chromatography
DNA	2'-deoxy-5'-ribonucleic acid
DO	Drop out
DTT	Dithiothreitol
<i>E. coli</i>	<i>Escherichia coli</i>
EDTA	Ethylenediaminetetraacetic acid

EEG	Electroencephalogram
EGTA	Ethylene glycol bis(2-aminoethyl ether)-N,N,N',N'-tetraacetic acid
ERK	Extracellular signal-regulated kinase
EST	Expressed sequence tag
FAK	Focal adhesion kinase
FBS	Fetal bovine serum
FGD	Faciogenital dysplasia
FISH	Fluorescence <i>in situ</i> hybridization
FITC	Fluorescein isothiocyanate
FLN1	Filamin 1
FMD	Frontometaphyseal dysplasia
FMR1	Fragile site mental retardation 1
GAP	GTPase activating protein
GDI α	GDP-associated inhibitor α
GEF	Guanine nucleotide exchange factor
HASA	Hydrocephalus due to congenital stenosis of aqueduct of sylvius
HEPES	4-(2-Hydroxyethyl)piperazine-1-ethanesulfonic acid sodium
hr	hour
HRP	Horseradish peroxidase
IL1RAPL	Interleukin-1 receptor accessory protein-like
IPTG	Isopropyl- β -D-thiogalactoside
IQ	Intelligence quotient
IS	Infantile spasms
JNK	c-Jun N terminal kinase
kb	Kilobase
L1CAM	L1 cell adhesion molecule
LIS	Lissencephaly
LTD	Long-term depression
LTP	Long-term potentiation
MAPK	Mitogen-activated protein kinase
MARK	Microtubule affinity regulatory kinase
MASA	Mental retardation, aphasia, shuffling gait, and adducted thumbs
Mb	Megabase

MECP2	Methyl- CpG-binding protein 2
MHC	Major histocompatibility complex
MID1	Midline defect 1
min	minute
mon	month
MR	Mental retardation
MRI	Magnetic resonance imaging
mRNA	Messenger RNA
MSK	Mitogen and stress-activated protein kinase
NBD	Nucleotide binding domain
NS-XLMR	Non-syndromic X-linked mental retardation
Ni-NTA	Nickel-nitrilotriacetic acid
OFD	Oral-facial-digital syndrome
OLB	Oligo labeling buffer
OMIM	Online mendelian inheritance in man
OPD	Otopalatodigital syndrome
OPHN1	Oligophrenin 1
PAC	P1 artificial chromosome
PAGE	Polyacrylamide gel electrophoresis
PAK	P21-activated kinase
PCR	Polymerase chain reaction
PEG	Polyethylene glycol
PtdIns	Phosphatidylinositol
PHA	phytohemagglutinin
Rac1	Ras-related C3 botulinum toxin substrate 1
Rho A	Ras homology member A
PIPES	Piperazine-N,N -bis(2-ethanesulfonic acid)
PKA	Protein kinase A
PKC	Protein kinase C
PLP1	Proteolipid protein 1
PLZF	Promyelocytic leukemia zinc finger protein
PMSF	Phenylmethanesulfonyl fluoride
PQBP1	Polyglutamine-binding protein 1

PVNH	Periventricular nodular heterotopia
RNA	Ribonucleic acid
RSK2	Ribosomal protein S6 kinase 2
RT	Reverse transcription
RTT	Rett syndrome
RZPD	Resource Center of the German Human Genome Project
SCLH	Subcortical laminar heterotopia
sec	second
SDS	Sodium dodecyl sulfatate
STK9	Serine/threonine kinase 9
S-XLMR	Syndromic X-linked mental retardation
T _A	Annealing temperature
TAP1	Transporter associated with antigen processing 1
Taq	<i>Thermus aquaticus</i>
TEAA	Triethylammonium acetate
TEMED	N,N,N',N'-Tetramethyl-1,2-diaminomethane
TM4SF2	Transmembrane 4 superfamily, member 2
TMD	Transmembrane domain
U	unit
UTR	Untranslated region
w/v	Weight per volume
XCI	X chromosome inactivation
X-Gal	5-Bromo-4-Chlor-3-indolyl- β -Galactosidase
XLAG	X-linked lissencephaly with abnormal genitalia
XLIS	Lissencephaly, X-linked
XLMR	X-linked mental retardation
XNP	X-linked nuclear protein
YAC	Yeast artificial chromosome

1 INTRODUCTION

1.1 Research Background

1.1.1 Mental retardation: definition, prevalence and causes

According to the American Association on Mental Retardation, mental retardation (MR) refers to conditions of sub-average intellectual ability associated with functional deficits in adaptive behavior (such as daily-living skill, social skills and communication) with an onset before age of 18 years (Luckasson et al. 1992). In practical terms, MR is defined by intelligence quotient (IQ) scores of 70 or below, with IQ<50 being considered as severe MR, and IQ 50-70 as mild MR (Kiely 1987; Roeleveld et al. 1997). Severe MR affects 0.3-0.5% of the population, the prevalence increases to 2-3 % if mild MR is included (Leonard and Wen 2002). Thus, MR is the most frequent cause of serious handicap in children and young adults (Chelly and Mandel 2001).

The underlying causes of MR are extremely heterogeneous, which include a variety of non-genetic factors that act prenatally or perinatally to cause brain injury, as well as genetic causes like chromosomal abnormalities or single gene defects. Because the pathogenesis of MR is unclear, early diagnosis, prevention or treatment is not possible in most of cases.

1.1.2 X-linked mental retardation (XLMR): a historical overview

An association of MR conditions with the X chromosome has long been noticed owing to two observations (Stevenson et al. 2000b). One is the consistent 30-40% excess of males in nearly all surveys of mental retardation, and the other is the existence of large families in which MR is inherited as an X-linked trait. However, it was not until the reports of Dr. Lehrke in the early 1970s that the principle of X linked mental retardation was clearly illustrated (Lehrke 1972a; Lehrke 1972b). He postulated that there existed X-linked loci that related to intellectual function, mutation of these genes could lead to MR, and the effects of mutation became more apparent in hemizygous males who could not compensate for mutations present on their single X chromosome. Still, the concept of XLMR was not fully accepted until 1977, when Sutherland described association of the

fragile X (folic acid sensitive) site— the cytogenetic marker on Xq27.3— with familial mental retardation and macroorchidism in males (later designated fragile X syndrome) (Sutherland 1977). The genetic mechanism of fragile X syndrome was uncovered in 1991. Three groups independently showed that an expansion of a CGG trinucleotide repeat in the Xq27.3 region co-segregated with the fragile X condition (Kremer et al. 1991; Oberle et al. 1991; Yu et al. 1991). The expanded CGG trinucleotide repeats, located in the 5' untranslated region of the fragile site mental retardation 1 gene (*FMRI*), was abnormally methylated in affected individuals, resulting in silencing of the *FMRI* gene (Verkerk et al. 1991).

The recognition of the fragile X syndrome has established XLMR as a distinct group in the MR field. To date, approximately 200 XLMR entities distributed along the whole X chromosome have been described (for a complete list, see the on-line XLMR database <http://www.rm.unicatt.it/xlmr>). Epidemiological studies in cohorts with MR suggest that XLMR accounts for 8-15% of all cases of MR (Laxova et al. 1977; Hunter et al. 1980; Farag et al. 1993; Crow and Tolmie 1998; Stevenson 2000). Using 2% as the overall prevalence of MR in the general population, X-linked genes are responsible for 1.6-3 cases per 1,000 births.

1.1.3 Studies in XLMR

Given that pedigrees of X-linked form are relatively easy to recognize, and molecular methodologies are more effective in mapping and cloning of X-linked genes, XLMR has attracted the focus of both clinicians and scientists. Multidisciplinary series of studies, including clinical delineation and classification, linkage analysis, and molecular investigation, have greatly improved our knowledge in XLMR.

1.1.3.1 Clinical delineation and classification of XLMR

Clinical delineation and classification are the first step to dissect the heterogeneous state of XLMR. Roughly, XLMR is categorized into two groups: non-syndromic XLMR (NS-XLMR) where the affected patients have no distinctive clinical or biochemical features in common other than MR, and syndromic XLMR (S-XLMR) where MR is associated with other clinically recognizable features. S-XLMR conditions are further divided into four sub-groups: malformation disorders,

neuromuscular disorders, metabolic disorders and dominant disorders. ‘Malformation disorders’ are characterized by somatic findings, particularly those that give the face a distinctive appearance. ‘Neuromuscular disorders’ are characterized by neurological and/or muscular abnormalities. ‘Metabolic disorders’ are characterized by biochemical abnormalities of metabolic transporters or enzymes. ‘Dominant disorders’ is the group separated considerably for their peculiar inheritance, affecting almost exclusively females (Stevenson 2000).

1.1.3.2. Linkage analysis in families with XLMR

Linkage analysis allows crude chromosomal localization of causative genes in families with XLMR. Using informative genetic markers, meiotic recombinant events in the X chromosome can be traced through XLMR pedigree. The region of the X chromosome that is consistently present in affected but not in unaffected members of an family with XLMR is considered to be linked with the relevant pathological condition, and therefore is assumed to contain the disease associated gene.

Linkage analysis is an important tool for further splitting of the XLMR entities (Stevenson 2000). S-XLMR conditions with similar clinical features can be separated based on linkage data. For example, patients with Coffin-Lowry syndrome (CLS, MIM 303600) and ATR-X syndrome (MIM 301040), both exhibiting MR and hypotonic faces, could be reliably separated according to the disease loci, which were mapped to Xp22 and Xq12-q21, respectively (Biancalana et al. 1992; Gibbons et al. 1992). Regional mapping is even more instructive for partitioning in the NS-XLMR conditions, where no additional clinical manifestations are available to distinguish one from another. In 70 mapped NS-XLMR families, 10-12 non-overlapping linkage regions have been identified, each of which might contain at least one XLMR gene (Stevenson 2000). Thus, it becomes apparent that NS-XLMR conditions, although clinically homogenous, are genetically heterogeneous.

1.1.3.3. Molecular identification of XLMR genes

Due to our limited understanding of cognitive mechanisms, identification of XLMR genes mostly rely on the knowledge of chromosomal localization rather than that of biochemical function of

disease-causing genes. Information about the genetic loci involved in XLMR has been obtained in two ways, e.g. by studying mentally retarded patients with X-chromosomal abnormalities, and by regionally mapping the relevant defects in large families with XLMR (Fig. 1).

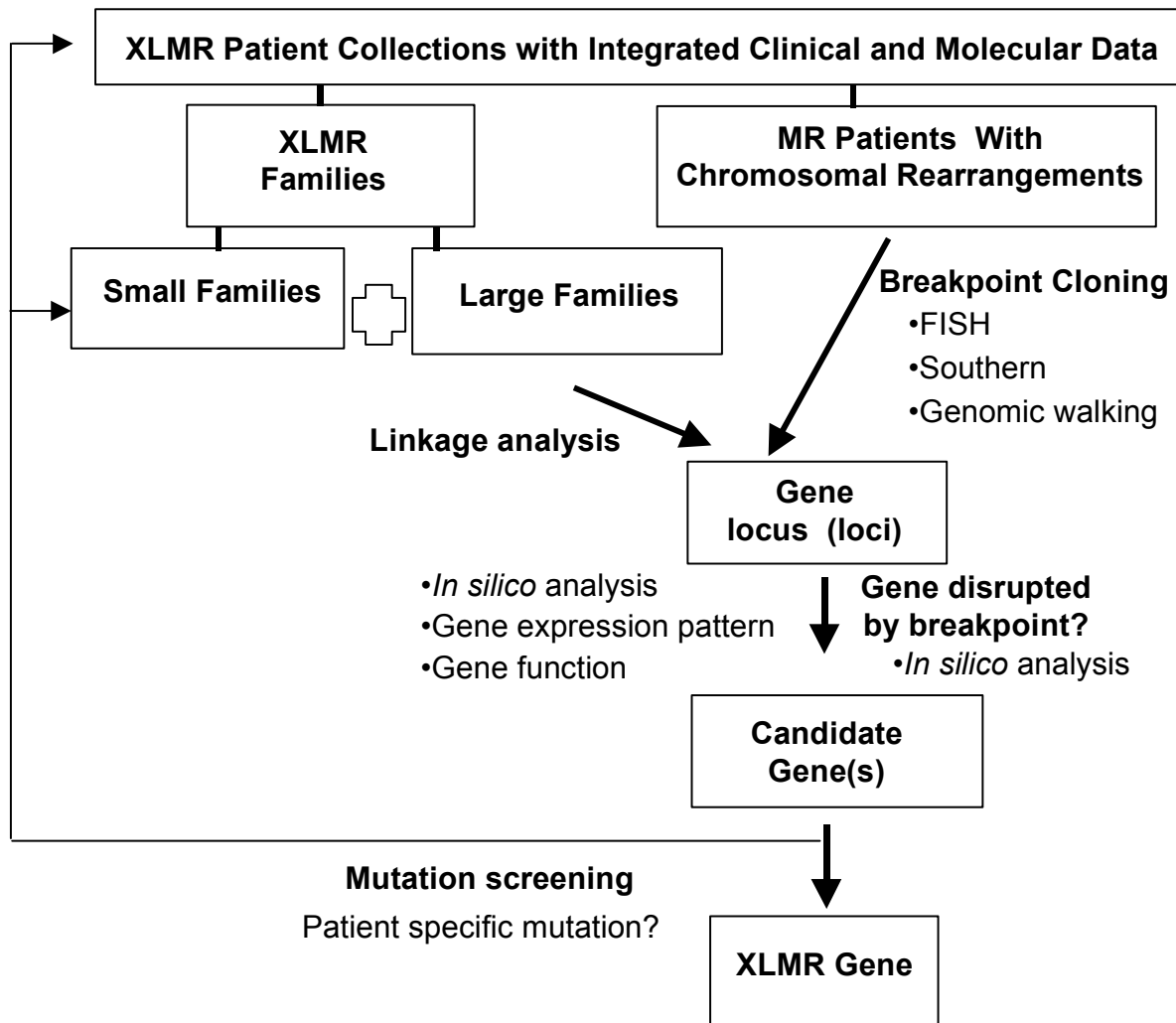


Figure 1. A schematic flow chart of the current strategies for identifying new XLMR genes. Patients with MR and X-chromosomal rearrangements and regionally mapped families with XLMR are the two main resources to obtain the positional information of disease-causing genes. For patients with chromosomal rearrangements, positional cloning of the breakpoints points to the location of the causative genes. Candidate genes identified by this approach need to be investigated for additional mutations in unrelated families. For families with XLMR, linkage analysis localizes the candidate regions, and causative genes can be identified by screening for disease-specific mutations in the linkage intervals.

Patients with MR and X chromosomal rearrangements, including balanced X;autosomal translocations, X inversions and microdeletions, form a unique resource for the identification of XLMR genes. The MR conditions in these patients are likely caused by the presence of chromosomal rearrangements, therefore the breakpoints on the X chromosome provide a valuable clue to the exact physical location of the disease-causing gene. Using a series of cytogenetic and molecular methods such as FISH, Southern blot hybridization and genomic walking, the location of breakpoints can be mapped to nucleotide level (for principles of these methods, see Fig. 2). Combined with *in silico* search for the genes disrupted by chromosomal breakpoints, the approach

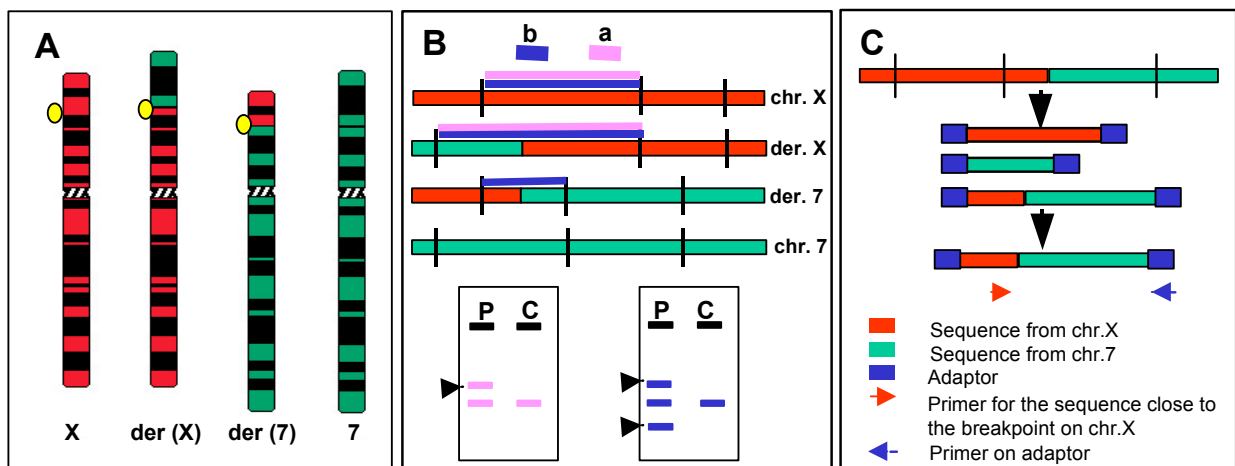


Figure 2. Principle of FISH, Southern blot hybridization and genomic walking used for identifying the breakpoint in an X;7 translocation. A, FISH. A genomic clone from the region of the breakpoint is used as hybridization probe on the patient metaphase chromosomes. The breakpoint-spanning clone shows signals on the normal chromosome X, derivative X and derivative 7. B, Southern blot hybridization. Genomic DNA from both the patient (P) and a normal control (C) are digested with rare-cutting restriction enzymes. Restriction fragments are separated by agarose-gel electrophoresis and are transferred to a nylon membrane. A probe derived from sequences within the junction fragment of the derivative X (probe a) recognizes this junction fragment and the fragment from the normal X chromosome (in pink). A probe spanning the breakpoint (probe b) recognizes the junction fragments from both derivative chromosomes and the fragment from the normal X chromosome (in blue). The junction fragments are indicated with arrows. C, Genomic walking. Genomic DNA from the patient is digested with frequent-cutting restriction enzymes. The restriction fragments are then ligated to adaptors on both ends. The junction fragments are amplified by PCR using one primer specific for the sequence on the X chromosome and the other for the sequence of the adaptor.

of positional cloning has identified 23 XLMR candidate genes, whose causative involvement was subsequently proven by the demonstration of mutations in unrelated families with XLMR (Fig. 3).

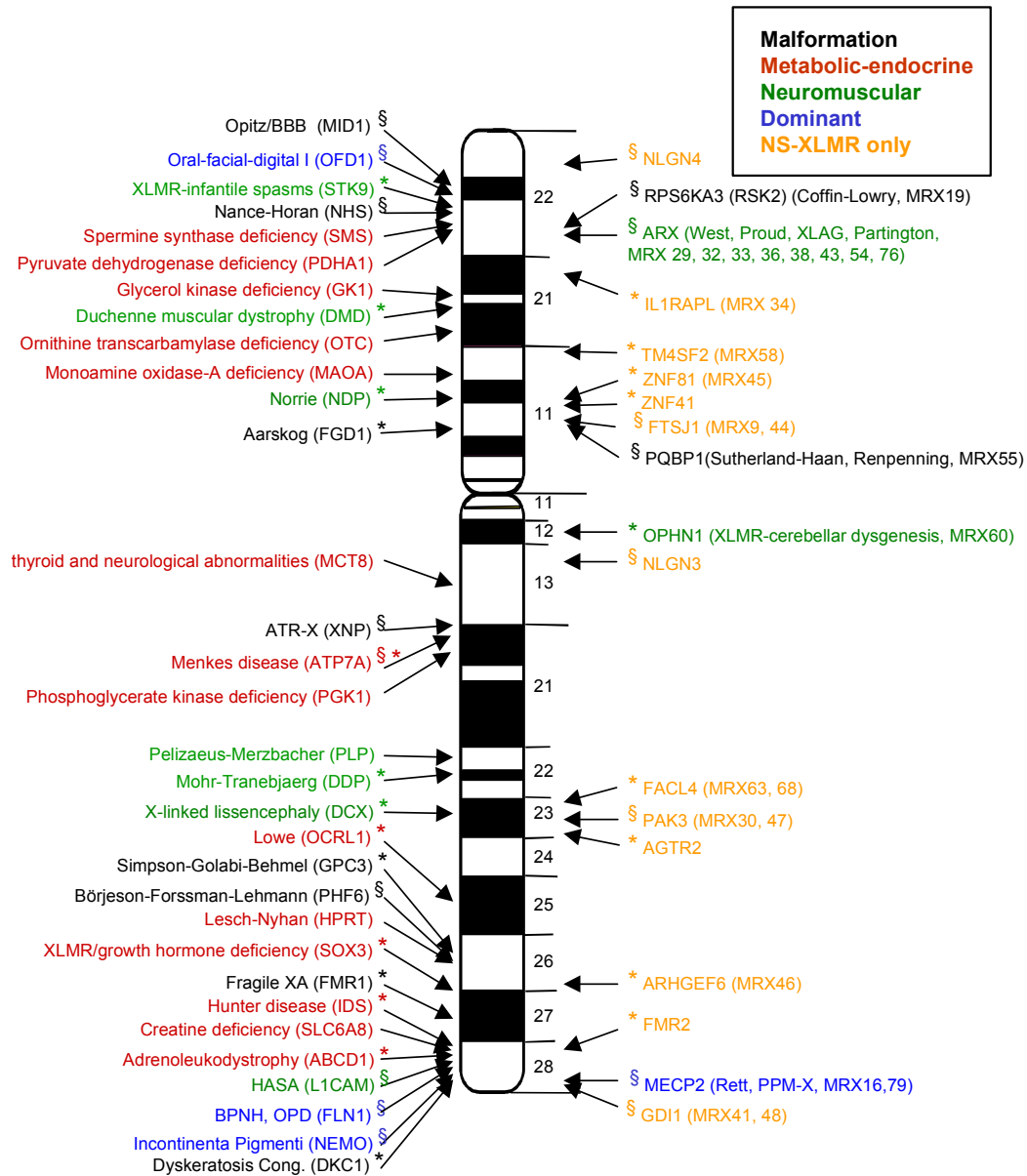


Figure 3. Location of the cloned XLMR genes. On the left side of the X chromosome are the genes involved in S-XLMR. On the right side of the X chromosome are the genes associated with NS-XLMR, among which, *RSK2*, *ARX*, *PQBP1*, *OPHN1*, and *MECP2* are occasionally associated with S-XLMR. The genes identified by positional cloning are indicated with an asterisk (*). The genes identified by positional candidate gene-mutation analysis are indicated with a paragraph (§). For references, see <http://www.xlmr.interfree.it>, and <http://www.ggc.org/xlmr.htm>.

As the number of such patients with X-chromosomal abnormalities is limited, regionally mapped families with XLMR remain a prominent resource in the search for XLMR genes. The genetic factor responsible for the MR condition in each family can be identified by screening for the disease-specific mutations within the linkage region. However, attempts to identify causative genes were often hindered by the broad linkage interval in an individual family, which in most of the cases comprises a region of about 10 Mb and may contain more than 100 genes. The breakthrough came during the last four years with the improved technology for high-throughput mutation analysis, and our accumulating knowledge about the regional distribution of the relevant genes on the X chromosome (Ropers et al. 2003). Prioritizing candidates according to their potential functions in brain development, the approach of positional candidate gene-mutation screening has been successful in identifying 18 of the XLMR genes (Fig. 3).

1.1.4 Impacts of XLMR studies

The concerted efforts of clinical and molecular investigations have made significant progress in the XLMR studies. To date, thirty-seven genes have been attributed to S-XLMR, of which *RSK2*, *ARX*, *PQBPI*, *OPHN1* and *MECP2* are occasionally associated with NS-XLMR. Another 13 genes have been attributed to NS-XLMR only (Fig. 3). This progress has greatly improved our insights into the nosology of XLMR, and advanced our understanding of cognitive function.

1.1.4.1 Contributions in the nosology of XLMR

Identification of XLMR genes provides the molecular basis for splitting and lumping in the nosology of XLMR. For example, X-linked spastic paraplegia, a heterogeneous neurological symptom characterized by progressive weakness and spasticity of the legs, could be splitted into at least two forms, with *LICAM* defects being responsible for spastic paraplegia type I (MIM 312900) (Jouet et al. 1994), and *PLP1* mutations underlying spastic paraplegia type II (MIM 312920) (Saugier-Weber et al. 1994). On the other hand, HSAS syndrome (MIM 307000), MASA syndrome (MIM 303350), and spastic paraplegia type I (MIM 312900), all due to *LICAM* mutations, are therefore allelic disorders. Likewise, the ATR-X syndrome (MIM 301040),

Holmes-Gang syndrome (Holmes and Gang 1984), Juberg-Marsidi syndrome (MIM 309590), Smith-Fineman-Myers syndrome (MIM 309580), and XLMR with spastic paraplegia (MIM 300465) all result from mutations in the *XNP* gene (Gibbons et al. 1995; Villard et al. 1996; Lossi et al. 1999; Stevenson et al. 2000a; Villard et al. 2000a). Defects of other XLMR genes give rise to syndromic as well as non-syndromic XLMR (Table 1). For example, *ARX* mutations were found in West syndrome (MIM 308350, a triad of infantile spasms, hypsarrhythmia, and MR), Partington syndrome (MIM 309510, MR with dystonic hand movements), X-linked lissencephaly with

Table 1 XLMR genes implicated in both S-XLMR and NS-XLMR conditions

Gene	XLMR entity (MIM No.)	Clinical features
<i>RSK2</i>	Coffin-Lowry (303600)	<ul style="list-style-type: none"> Severe MR, facial and digital dysmorphisms, and progressive skeletal deformations
<i>ARX</i>	MRX19	<ul style="list-style-type: none"> NS-XLMR
	West (308350)	<ul style="list-style-type: none"> Infantile spasms, hypsarrhythmia, MR
	Partington/MRXS1 (309510)	<ul style="list-style-type: none"> Dysarthria, dystonic hand movements, ataxia, seizures
	Myoclonic epilepsy & spasticity (300432)	<ul style="list-style-type: none"> Myoclonic and tonic-clonic seizures, spasticity, ataxia
	Myoclonic epilepsy & spasticity (300432)	<ul style="list-style-type: none"> Myoclonic and tonic-clonic seizures, spasticity, ataxia
<i>PQBP1</i>	XLAG (300215)	<ul style="list-style-type: none"> Lissencephaly with ambiguous genitalia
	Proud (300004)	<ul style="list-style-type: none"> Agenesis of the corpus callosum, with seizure and microencephaly
	MRX29, 32, 33, 36, 43, 54, 76	<ul style="list-style-type: none"> Non-syndromic MR
<i>OPHN1</i>	Renpenning (309500)	<ul style="list-style-type: none"> MR, microcephaly, short stature, and small testes
	Sutherland-Haan (309470)	<ul style="list-style-type: none"> MR, short stature, microcephaly, brachycephaly, spastic diplegia, small testes, and anal stenosis or atresia
<i>MECP2</i>	MRX55	<ul style="list-style-type: none"> NS-XLMR
	Cerebellar hypoplasia	<ul style="list-style-type: none"> Cerebellar hypoplasia
<i>MECP2</i>	MRX60	<ul style="list-style-type: none"> NS-XLMR
	Rett (312750)	<ul style="list-style-type: none"> Developmental stagnation, loss of speech and hand skills
	PPM-X (300555)	<ul style="list-style-type: none"> MR, psychosis with pyramidal signs
	MR with progressive spasticity (300279)	<ul style="list-style-type: none"> Severe MR, ataxia, spasticity and convulsions
	MRX16, 79	<ul style="list-style-type: none"> NS-XLMR

abnormal genitalia (XLAG, MIM 300215), and in NS-XLMR (Bienvenu et al. 2002; Kitamura et al. 2002; Stromme et al. 2002). Similarly, *MECP2* mutations were found in females with Rett syndrome (RTT, MIM 312750, cessation and regression of development in early childhood), and in male patients with NS-XLMR (Amir et al. 1999; Yntema et al. 2002). With increasing numbers of XLMR genes implicated in S-XLMR and NS-XLMR, it becomes obvious that there is no molecular basis for strictly separating these two categories.

1.1.4.2 Understanding the molecular and cellular basis of MR

Identification of genes that play a role in XLMR provides a starting point for elucidating their molecular and cellular functions. Genes mutated in XLMR encode a range of proteins that fall into distinct subclasses, including membrane proteins, signaling pathway components, transcription regulators, cytoskeleton-associated proteins and enzymes that catalyze metabolic reactions. A proportion of these proteins has been suggested to play a role in regulation of cytoskeletal dynamics (Table 2), which is a critical cellular process for neural morphogenesis.

Three XLMR genes, namely filamin 1 (*FLNI*), doublecortin (*DCX*) and midline defect 1 (*MIDI*), encode proteins that are directly associated with actin filaments or microtubules, two

Table 2 Properties of the XLMR genes associated with cytoskeletal dynamics

XLMR gene	Protein function	Corresponding XLMR entity
<i>FLNI</i>	Actin-binding protein	OPD spectrum/ PVNH
<i>DCX</i>	Microtubule-associated protein	SCLH/XLIS
<i>MIDI</i>	B BOX family of RING finger protein, microtubule –anchoring protein	Opitz G
<i>OFD1</i>	LIS1 homology motif, regulating microtubule dynamics?	OFD1
<i>ARHGEF6</i>	GEF for Rac/Cdc42	NS-XLMR
<i>FGD1</i>	GEF for Cdc42	Aarskog-Scott
<i>OPHN1</i>	RhoGAP	NS-XLMR
<i>PAK3</i>	Ser/Thr protein kinase, Cdc42/Rac1 effector	NS-XLMR
<i>LICAM</i>	Ig superfamily of cell adhesion molecules	HASA spectrum
<i>TM4SF2</i>	Four transmembrane protein, integrin-mediated signaling?	NS-XLMR

main components of the cytoskeletal structure. Loss-of-function defects in *FLNA* cause periventricular nodular heterotopia (PVNH, MIM 300049, failure in neuronal migration into the cerebral cortex with consequent formation of nodules in the ventricular and subventricular zones in females) (Fox et al. 1998); whereas gain-of-function defects lead to a spectrum of disorders with congenital malformations in a wide range of tissues, including otopalatodigital syndrome types I (OPD1, MIM 311300) and II (OPD2, MIM 304120), frontometaphyseal dysplasia (FMD, MIM 305620), and Melnick-Needles syndrome (MNS, MIM 309350) (Robertson et al. 2003). The gene product *FLNA* is an actin-binding protein, which stabilizes actin filaments into three-dimensional networks and links them to cellular membranes (Stossel et al. 2001). Mutations in *DCX* cause lissencephaly (also called smooth brain) in males, and subcortical laminar heterotopia (also called double cortex) in females (MIM 300067) (des Portes et al. 1998; Gleeson et al. 1998). The coding protein *DCX* is a microtubule-associated protein that binds to tubulin and affects microtubule polymerization and stability (Gleeson et al. 1999). The third gene, *MIDI*, is involved in Opitz syndrome (OMIM 300000, a midline defect often associated with hypertelorism, laryngotracheoesophageal cleft, hypospadias and imperforate anus) (Quaderi et al. 1997). The gene product of *MIDI* is a microtubule-anchoring protein recruiting the proteins that are required for microtubule dynamics into the microtubule compartment (Cainarca et al. 1999; Schweiger et al. 1999). A fourth gene, *OFDI*, mutated in oral-facial-digital syndrome 1 (OFD1, OMIM 311200, abnormalities in the face, oral cavity, and digits), might be functionally associated with the cytoskeleton as well. OFD1 protein contains a predicted LIS1 homology motif (Emes and Ponting 2001), which is present in the product of the gene mutated in autosomal form of lissencephaly (Miller-Dieker lissencephaly, OMIM 247200). The LIS1 motif is suggested to play a role in microtubule dynamics, potentially through interaction with the dynein motor protein complex (Emes and Ponting 2001). Recent studies have shown that these cytoskeleton-associated proteins serve as targets of a number of signaling pathways. For example, *FLNA* can be phosphorylated by PAK1 and protein kinase C (PKC) (Vadlamudi et al. 2002; Tigges et al. 2003; Ueda et al. 2003). *DCX* can be phosphorylated by cyclin-dependent kinase 5 (Cdk5), c-Jun N-terminal kinase (JNK), microtubule affinity regulatory kinase (MARK) and protein kinase A (PKA) (Gdalyahu et al. 2004; Schaar et al. 2004; Tanaka et al. 2004). Moreover, phosphorylation of *DCX* has been shown to be

critical in regulating its affinity to microtubules and thus modulating its effect on microtubule polymerization. Similarly, the regulation of microtubule association of MID1 involves its phosphorylation by mitogen-activated protein kinase (MAPK) and dephosphorylation by a ternary MID1- α 4-PP2Ac complex (Schweiger and Schneider 2003). These data suggest an emerging role of these cytoskeleton-associated proteins as signaling integrators to modulate the cytoskeletal architectures in response to various extra- or intra-cellular stimuli (Schaar et al. 2004; Tanaka et al. 2004).

Another four XLMR gene products, namely, OPHN1, ARHGEF6, FGD1 and PAK3, are components of the Rho GTPase signaling cascade, which is one of the prominent signaling pathways in regulating the assembly and organization of the actin cytoskeleton (Etienne-Manneville and Hall 2002). Central to this pathway are the Rho GTPases, acting as intracellular molecular switches cycling between a GTP-bound active state and a GDP-bound inactive state. The activities of Rho GTPases are regulated by two main classes of proteins, guanine nucleotide exchange factors (GEFs) and GTPase activating proteins (GAPs). GEFs stimulate the exchange of GDP for GTP, thereby switching on Rho GTPases. In contrast, GAPs increase the endogenous GTPase activity of Rho GTPases, thereby helping to switch them off. In the active form, Rho-GTPases are able to interact with downstream effectors to elicit their biological functions. In mammals, over a dozen of Rho GTPases, 30 GEFs and 20 GAPs have been identified to date (Bishop and Hall 2000). The abundant Rho GTPases and their upstream regulators together with diverse downstream effectors constitute a complex regulatory network transducing various extracellular signals to the intracellular actin cytoskeleton. Of the four Rho-linked XLMR genes, *ARHGEF6* and *PAK3* are associated with NS-XLMR (Allen et al. 1998; Kutsche et al. 2000), while *OPHN1* is implicated in both NS-XLMR and S-XLMR with epilepsy and cerebellar hypoplasia (Billuart et al. 1998; Bergmann et al. 2003), and *FGD1* in Aarskog syndrome (MIM 305400, disproportionately short stature and anomalies in the face, skeleton, and urogenital tract) (Pasteris et al. 1994). The gene products of *ARHGEF6* and *FGD1* are RhoGEF proteins (Zheng et al. 1996; Manser et al. 1998), the OPHN1 protein is a RhoGAP (Billuart et al. 1998), and the PAK3 protein is one of the PAK family members that mediate downstream effects of Rho GTPases on regulation of the actin cytoskeleton (Bagrodia et al. 1995; Manser et al. 1995).

Two other XLMR genes encoding cell surface proteins might be involved in cytoskeleton regulation as well. One of them is *L1CAM*, implicated in a spectrum of disorders, including HSAS syndrome (MIM 307000), MASA syndrome (MIM 303350), and spastic paraplegia type I (MIM 312900) (Fransen et al. 1997; Weller and Gartner 2001). The L1CAM protein is a member of the immunoglobulin superfamily of neuronal adhesive molecules and plays a key role in axon outgrowth and path finding. Recent studies demonstrated that the cytoplasmic domain of L1CAM interacts with ankyrin, a linker molecule of the spectrin-actin based membrane cytoskeleton network. The binding of L1CAM with ankyrin plays a crucial role in regulating L1CAM mediated effects (Gil et al. 2003; Nishimura et al. 2003). These data indicate that the biological function of L1CAM depends critically on its interaction with the dynamic components of the cytoskeleton. The other gene is *TM4SF2*, which encodes a four-transmembrane-domain protein and is mutated in NS-XLMR (Zemni et al. 2000). The specific biochemical function of TM4SF2 has not been determined, except for its association with PtdIns 4-kinase (Yauch and Hemler 2000). However, as proteins with four-transmembrane-domain have the potential to associate with cell adhesion molecules of the integrin family, TM4SF2 is proposed to play a role in integrin-dependent cell mobility and migration (Hemler 2001). TM4SF2 may contribute to cytoskeletal dynamics through recruiting PtdIns 4-kinase into the vicinity of integrin-associated cytoskeleton proteins, e.g. α -actinin, vinculin and talin (DeMali et al. 2003), and regulating the actin-binding properties of those proteins.

Properly controlled cytoskeletal dynamics are crucial for brain development. To establish the neuronal network, newborn neurons must migrate to their characteristic locations, send out axons and dendrites into proper target regions and form synapses with appropriate partners. These seemingly different processes all depend on the regulation of the cytoskeletal organization in response to diverse extra or intra-cellular cues (Luo 2000).

Given the fact that functions of many XLMR genes converge on the control of cytoskeletal dynamics, it is conceivable that MR in the relevant conditions may result from deficits in cytoskeleton-dependent neuronal structure. In support of this assumption, macro-anatomical abnormalities such as brain malformation, microcephaly and lissencephaly are often found in patients with defects in cytoskeleton-associated proteins, e.g. FLNA, DCX, MID1, OFD1 and

LIS1. The severe MR present in these patients is likely caused by gross alterations in brain structure. Likewise, abnormalities in dendrites and dendritic spines, which are likely to reflect a more general micro-structural defect in neuronal connectivity, are common findings in patients with milder forms of MR (Ramakers 2002; Chechlacz and Gleeson 2003). In these patients, the sub-optimized neuronal connectivity during brain development would limit the capability of the brain to process information and give rise to a milder MR manifestation.

In addition to the regulation of cytoskeletal dynamics, synaptic functions are also likely to be affected in XLMR. *GDII* and *IL1RAPL*, two genes that have been implicated in NS-XLMR (D'Adamo et al. 1998; Carrie et al. 1999), are associated with synaptic vesicle transport. $GDI\alpha$, the protein encoded by *GDII*, regulates the activity of Rab3a and Rab 3c, the small Ras-like GTPases that are involved in synaptic vesicle fusion (Geppert and Sudhof 1998). In brain of *GDI1*-deficient mice, the concentration of Rab4 and Rab5 are markedly reduced (D'Adamo et al. 2002), which suggests a role of *GDI1* in endocytosis. *IL1RAPL* has recently been shown to interact with neuronal calcium sensor-1 (NCS-1), and may regulate calcium-dependent exocytosis of neurotransmitters in synapses (Bahi et al. 2003).

1.1.5 Perspectives

The abnormalities in neuronal connectivity offer a plausible explanation for the impaired cognition in XLMR. However, as the genes that fit into the theme of cytoskeletal dynamics represent only a fraction of the known XLMR genes, the pathogenesis of XLMR in general is still poorly understood. Further characterization of the remaining genetic defects in XLMR and their functional link with cognitive processes, together with the ongoing effort to search for new XLMR genes will expand our limited knowledge on the pathology of MR. Our increasing knowledge of the cellular processes that are crucial for appropriate cognitive functions will hopefully lead to the development of effective treatments beneficial to mentally retarded patients.

1.2 Outline of the project

Our group is interested in finding new causative genes for XLMR, and in further elucidating their functions in cognitive processes and normal brain development. To achieve this goal, we employ two complementary approaches: large-scale mutation screening in regionally mapped families with XLMR and breakpoint cloning in patients with MR and chromosomal rearrangements.

As part of these systematic studies, this project started with investigations in a mentally retarded female who carried an X;autosome translocation. Breakpoint cloning in the patient identified serine/threonine kinase 9 (*STK9*) as a potential causative gene for XLMR. The second part of the project focused on mutation analysis of *STK9*. Disease-causing mutations were identified from three selected cohorts with MR. To obtain insights into the function of STK9, a polyclonal antibody against STK9 protein was generated and the intracellular distribution of STK9 was also studied. Furthermore, to search for proteins that interact with STK9, a yeast two-hybrid library screening was performed. The primary data of the yeast two-hybrid assay and immunocytochemistry studies, together with the preparation of specific anti- STK9 antibody, enable us to further elucidate the role of STK9 in brain development.

2 MATERIALS, SUBJECTS AND METHODS

2.1 Materials

2.1.1 Chemicals and reagents

Standard chemicals and reagents are listed in Table 3 in an alphabetical order. Culture reagents are listed separately in Table 4.

Table 3 Standard chemicals and reagents

Chemical/ Reagent	Company
Acetonitrile	Transgenomic
30% Acrylamide mix	Merck
Adenine	Sigma
Agar	Difco
Agarose	Invitrogen
Ammonium persulfate (APS)	Invitrogen
Bactopeptone	Difco
Bovine serum albumin (BSA)	Sigma
Bromophenol blue	Fluka
Complete mini protease inhibitor cocktail tablets	Roche
Coomassie Brilliant Blue R250	Fluka
4'6-diamino-2-phenyl-indole (DAPI)	Serva
[α - ³² P]dCTP	Amersham
Dextran blue	Fluka
Diethylpyrocarbonate (DEPC)	Sigma
Disodiumhydrogen phosphate	Merck
Dithiothreitol (DTT)	Sigma
dNTPs	MBI Fermentas
DO Supplement	BD Biosciences
Ethylene glycol bis(2-aminoethyl ether)-N,N,N',N'-tetraacetic acid (EGTA)	Sigma
Ethanol	Merck
Ethidium bromide	Serva
Ethylenediaminetetraacetic acid (EDTA)	Merck

MATERIALS, SUBJECTS AND METHODS

GeneRuler 1 kb and 100 bp DNA ladders	MBI Fermentas
Glacial acetic acid	Merck
Glass beads (425-600 μm)	Sigma
Glucose	Merck
Glycerol	Merck
Glycine	Sigma
Herring sperm DNA	Roche
Histidine	Sigma
Hybridime human placental DNA	HT Biotechnology
Hydrochloric acid	Merck
4-(2-Hydroxyethyl)piperazine-1-ethanesulfonic acid sodium (HEPES)	Sigma
Imidazole	Fluka
Isopropanol	Merck
Isopropyl β -D-thiogalactoside (IPTG)	Serva
Kanamycin	Invitrogen
Magnesium chloride	Merck
β -Mercaptoethanol	Merck
Methanol	Merck
Ni-NTA agarose	Qiagen
N,N,N,N -Tetramethylethylenediamine (TEMED)	Invitrogen
Paraformaldehyde	Sigma
pd(N) ₆ random hexamers	Pharmacia
Phenol	Roth
Phenol red	Fluka
Phenylmethylsulphonyl fluoride (PMSF)	Sigma
Phytohemagglutinin (PHA)	Roche
Piperazine-N,N -bis(2-ethanesulfonic acid) (PIPES)	Sigma
Polyethylene glycol 6000 (PEG 6000)	Merck
Potassium chloride	Merck
Potassium dihydrogen phosphate	Merck
Pre-stained protein molecular weight marker	MBI Fermentas
Protein A agarose	Roche
Protein G agarose	Roche
RNAguard RNase inhibitor	Amersham

Sephadex G-50	Pharmacia
Sodium chloride	Merck
Sodium citrate	Merck
Sodium dihydrogen phosphate	Merck
Sodium dodecyl sulfate (SDS)	Serva
Sodium hydroxide	Merck
Sorbitol	Sigma
Triethylammonium acetate (TEAA)	Transgenomic
Tris (hydroxymethyl)-aminomethane	Merck
Triton X-100	Roth
TRIZol reagent	Invitrogen
Trypton	Difco
Tween 20	Sigma
Urea	Merck
Vectashield mounting medium	Vector
X- α - gal	BD Biosciences
Yeast extract	Difco
Yeast nitrogen base without amino acids	Difco

Table 4 Cell culture and transfection reagents

Reagent	Company
Minimal essential medium eagle's with earles salts (EMEM)	Biowhittaker
L-glutamine	Invitrogen
Opti-MEM medium	Invitrogen
Penicillin/ streptomycin antibiotic solution	Invitrogen
Fetal bovine serum (FBS)	Biowhittaker
Polyfectamine transfection reagent	Qiagen

2.1.2 Solutions and media

Aqueous solutions were prepared using autoclaved Millipore water. For sterilization, if necessary, solutions and media were autoclaved or passed through a 0.45 μm filter (Millipore). Solutions used for Southern blot hybridization are listed in Table 5. Solutions used for SDS PAGE, Western blot analysis and immunofluorescence are listed in Table 6. Solutions used for expression and

purification of 6 × His tagged proteins are listed in Table 7. Solutions used for yeast two-hybrid assay are listed in Table 8.

Table 5 Solutions used for Southern blot hybridization

Solution	Component
Nuclear buffer (pH 7.5)	10 mM Tris-HCl 25 mM EDTA 75 mM NaCl
20 × SSC (pH 7.0)	300 mM sodium citrate 3 mM NaCl
Denaturing solution	0.4 N NaOH 1 M NaCl
PEG hybridization solution	250 mM NaCl 125 mM Na ₂ HPO ₄ 1 mM EDTA 7% (w/v) SDS 10% (w/v) PEG 6000
5 × OLB (-dCTP)	0.1 mM each dATP, dGTP, dTTP 1 M HEPES 0.425 mM pd(N) ₆ 25 mM MgCl ₂ 250 mM Tris 0.36% (v/v) β-Mercaptoethanol
Stop solution (pH 7.5)	10 mM Tris 5 mM EDTA 2% SDS 0.1% Dextran blue 0.1% Phenol red
TES (pH 7.5)	10 mM Tris-HCl 5 mM EDTA 0.2% SDS
Washing buffer	0.2% SSC 0.1% SDS

Table 6 Solutions used for SDS PAGE, Western blot analysis and immunofluorescence

Solution	Component
Protein loading buffer (pH 6.8)	50 mM Tris 100 mM DTT 2% SDS 0.1% bromophenol blue 10% glycerol
1 × electrophoresis buffer	25 mM Tris 250 mM glycine 0.1% SDS
Coomassie blue staining solution	0.25% Coomassie brilliant blue R250 10% glacial acetic acid 45% methanol
Destaining solution	10% glacial acetic acid 45% methanol
Blot transferring buffer	39 mM glycine 48 mM Tris 0.037% SDS 20% methanol
1 × PBS (pH 7.3)	137 mM NaCl 2.7 mM KCl 10.1 mM Na ₂ HPO ₄ 1.8 mM KH ₂ PO ₄
PEM buffer (pH 6.8)	80 mM PIPES 5 mM EGTA 2 mM MgCl ₂
Blocking buffer	5% (w/v) nonfat dry milk 1 × PBS
PBST	0.1% Tween 20 1 × PBS

Table 7 Solutions used for expression and purification of 6 × His tagged proteins

Solution	Component
LB medium	10 g/l trypton
	5 g/l yeast extract
	10 g/l NaCl
LB agar	5 g agar per 1 l LB medium
Lysis buffer (pH 8.0)	100 mM NaH ₂ PO ₄
	10 mM Tris-HCl
	8 M urea
Washing buffer 1 (pH 8.0)	100 mM NaH ₂ PO ₄
	10 mM Tris-HCl
	8 M urea
	20 mM β-mercaptoethanol
	20 mM imidazole
	0.1% Tween 20
Washing buffer 2 (pH 6.5)	100 mM NaH ₂ PO ₄
	10 mM Tris-HCl
	8 M urea
	20 mM β-mercaptoethanol
	20 mM imidazole
	0.1% Tween 20
Elution buffer (pH 5.0)	100 mM NaH ₂ PO ₄
	10 mM Tris-HCl
	8 M urea
	20 mM β-mercaptoethanol
	100 mM imidazole
	0.1% Tween 20

Table 8 Solutions used for yeast two-hybrid assay

Solution	Component
YPDA medium	2% bactopectone 1% yeast extract 2% glucose 0.003% adenine
YPDA agar	2% agar in YPDA medium
YCM medium (pH 3.5)	1% yeast extract 1% bactopectone 2% glucose
YCM agar (pH 4.5)	2% agar in YCM medium
SD medium	0.67% yeast nitrogen base without amino acids 2% glucose 1 × appropriate DO supplement
SD agar	2% agar in SD medium
10 × Protease inhibitor stock	1 tablet of complete mini protease inhibitor cocktail per 1 ml H ₂ O
100 × PMSF stock	0.1742 g PMSF in 10 ml isopropanol
Cracking buffer	8 M Urea 5% (w/v) SDS 40 mM Tris-HCl 0.1 mM EDTA 0.4 mg/ml Bromphenol blue 1 × Protease inhibitor solution 1 × PMSF

2.1.3 Enzymes

All restriction endonucleases for cloning and genomic DNA digestion were purchased from New England Biolabs, Invitrogen or MBI Fermentas. Reactions were performed in supplied reaction buffers following the manufacturers' instruction. Additional enzymes used are listed in Table 9.

Table 9 Additional enzymes

Enzyme	Concentration	Company
AmpliTaq	5 U/μl	Perkin Elmer
Pfu DNA polymerase	2.5 U/μl	Stratagene
TaKaRa LA Taq polymerase	5 U/μl	TaKaRa
BIO-X-ACT DNA polymerase	4 U/μl	Bioline
Klenow fragment	2 U/μl	Roche
Omniscript reverse transcriptase	200 U/μl	Qiagen
Proteinase K	10 mg/ml	Invitrogen
RNase A	50 μg/ml	Roche
T4 DNA ligase	400 U/μl	Promega
Calf intestine alkaline phosphatase	10,000 U/μl	Sigma

2.1.4 Kits

All kits used are listed in Table 10.

Table 10 Kits

Kit	Company
BigDye terminator cycle sequencing ready reaction kit	PE Biosystems
QIAprep spin miniprep kit	Qiagen
QIAGEN plasmid midi and maxi kits	Qiagen
QIAquick gel extraction kit	Qiagen
Enhanced chemiluminescence HRP detection kit	Amersham

2.1.5 Vectors

All vectors used for expression studies as well as those used for intermediate cloning steps are listed in Table 11.

Table 11 Cloning vectors

Vector	Size (kb)	Resistance gene	Company
pBluescript II SK	3.0	Ampicillin	Stratagene
pQE-30	3.4	Ampicillin	Qiagen
pCMV-Tag 3B	4.3	Kanamycin/Neomycin	Stratagene
pGBKT7	7.3	Kanamycin/Tryptophan	BD Biosciences

2.1.6 Antibodies

All primary and secondary antibodies used in this study are listed in Table 12.

Table 12 Antibodies

Antibody	Company
Monoclonal anti- 6 × His antibody	Qiagen
Monoclonal anti- γ -tubulin antibody (clone GTU-88)	Sigma
Monoclonal anti- c-myc antibody	Invitrogen
Polyclonal anti- c-myc antibody	Santa Cruz
Horseradish peroxidase (HRP) conjugated anti- rabbit Ig	Amersham
Horseradish peroxidase (HRP) conjugated anti- mouse Ig	Dianova
Fluorescein isothiocyanate (FITC) conjugated anti- rabbit Ig	Dianova
Cyanine 3 (C3) conjugated anti- mouse Ig	Dianova

2.1.7 Primers

All primers used in this study were synthesized at MWG Biotech, Germany.

2.1.8 Human genomic clones

All human YAC, BAC and PAC clones were obtained from the Resource Centre of the German Human Genome Project (RZPD).

2.1.9 Bacterial materials

For all recombinant DNA techniques, competent *Escherichia coli* strain DH5 α or XL1-Blue cells (Stratagene) were used.

2.1.10 Mammalian cell line

Transient transfection experiments were performed in COS-7 cells (African green monkey kidney cells).

2.2 Subjects

The female patient with a chromosome translocation $t(X;7)(p22.3;p15)$ (designated patient 1) was originally referred to the Institute for Human Genetics Lübeck, Germany. The translocation was observed using high resolution Giemsa banding in the diagnostic cytogenetic laboratory. A patient-derived fibroblast cell line was available.

For *STK9* mutation analysis, three cohorts of mentally retarded patients were selected. The cohort with infantile spasms included 96 male patients, in whom no mutation had been identified in the *ARX* coding region. The panel of XLMR families was collected by the European XLMR Consortium. 150 families were selected for this study, in which either linkage analysis was not applicable due to the small family size or linkage to Xp22 could not be excluded. The cohort with RTT-like features included 25 females and 7 males, in whom no mutation had been identified in the *MECP2* coding region. The control panel consisted of 275 normal males and 65 normal females. All DNA samples were obtained with informed consent.

2.3 Methods

2.3.1 DNA isolation

Genomic DNAs from fibroblast cell lines were extracted according to standard protocols (Sambrook et al. 1989). Essentially, approximately 1×10^8 cells were suspended in 10 ml of nuclear buffer (see Table 5), and lysed by addition of SDS to a final concentration of 0.5%. Cell lysates were subjected to overnight proteinase K digestion. DNAs were extracted by phenol/chloroform, and precipitated by ethanol.

Plasmid DNAs were isolated using QIAprep miniprep kit or QIAgen plasmid midi and maxi kits according to the manufacturer's instruction.

2.3.2 RNA isolation

Total RNAs from fibroblast cell lines were isolated using TRIzol reagent (Invitrogen) according to the manufacturer's instruction.

2.3.3 Fluorescence *in situ* hybridization (FISH)

Metaphase chromosomes were prepared from the PHA-stimulated fibroblast cell line which was derived from patient 1 with t(X;7)(p22.3;p15) chromosome translocation. CEPH and ICRFy900 YAC probes selected from the Whitehead Institute and the Integrated X chromosome database, and BACs and PACs from the Sanger Institute and UCSC "Golden Path" database were used for breakpoint mapping. YAC, PAC and BAC DNAs were prepared according to standard protocols (Sambrook et al. 1989). Purified DNAs were labelled with either biotin-16-dUTP or digoxigenin-11-dUTP, by nick translation. Immunocytochemical detection of probes was performed as described previously (Wirth et al. 1999).

2.3.4 Preparation of DNA probes for Southern blot hybridization

DNA probes for Southern blot hybridization were amplified by PCR with AmpliTaq DNA

Table 13 Probes for Southern blot hybridization

Probe	Primer name	Primer sequence	T _A
245G19-1 (735bp)	Z92542-38913for Z92542-39648rev	GCATCTCAGGGTGGTGGT CAGGACTGGCATTG GCC	58°C
*245G19-2 (1121bp)	Z92542-76261for Z92542-77382rev	GTATTTGAAGCCTCCCATCG CTAAACTGGCAGAAGCACAGG	58°C
245G19-3 (966bp)	Z92542-80637for Z92542-81603rev	GGTCTGGGAGAGCATCC GAGACAAGGCAGGGGAG	58°C
245G19-4 (874bp)	Z92542-100069for Z92542-100943rev	AGGTCTTCAACAGCATGGA CCCTAAAATCCCAGATACG	56°C
245G19-5 (804bp)	Z92542-120709for Z92542-121513rev	TCACTGTTTCCTCCTCTCCT GACCATGTAGCTTTTCCCT G	57°C
245G19-6 (490bp)	Z92542-141051for Z92542-141541rev	GCCAGTCTCTAAGTTCAAAG CCCTAACCTTCATTGCTAC	57°C

* breakpoint-spanning probe

polymerase (Perkin Elmer) in the supplied buffer (1.5 mM MgCl₂ final concentration). PCR reactions were carried out in 50 µl reaction volumes containing 30 pmol of each primer pair, 0.4 mM dNTPs, and 1 U AmpliTaq DNA polymerase. Cycling conditions included an initial denaturation step at 95°C for 4 min, followed by 30 cycles of 40 sec at 95°C, 40 sec at the specific annealing temperature, 2 min at 72°C, and a final extension step at 72°C for 10 min. The PCR products were purified using the QIAquick gel extraction kit (Qiagen), according to the manufacturer's instruction. Probes used for Southern blot hybridizations, and the respective primer sequences (in 5' to 3' orientation), together with the annealing temperature (T_A) in each PCR reaction are given in Table 13.

2.3.5 Isotope-labeling of probes for Southern blot hybridization

Gel purified DNA probes were denatured for 10 min at 95°C, chilled on ice and radiolabelled using random hexanucleotide primers in 1 × OLB buffer. Essentially, reaction was carried out at 37°C for at least 1 hr in 20 µl volume containing 50 ng of DNA probe, 20 µCi [α -³²P]dCTP and 5 U Klenow fragment. Reaction was stopped by adding 50 µl of stop solution. To remove excess non-incorporated dNTPs and random hexamers, the reaction mixture was separated by passing through a Sephadex G-50 column and the labeled probe was eluted with TES buffer. Solutions used in this section are listed in Table 5.

2.3.6 Southern blot hybridization

Genomic DNAs from patient 1 with t(X;7)(p22.3;p15) chromosome translocation and controls were digested with appropriate restriction enzymes, separated in 0.7% agarose gels, and capillary transferred to nylon membranes (Roth) using 10 × SSC. For transferring large DNA fragments, if necessary, gels were pre-incubated with 0.1 M HCl for 5 min followed by denaturing solution for 30 min. After overnight transfer, membranes were rinsed in 2 × SSC, and the DNAs were fixed by UV crosslinking at 254 nm for 2 min. For hybridization, membranes were pre-hybridized in PEG hybridization buffer supplemented with 0.1 mg/ml denatured herring sperm DNA as blocking reagent for at least 2 hr at 65°C. Isotope-labelled DNA probes were denatured for 10 min at 95°C, chilled on ice and blocked with human placental DNA Hybridime (HT Biotechnology) in PEG

hybridization buffer for 1 hour at 65°C before added to the prehybridization solution. Membranes were hybridized with isotope-labelled probes at 65°C overnight, washed with washing buffer and exposed to Kodak X-Omat AR film at –80°C for 3-7 days. Solutions used in this section are listed in Table 5.

2.3.7 Genomic walking

For breakpoint cloning in patient 1, genomic walking was performed essentially as described elsewhere (Siebert et al. 1995). Genomic DNAs from the patient and a control were digested with appropriate restriction enzymes, phenol/chloroform extracted, and ethanol precipitated. Approximately one µg of each digested DNA was ligated to pre-annealed adaptor oligos using T4 DNA ligase (Promega) in supplied buffer. After overnight ligation at 4°C, the reaction was stopped by heating at 70°C for 10 min. One µl of each ligation mixture was used as a template in the first round of nested PCR. All PCR reactions were carried out with TakaRa LA Taq polymerase (TaKaRa) in 50 µl volume of 1× PCR buffer provided by the manufacturer. The first round PCR contained 30 pmol each of adaptor primer AP1 and sequence-specific primer STK9-77362rev. Cycling condition comprised an initial denaturation step at 94°C for 3 min, followed by 30 cycles of 42 sec at 94°C, 40 sec at 60°C, 3 min at 72°C, and a final extension at 72°C for 10 min. One µl of each first round PCR product was used as a template in the second round PCR reaction, which contained 30 pmol each of nested adaptor primer AP2 and sequence-specific primer STK9-77293rev. Cycling condition for the second round PCR was

Table 14 Primer/Adaptor sequences for genomic walking

Name	Sequence
Adaptor-long	CTAATACGACTCACTATAGGGCTCGAGCGGCCCGCCCGGGCAGGT
Adaptor-short*	AATTACCTGCCCGG
AP1	GGATCCTAATACGACTCACTATAGGGC
AP2	TATAGGGCTCGAGCGGC
STK9-77362rev	CTAAACTGGCAGAAGCACAGG
STK9-77293rev	TACCACACTGATGCTTGGCA

* 5' phosphate modification

essentially the same as the first round, except for annealing temperature adjusted to 57°C. Primers and adaptor sequences (in 5' to 3' orientation) are listed in Table 14.

2.3.8 RT-PCR

Reverse transcription (RT) reactions were performed using the Omniscript reverse transcriptase (Qiagen) and random hexanucleotide primers, according to the manufacturer's instruction. The derived cDNAs were used as templates for following PCR amplifications. To avoid genomic DNA contamination, only intron spanning primer pairs were used in RCR reactions. For studies on *STK9* expression, PCR reactions were performed essentially as described for DNA probe amplification in section 2.3.4. For studies on *ARX* expression, semi-nested PCR was carried out essentially as described for genomic walking in section 2.3.7, with primer pair ARX-1274for and ARX-1752rev in the first round of PCR, and primer pair ARX-1274for and ARX-1696rev in the second round of PCR. Cycle number and extension time were adjusted as necessary. Amplification of *G3PDH* served as a control for the amount of cDNA template in each sample. Sequences of primers (in 5' to 3' orientation) and annealing temperatures are listed in Table 15.

Table 15 Primers for *STK9* and *ARX* expression

Product	Primer name	Primer sequence	T_A
5BP <i>STK9</i> (678 bp)	STK9-96for	TGAAAGTTCCCACCAACCAG	57°C
	STK9-773rev	AAGTAAGAGTTCTGGGGACC	
BP <i>STK9</i> (1029bp)	STK9-811for	TGGGCTGTATTCTTGGGGA	57°C
	STK9-1839rev	TTCTCGTGTCACTGTGTCTG	
<i>ARX</i> (422bp)	ARX-1274for	CGCTCG ACTCCGCTTGGACTG	62°C
	ARX-1752rev	GAGTGGTGCTGAGTGAGGTGA	
	ARX-1696rev	GCAGCCTTTAGCACACCTCCT	
<i>G3PDH</i>	<i>G3PDH</i> for	TGGCGTCGTGATTAGTGATG	57°C
	<i>G3PDH</i> rev	TATCCAACACTTCGTGGGGT	

2.3.9 Denaturing high performance liquid chromatography (DHPLC) analysis

STK9 mutation screening was performed by DHPLC analysis with the WAVE DNA fragment analysis system (Transgenomic). All 21 coding exons of *STK9* (exons 2-21) and the flanking splicing sites were PCR amplified from genomic DNA. Exon 12 was amplified in three overlapping fragments. PCR reactions were carried out with the Amplitaq DNA polymerase (Perkin Elmer) in 50 μ l reaction volume, essentially as described for DNA probe amplification in section 2.3.4. Sequences of primer pairs (in 5' to 3' orientation) and specific amplification conditions (T_A and $MgCl_2$ concentration) are indicated in Table 14. All amplicons were analyzed by DHPLC, with the exception of amplicon 6. Samples of amplicon 6 gave uninterpretable chromatograph patterns in DHPLC analysis and therefore were subjected to direct sequencing. For introducing heteroduplexes in DHPLC analysis, paired PCR products were denatured at 95°C for 5 min and gradually re-annealed from 95°C to room temperature over 45 min. Re-annealed DNA duplexes were injected into the HPLC column (10 μ l per sample) and eluted with a linear acetonitrile gradient at a flow rate of 0.9 ml/min, with a mobile phase consisting of a mixture of buffer A (0.1 M TEAA, with 0.1% acetonitrile) and buffer B (0.1 M TEAA with 25% acetonitrile). Elution condition for each amplicon, including start and end concentration of elution buffer A and B, as well as resolution temperatures, were predicted by the Transgenomic WAVEMAKER software version 4.1 (Transgenomic). DHPLC data analysis was based on visual inspection of the chromatograms. Heterozygous profiles were detected as distinct elution peaks from homozygous wild-type peaks. For each pair of patient or control samples exhibiting exceptional elution profiles, DNA was re-amplified and gel purified using the QIAquick gel extraction kit (Qiagen). Purified PCR products, including samples of amplicon 6, were bidirectionally sequenced using the BigDye terminator cycle sequencing ready reaction kit (PE Biosystems). Samples were analyzed on an ABI 377 DNA sequencer (PE Biosystems), according to the manufacturer's instructions. Sequence data from both orientations were aligned for comparison with corresponding wild-type sequence using SeqMan II software (DNASTAR).

Table 16 Primers and conditions for PCR amplification of *STK9* fragments for DHPLC analysis

<i>STK9</i> amplicon	Forward primer	Reverse primer	Size (bp)	T _A (°C)	MgCl ₂ (mM)
2	TCTTTTGGTGCCA TGTTTTG	TTCATTGCTCAAA ACTCAAGG	156	55	3
3	GAAGCAATGTCA GTATAGCAGAGC	CAACCTGTACATG CCCACAC	201	63	2
4	GAATCCCCAGTC GGAAAAAC	TGACCAGCTAGAT CCCCTTC	209	61	3
5	CAAAGCAGAAG GTGAAATTGG	AAATAAAAGAATC GGGCAAATG	288	56	3
6	TTACGGGCCTAC CTAATTTG	AAATACTCTTAACT TTATTTGATG	229	56	3
7	TCTAACAGTGTC AATCAGGAGAAC	TTCCTTTAAAAGCT ACCTATGTGTTAC	202	60	4
8	CAACTTTGGACT TTGCTATCTTTC	GAATCAGCAGATG TGGAATG	165	59	3
9	CAGTTGCCAAAA TAATCTCTTCC	ATCCATTTTGGGT TTCAGC	257	57	3
10	GTGCACACACAT GTCCTTCC	CAAAAGAATCCAC AAACCAAAG	193	59	3
11	TGACTTTGTAATG TTCTTAACGATCC	CCAACCTCCTCCA CCTACTTG	261	61	3
12a	TGTCAGCTATTG AGGGAAACTG	ATGAATGAGTGGC GGTTCTG	414	61	3
12b	GCCCAGGGACAA AGTACCTC	GAATGTCTGGTTG TGGTTCG	412	61	3
12c	AAATGAGGGAAC GCTGGAC	GCCACCAGATTCA GTCAAGG	328	60	2
13	CATCCCTAGGAA CAGGATGC	GGCAGTAATGATG TTGAACAAATG	205	61	3
14	GCAATATTGTCAT CAATGTGTGG	GAGGAGAGGGGA ACCTGTTG	201	61	3
15	AAGTCCATCAGT GACTTACTTTTTTC	AAGCTCATCCAGA ATTTATTTCAAC	236	60	2
16	TCACACAATGGC AAGAAAATG	TTTGATTGCCAAGT GCAAAG	245	55	3
17	GGCTTCTCAGTG TGCTTATTG	CCGCTCCTCAGGA CAGTTAC	228	62	2
18	TGGTCGCTCTAA CTTGAATCC	GTGGCACTCCTGG TCACAG	314	61	3
19	GTCATGCGCACT CTGCTG	GTCGTTATGGCAG CTTGATG	170	61	3
20	CACTGTCACCTT GGCTTCAG	GGCAATTCCGAGG TACAGC	331	62	2
21	CTGGCAGCTCTG AGTGACC	TTAACAACACAGA TATTTTCAG	285	57	2

2.3.10 Construction of bacterial, yeast and mammalian expression vectors

DNA manipulations were carried out using standard techniques (Sambrook et al. 1989). Various *STK9* coding sequences were amplified by RT-PCR on human fetal brain total RNA (BD Biosciences), essentially as described in 2.3.8. Gene specific primers used in PCR amplification were incorporated with appropriate restriction sites, if necessary, to facilitate cloning. Amplified DNA fragments were digested with relevant restriction enzymes and cloned into the complementary sites of pBluescript II SK vector (Stratagene) as intermediate constructs. Sequence identity of each insert was verified by direct sequencing. All cloned fragments and respective primers for sequence amplification together with restriction sites used for cloning are indicated in Table 17.

The bacterial expression construct pQE-STK9AB was generated by subcloning of the STK9AB fragment from the respective pBluescript II intermediate construct into pQE-30 vector (Qiagen) using the 5'-*Bam*H I and 3'-*Pst* I sites. The yeast two-hybrid pGBKT-STK9-WT bait construct was cloned in two steps. In the first step, the STK9Cterm fragment was subcloned from the respective pBluescript II intermediate construct into pGBKT7 vector (BD Biosciences) using the 5'-*Eco*R I and 3'-*Bam*H I sites. In the second step, the resulting pGBKT7-STK9Cterm construct was digested with *Eco*R I, dephosphorylated with calf intestinal phosphatase (Sigma), and ligated with the STK9Nterm fragment from the respective pBluescript II intermediate

Table 17 Primers and restriction sites used for coding sequence amplification and cloning

Cloned fragment ^a	Restriction site(s)	PCR product ^a	Forward primer	Reverse primer
STK9AB (1781-2711)	<i>Bam</i> H I/ <i>Pst</i> I	<i>STK9</i> (1781-2853)	<u>GTTCAGGATCCTGC</u> TTAGACTTGAATTC TCCCAC	GGTGAATCCGA ATTTCTGAG
STK9Nterm (222-1798)	<i>Eco</i> R I	<i>STK9</i> (222-1840)	ATCT <u>GAATTC</u> ATGA AGATTCCTAACATT GGTAATGT	GTTCTCGTGTCA CTGTGTCTG
STK9Cterm (1793-3311)	<i>Eco</i> R I/ <i>Bam</i> H I	<i>STK9</i> (1820-3311)	ACCAGTAGGTA <u>CTT</u> CCCATC	AGATATGGAT <u>CC</u> CTTGCCCGTCAG TGCCGCATTC

Note—incorporated restriction sites are underlined

a: position corresponding to the *STK9* mRNA sequence NM_003159

construct. The mammalian expression construct pCMV-STK9FL was generated by subcloning the full insert of the pGBKT7-STK9-WT construct into pCMV-Tag 3B vector (Stratagene) using the 5'-*EcoR* I and 3'-*Xho* I sites. The mammalian expression construct pCMV-STK9Nterm was generated by subcloning the STK9Nterm fragment from the respective pBluescript II intermediate construct into pCMV-Tag 3B vector using the *EcoR* I site. For all final constructs, the frame of the insert as well as the ligation junction were confirmed by sequence analysis.

2.3.11 Construction of STK9 kinase-deficient mutant

Substitution of lysine 42 to arginine in the STK9 protein was created by PCR based site-directed mutagenesis. The pBluescript II intermediate construct containing the wild-type coding sequence of STK9Nterm was used as a template. PCR reactions were carried out with *Pfu Turbo* DNA polymerase (Stratagene) with the supplied buffer in the presence of 10 ng of pBluescript-STK9Nterm plasmids and 30 pmol of each of the mutagenic primers. Primer sequences are indicated in Table 18. Cycling conditions included an initial denaturation step at 95°C for 30 sec, followed by 16 cycles of 30 sec at 95°C, 1 min at 55°C, 5 min at 68°C. Subsequently, the PCR product was treated with *Dpn* I to digest the parental DNA template. The nicked DNAs containing the desired mutations were then transformed into the competent *E. coli* DH5 α cells, and nicks in the mutated plasmids were repaired in the host *E. coli* cells. Sequence identity of the resulting pBluescript II intermediate construct containing the STK9Nterm-K42R mutation was confirmed by sequence analysis.

The pGBKT-STK9-K42R and pCMV-STK9-K42R constructs were cloned in a manner similar as their wild-type STK9 counterparts by replacing STK9Nterm-K42R for STK9Nterm in the first step of cloning.

Table 18 Primers used for K42R site-directed mutagenesis

Primer Name	Primer sequence
K42Rplus	GAAATTGTGGCGATCC <u>CGG</u> AAATTCAAGGACAGTG
K42Rminus	GTCCTTGAAT TT <u>CCG</u> GATCGCCACAATTTTCATGTG

Note—nucleotides corresponding to the mutagenic codon Arg 42 are underlined.

2.3.12 Expression of 6 × His tagged STK9 peptides in *E. coli*

The bacterial expression construct pQE-STK9AB was heat shock transformed into the *E. coli* strain M15 (Qiagen) containing the lac repressor pREP4 plasmid. For protein production, cells were grown overnight at 37°C in LB medium containing 50 µg/ml kanamycin and 100 µg/ml ampicillin. 50 ml of overnight culture was used to inoculate 2000 ml of LB medium supplemented with antibiotics as described above. Cultures were grown at 37°C until the OD₆₀₀ reached to 0.6. Protein expression was then induced by addition of IPTG to a final concentration of 1 mM. Cells were grown for another 3 hr before they were harvested by centrifugation at 4000 × g for 20 min (Kendro Laboratory). Cell pellets were resuspended in 50 ml of cold lysis buffer and lysed by sonication (Branson). Cell lysates were clarified by centrifugation at 10,000 g at 4°C for 30 min (Kendro Laboratory). Solutions used in this section are listed in Table 7.

2.3.13 Purification of 6 × His tagged fusion proteins

To purify 6 × His-tagged proteins, 50 ml of the cleared cell lysates supplemented with 20 mM β-mercaptoethanol, 20 mM imidazole, and 0.1% Tween 20 were mixed with 5 ml of 50% Ni-NTA (Qiagen) slurry previously equilibrated with lysis buffer, and incubated 3 hr at 4°C with gentle agitation. The Ni-NTA beads were pelleted by centrifugation at 120 × g for 1 min at 4°C. The beads were further transferred to a polypropylene column (Qiagen), washed two times with 50 ml of washing buffer 1, followed by two times with 50 ml of washing buffer 2. Bound proteins were then eluted with 10 ml of elution buffer. The elution fraction was concentrated to a final volume of 800 µl using centriplus YM-10 centrifugal filter (Amicon), according to the manufacturer's instruction. Solutions used in this section are listed in Table 7.

2.3.14 Immunization

Two New Zealand rabbits were immunized with the purified 6 × His tagged STK9 peptides at BioGenes, Germany. Injection was performed on 1st, 7th, 14th, 28th, 42th and 56th day, each time with 100 µg of the purified 6 × His tagged STK9 peptides.

2.3.15 Yeast two-hybrid library screening

The yeast two-hybrid library screening was carried out using the MATCHMAKER 3 system (BD Biosciences). The yeast MAT α strain Y187 pre-transformed with the human brain cDNA prey library was purchased from BD Biosciences. The pGBKT7-STK9-K42R bait construct was transformed into the yeast MAT α strain AH109, according to the manufacturer's instruction. Yeast mating was performed essentially as described elsewhere (Soellick and Uhrig 2001). Briefly, approximately 5.6×10^7 thawed Y187 cells harboring the cDNA prey library were re-activated in YPDA medium for 4 hr at 30°C, and then mixed with an overnight culture of AH109 cells harboring the pGBKT7-K42RFL construct at a ratio of 1:3. The mixed two yeast strains were suspended in 2 ml YCM (pH 3.5) and incubated for 2 h at 30°C with vigorous shaking. The cells were diluted with 200 ml sterile water and cell clumps were dispersed by sonication (Branson). The cells were then transferred onto a 50 mm membrane filter (0.45 μ m, Millipore) using a filter funnel and incubated for 4.5 hr at 30°C on YCM (pH 4.5) solid medium. Cells were collected with 1 M sorbitol, sonicated, and resuspended in 3 ml of 1 M sorbitol. A total of $\sim 2.5 \times 10^8$ cells were spread onto 30 plates (150 mm diameter) of selective SD medium lacking leucine, tryptophan, histidine and adenine and incubated for 8 days at 30°C. The clones surviving from the nutrition selection were re-streaked on the same SD medium supplemented with 20 μ g/ml X- α -Gal for colorimetric selection. Solutions used in this section are listed in Table 8.

2.3.16 Analysis of prey inserts in yeast positive clones

For all positive yeast clones that survived from nutrition selection and turned blue in the presence of X- α -Gal, inserts of prey plasmids were amplified by colony PCR. Briefly, each isolated yeast colony was dispersed in 50 μ l H₂O by vigorous vortexing. Cell suspensions were subjected to three times freeze/thaw treatment (frozen for ~ 10 sec in liquid nitrogen, and thawed at room temperature) and centrifuged at 4000 \times g for 1 min. Five μ l of the supernatant containing the released plasmids were used as template for PCR. PCR was carried out using the BIO-X-ACT DNA polymerase (Bioline) in the supplied buffer, with forward primer 5'-CGATGATGAAGATACCCAC, and reverse primer 5'-CACGATGCACAGTTGAAGTG. Cycling conditions included an initial denaturation step at 95°C for 4 min, followed by 40 cycles of 40 sec at 95°C, 40 sec at 56°C, 3 min

at 68°C, and a final extension step at 68°C for 10 min. PCR products were gel purified and sequenced as described in section 2.3.9. Sequences were analyzed by BLAST searches against the non-redundant nucleotide database at NCBI.

2.3.17 Preparation of yeast protein extracts

The yeast expression construct pGBKT-STK9-WT, pGBKT-STK9-K42R and control pGBKT-53 (BD Biosciences) were transformed to the yeast cells AH109 according to the manufacturer's instruction. For each transformed strain, a 5 ml overnight culture was prepared from a single isolated colony in SD medium lacking tryptophan. Each overnight culture was used to inoculate 50 ml of the same SD medium, and cells were continued to grow at 30°C until the OD₆₀₀ reached to 0.6. Cells were pelleted by centrifugation at 1000 × g for 5 min (Kendro Laboratory), washed once in sterile H₂O and resuspended in 400 µl of cracking buffer. Cell suspensions were mixed with 300 µl of glass beads, heated at 70°C for 10 min, and vigorously vortexed for 1 min. Cell lysates were clarified by centrifugation at 10,000 g at 4°C for 30 min (Kendro Laboratory). For each sample, 20 µl of protein extracts were used for SDS-PAGE analysis. Solutions used in this section are listed in Table 7.

2.3.18 Cell culture and DNA transfection

COS-7 cells were grown in EMEM medium supplemented with 10% FBS, 2 mM glutamine, 50 µg/ml penicillin and 50 µg/ml streptomycin at 37°C in 5% CO₂. For immunofluorescence studies, cells were grown on glass cover slips. Transient transfections were performed using Polyfect transfection reagent (Qiagen), according to the manufacturer's protocol. Typically, 1 × 10⁵ cells per 35 mm dish were seeded the day before the experiment, and transfected at approximately 50-70% cell confluency, with 1.5-3 µg plasmid DNA and 7 µl Polyfect Transfection Reagent. Following transfection, cells were maintained in medium free of antibiotics.

2.3.19 Immunofluorescence

Immunofluorescence experiments were performed 24 or 48 hr post-transfection. After rinsing once with PEM buffer, cells on cover slips were fixed in 3.7% paraformaldehyde/PEM for 20 min

at room temperature and washed three times with PBS to remove excess paraformaldehyde. Subsequently, cells were blocked/ permeabilized in blocking buffer supplemented with 0.1% Triton X-100 for 1 hr at 37°C, and incubated for 1 hr at 37°C with primary antibodies diluted in blocking buffer. After washing four times with PBS, cells were incubated for another 30 min at 37°C with the appropriate conjugated anti- mouse or anti- rabbit secondary antibody diluted in blocking buffer. Cells were washed 5 times with PBS, and mounted in antifade Vectashield mounting medium (Vector Laboratories), containing one µg/ml DAPI. The anti- STK9 antiserum and anti- c-myc polyclonal antibodies were used at 1:100 and 1:200 dilutions, respectively. The anti- γ -tubulin and anti- c-myc monoclonal antibodies were used at 1:3000 and 1:100 dilutions, respectively. The FITC conjugated goat anti- rabbit antibodies were used at 1:100 dilution, and Cy3 conjugated donkey anti- mouse antibodies were used at 1:2000 dilution. Cells were visualised using either a 63 \times or a 100 \times oil-immersion lens on an Axioskop epifluorescence microscope (Carl Zeiss) equipped with single band pass filters for excitation of green, red, blue and infrared fluorescence (Chroma Technologies). Digital images were captured using a cooled CCD camera (Hamamatsu Photonics) and the ISIS fluorescence image analysis software (MetaSystems). Images were further processed with the PaintShop Pro 8 software (Jasc). Solutions used in this section are listed in Table 6.

2.3.20 SDS PAGE and Western blot analysis

Protein samples were heated at 95°C in protein loading buffer for 5 min and separated by 10-12% SDS-PAGE. For Coomassie blue staining, gels were stained with Coomassie blue staining solution for 4 hr at room temperature, and then incubated with destaining solution until background removed. For Western blot analysis, proteins were transferred from gels to microporous polyvinylidene difluoride (PVDF) membrane (Roche) using a semi-dry transfer unit (Bio-rad) at 15 V for 30-45 min. After transfer, blots were incubated with blocking buffer for at least 1 hr at room temperature, and then incubated overnight at 4°C with the first antibody diluted in blocking buffer. Blots were washed three times in PBST, and incubated for 1.5 hr at room temperature with HRP conjugated anti- rabbit IgG or anti- mouse Ig. Following 5 times washes in PBST, blots were incubated with ECL Western blotting reagent (Amersham) and exposed to Fuji

MATERIALS, SUBJECTS AND METHODS

X-ray film. The anti- STK9 serum was used at 1:6000 dilution. The anti- c-myc monoclonal antibodies were used at 1:5000 dilutions. The HRP conjugated anti- mouse and anti- rabbit antibodies were used at 1:2000 dilution. Solutions used in this section are listed in Table 6.

3 RESULTS

3.1 Disruption of serine/threonine kinase 9 gene in a female patient with severe infantile spasms, global developmental arrest and profound mental retardation (patient 1)

Disease associated chromosomal rearrangements, especially balanced chromosomal translocations, inversions and micro-deletions, form a unique resource in bridging genotypes and phenotypes (Bugge et al. 2000). Fine mapping of chromosomal breakpoints in these patients has been instructive in the positional cloning of many disease genes. In order to search for new XLMR genes, we set out with an X;autosomal translocation in a patient with severe infantile spasms, global developmental arrest and profound mental retardation (designated patient 1).

Infantile spasms (IS), one of the main neurological features presented in this patient, is an age-specific epileptic encephalopathy with an incidence rate of about 2-5 per 10,000 live births (Wong and Trevathan 2001; Koehn and Duchowny 2002). The disease typically begins in the first year of life, with peak age of onset at 4-6 months. Clinically, epileptic spasms occur in clusters, consisting of a sudden and brief axial muscle contraction involving the neck, the trunk, or the extremities. Diagnostically, interictal electroencephalograms (EEG) show the characteristic pattern of hypsarrhythmia, a massive disturbed pattern consisting of multi-focal spikes and high-voltage slow waves in all cortical areas. Moderate to severe mental retardation is found in 60-70% of patients following the onset of infantile spasms. The triad of infantile spasms, hypsarrhythmia, and mental retardation is referred to as infantile spasms syndrome or West syndrome.

Despite its distinctive clinical features, IS is an etiologically heterogeneous disease. About 80% of the cases are symptomatic, and can be due to a wide variety of causes, including neurocutaneous diseases (especially tuberous sclerosis), metabolic diseases (such as phenylketonuria), cortical dysplasia, tumor, porencephalic cyst, trauma, birth hypoxia, central

nervous system infections, and stroke (Shields 2000). In the remaining 20% of cases, the so-called idiopathic ones, the etiology is still largely unknown. Recently, mutations in the X-linked *ARX* gene, an ortholog of the drosophila aristaless-related homeobox gene, have been found in four families where IS segregated in an X-linked pattern (Stromme et al. 2002).

To identify the molecular cause of the severe phenotype in patient 1 who carried an X;autosomal translocation, we cloned the translocation breakpoints on both chromosomes.

3.1.1 Clinical investigation of patient 1

Patient 1 (Fig. 4) was the second child of healthy unrelated parents. The pregnancy was normal, only complicated by bleeding in the second month. She was delivered 10 days after term with Apgar scores 9 at one minute and 10 at five minutes. Her birth weight (3410g), length and head circumference were normal. She showed mild hyperexcitability at the age of 3 weeks, and abnormal turning of the eyes at the age of 6-8 weeks. Initially motor development was normal and EEGs gave normal results. At the age of 3 months, the EEG showed hypsarrhythmia and IS was diagnosed. At the age of 4 1/2 months, tonic-clonic seizures became more frequent and motor retardation and generalized hypotonia were evident. Initially, the seizures responded to clonazepam, but from the age of 5 months anti-epileptic drugs could no longer control them. With time, the seizures evolved into tonic seizures and after the age of 7 years, dyskinesias with short choreatiform or myoclonic-like movements also appeared. During the following years the frequency of seizures diminished, but there was no developmental progress. The patient had slightly dysmorphic features with hypertelorism, high nasal bridge, large, but narrow and not well-modeled ears, a low posterior hairline and a simian crease. Eye movements were uncoordinated and there was no fixation to light or movement. The fundi were pale with fine pigmentation. Cranial magnetic resonance imaging (MRI) at age 6 years showed ventricular enlargement and hypoplasia of corpus callosum, cerebellum and white matter. There was a mild conduction defect (43m/s) in the median nerve, but

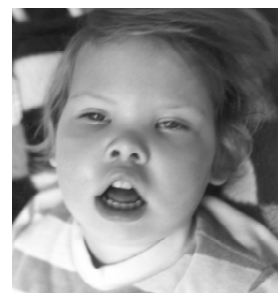


Figure 4. Patient 1 at the age of 3 years

normal values in the lower limbs. Urine amino acids and organic acids, plasma lactate and pyruvate were normal, and GM-1 and GM-2 gangliosidosis were excluded. At age 7 years and 4 months, length was 126 cms (50th centile), weight was 17,4 kg (<3rd centile) and head circumference was 49 cms (3rd centile). She died at the age of 17 years.

3.1.2 Cytogenetic investigation of the translocation breakpoints

Patient 1 carried a balanced translocation between the distal short arm of chromosome X and the distal short arm of chromosome 7. Her karyotype was 46,X,t(X;7)(p22.3;p15) (Fig. 6A). The translocation was not detected in her parents and thus was considered as *de novo*.

We first focused on the X chromosomal breakpoint (Fig. 5). Several rounds of FISH with YAC clones from the Xp22 region were performed to narrow the breakpoint region. YAC 939h7 was identified as breakpoint-spanning clone, giving split signals on both derivative chromosomes

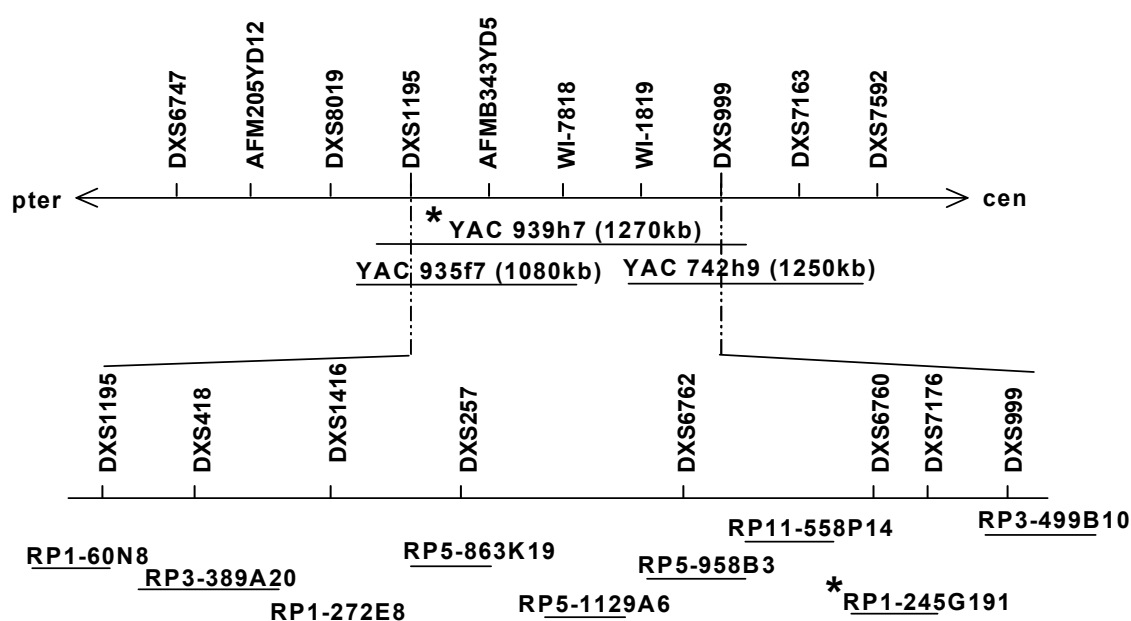


Figure 5. Schematic map of the Xp22.3 breakpoint region in patient 1. The upper panel shows the YAC clones in Xp22.3, and the lower panel shows the BAC and PAC clones in the DXS1195-DXS999 interval in Xp22.3. The breakpoint-spanning YAC and PAC clones are indicated by an asterisk (*).

(Fig. 6B), whereas YAC 935f7 gave a signal only on der(7) and YAC 742h9 only on der(X). The results placed the X chromosomal breakpoint within the interval between markers DXS1195 and DXS999 (Fig. 5). Subsequent FISH with BAC and PAC clones selected from this region further narrowed the breakpoint. RP1-245G19 (GenBank accession number Z92542) was identified as breakpoint-spanning PAC clone, showing split signals on both derivative chromosomes (Fig. 6C).

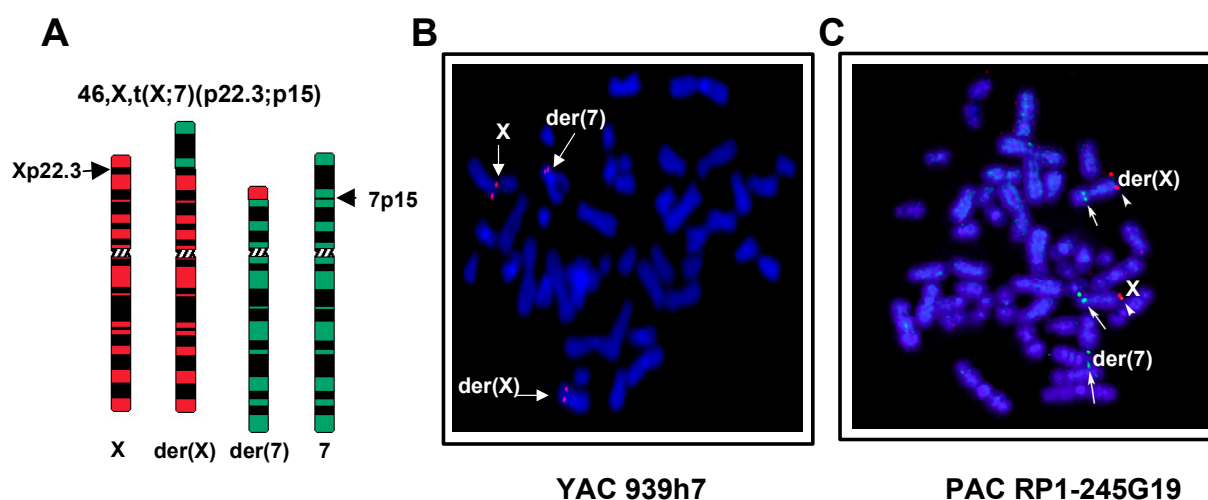


Figure 6. FISH mapping of the Xp22.3 translocation breakpoint in patient 1. A, Ideograms showing the translocation breakpoints in patient 1 with 46,X,t(X;7)(p22.3;p15). B-C, The breakpoint-spanning YAC and PAC clones identified by FISH. Metaphases of patient 1 were hybridized with YAC 939h7 (red in B), or PAC clone RP1-245G19 (green in C), The split signals (arrows) on the der(X) and the der(7) indicated that they are breakpoint-spanning. Co-hybridization with an Xptel-specific cosmid probe (red) was used in C to indicate the normal and derivative X chromosomes (arrowheads).

3.1.3 Molecular investigation of the translocation breakpoints

Further localization of the X chromosomal breakpoint was achieved by Southern blot hybridization. Genomic DNAs from patient 1 and a normal female control were digested with *EcoR* I, *EcoR* V, or *Hind* III enzymes, gel separated and hybridized with probes derived from sequence of the breakpoint-spanning PAC clone. A probe generated by PCR and corresponding to bps 76261-77382 of PAC RP1-245G19 detected aberrant fragments from both derivative chromosomes in each independent digest of the patient DNA but not control (Fig. 7), indicating

that this probe spans the breakpoint (for principle, see Fig. 2B). In the patient DNA, the probe detected a normal fragment at 5.5 kb, and two aberrant fragments at 4.2 kb and 7.4 kb in the *EcoR*I digest, a normal fragment at 17.3 kb, and two aberrant fragments at 10.0 kb and 12.2 kb in the *EcoR*V digest, and a normal fragment at 13.6 kb, and two aberrant fragments at 7.8 kb and 17.8 kb in the *Hind* III digest.

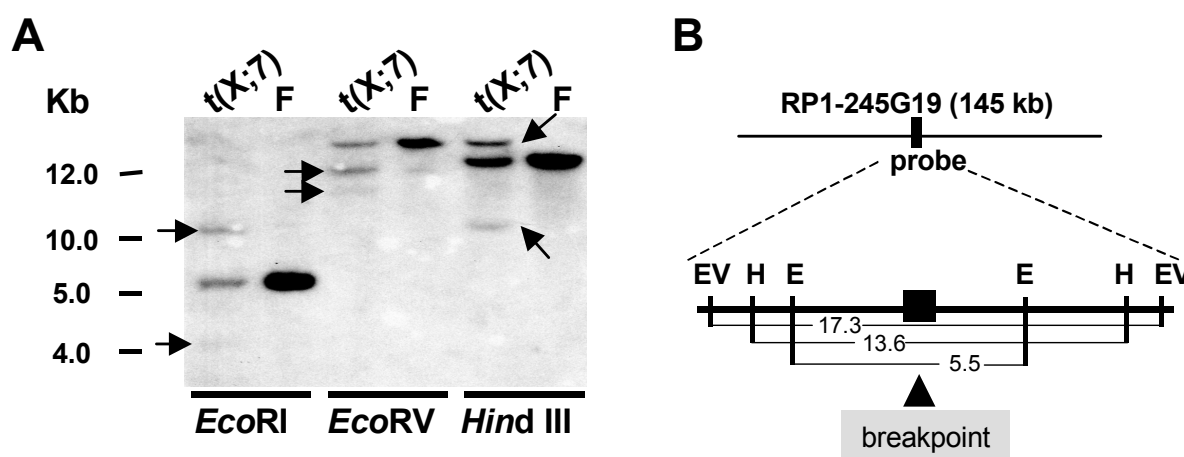


Figure 7. Localization of the Xp22.3 breakpoint region by Southern blot hybridization. A, Southern blot analysis with the probe spanning the breakpoint. DNAs from the patient [(t(X;7))] and a female control (F) were digested with the indicated enzymes. The probe corresponding to bps 76261-77382 of clone RP1-245G19 detected two aberrant fragments (arrows) in each digest of the patient but not in the control DNA, indicating that it spans the breakpoint. B, Diagram depicting the genomic structure around the probe used in A. The upper panel shows the relative location of the probe within the PAC RP1-245G19. The lower panel shows a restriction map of the area surrounding the probe (solid rectangle). Position and size of the normal restriction fragments detected by the probe are indicated (E = *EcoRI*, EV = *EcoRV*, H = *HindIII*).

The precise location of the translocation breakpoints on both chromosomes was determined by genomic walking (for principle, see Fig. 2C). Genomic DNA from patient 1 was digested with *Dra* I, *EcoR* I, *Hae* III, or *Ssp* I, and the restriction fragments were ligated to the adaptor oligos at both ends. The aberrant der(X) junction fragment was amplified by nested PCR, with adaptor primer AP1 and sequence specific primer STK9-77362rev in the first round PCR, and adaptor primer AP2 and sequence specific primer STK9-77293rev in the second round PCR. From *EcoR* I digested DNA, a fragment of approximate 1000 bp was amplified. Sequencing of the specific PCR

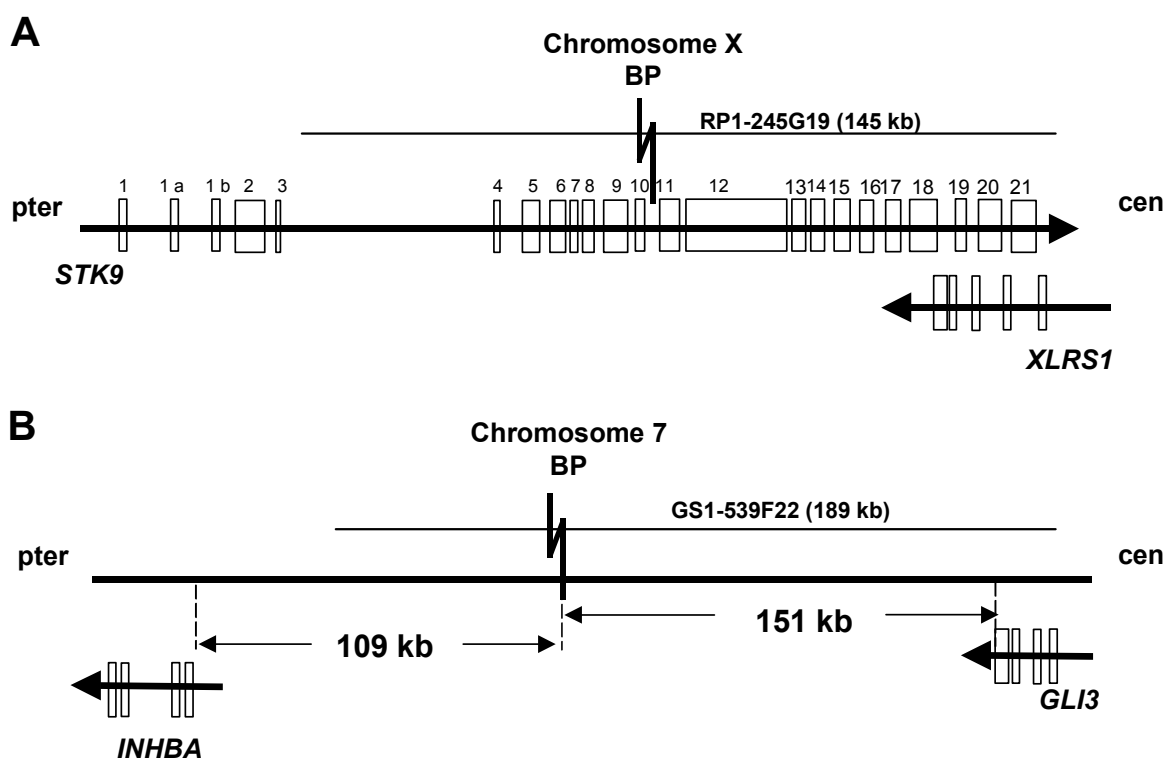


Figure 9. Diagram depicting the genes in the regions around the translocation breakpoints. A, On the X chromosome, the breakpoint-spanning clone RP1-245G19 contains exons 4-21 of the *STK9* gene and the last five exons of the *XLRS1* gene. The X-chromosomal breakpoint of patient 1 disrupted *STK9* in intron 10. B, On chromosome 7, the breakpoint-spanning clone GS1-539F22 contains part of the *GLI3* gene. No transcript was found disrupted by the breakpoint. Exons of the genes are shown in boxes (not to scale). Arrows across the exons indicate transcriptional direction. BP = breakpoint.

STK9 has been isolated in the course of a transcriptional mapping effort in the Xp22 region (Montini et al. 1998). The genomic structure of the *STK9* gene was revisited by aligning the cDNA and EST sequences (NM_003159, AL704691, and BI559845) with the genomic sequences (Z92542 and AL109798); several discrepancies were found related to the exon numbers and sizes given by Montini et al. (Y15057) (Table 19). The translational start site is in exon 2 and the first three exons (exons 1, 1a and 1b) form the 5' untranslated region (5'UTR). EST sequences in the Genbank database suggest that there are at least two *STK9* isoforms, which are different in their 5' UTR (Fig. 10A). The isoform containing exon 1 (designated isoform I) is ubiquitously expressed (Montini et al. 1998), while the isoform containing exons 1a and 1b (designated isoform II) is

transcribed at a very low level in human fetal brain and testis (supporting EST and mRNA sequences: AL704691, BI559845 and BC036091).

Table 19 Exon numbers, splice junction sequences and exon sizes of the *STK9* gene

Exon No.	3' Splice Site	5' Splice Site	Exon Size
1		ACTCGGCGGG <u>gt</u> gagtagtc	111
1a		GGAAGTTGAG <u>gt</u> atcatatc	73
1b	tggtgtcc <u>ag</u> CTGTACTCTC	CTCCCTTCAG <u>gt</u> actctcct	49
2	tttttttc <u>ag</u> GGAGTCATTT	GTAGGTGAAG <u>gt</u> aagttgga	126
3	tttattata <u>ag</u> GAGCCTATGG	CAGACACAAG <u>gt</u> caagtacat	35
4	tcccttgca <u>ag</u> GAAACACATG	GACAGTGAAG <u>gt</u> agatatat	46
5	tacattctagAAAATGAAGA	TGTTGAAAAA <u>gt</u> aagtcatt	137
6	taatTTTT <u>ag</u> AATATGCTCG	GTCCATCGAG <u>gt</u> gagtatga	121
7	gacactcc <u>ag</u> ATATAAAACC	TGTGACTTTG <u>gt</u> aagttaaa	60
8	tatctttc <u>ag</u> GTTTTGCTCG	TCTTACTTGG <u>gt</u> gagttacc	91
9	tatTTTTc <u>ag</u> CGCTCCCTAT	TGGGCTCCG <u>gt</u> aagaggtt	190
10	tgtctcac <u>ag</u> TTTCCAGCTG	CCTAATGAAG <u>gt</u> aaggccaa	81
11	atctccta <u>ag</u> AATTTACTGA	TGTCTAATAG <u>gt</u> aaatattc	152
12	tttaacata <u>ag</u> AAACCAAGCC	GTCACCCCAG <u>gt</u> acagttga	967
13	ttacttcc <u>ag</u> CCTGGAGAAC	GAAGTCTGAG <u>gt</u> atgtcaca	102
14	cctgcctc <u>ag</u> GGTGGACTGT	TTTTACAGAG <u>gt</u> aagccac	106
15	ctttattc <u>ag</u> TGCCATCTCC	TCGATCCATG <u>gt</u> gagcattt	124
16	tctcattt <u>ag</u> GAAAAGTCCT	ATCTCAAACAg <u>gt</u> aagtagat	100
17	tttgctct <u>ag</u> GTACCCAATT	GCAGACCCAA <u>gt</u> gagtgat	120
18	tttctttc <u>ag</u> AGCCAGCCAT	CAGCTGCCAG <u>gt</u> cagatgga	217
19	caccaact <u>ag</u> ACGGTGGATG	GAACAACAAG <u>gt</u> agagtctg	84
20	tatTTTTcc <u>ag</u> GAGAATACTT	CAGCAATCCG <u>gt</u> aagcagag	183
21	tgctttcc <u>ag</u> GGTTCTCTTT		198

Note— Lowercase letters indicate intron sequence; uppercase letters indicate exon sequences; and consensus dinucleotides in exon-intron boundaries are underlined.

To determine the expression status of *STK9* in the patient, RNA from the patient-derived fibroblast cell line was reverse-transcribed and amplified with *STK9* gene specific primers. RT-PCR with the primer pair 5' to the breakpoint (STK9-96for and STK9-773rev, see Table 15) resulted in a product of 678 bp in both the patient and a control, whereas RT-PCR with the breakpoint-spanning primer pair (STK9-811for and STK9-1893rev, see Table 15) resulted in a product of 1029 only in the control (Fig. 10B). This result showed that expression of *STK9* was disrupted by the X-chromosomal breakpoint in patient 1, and that *STK9* is subjected to X inactivation. The truncated *STK9* transcripts containing the region of exons 1-10 would encode a protein of 275 amino acids.

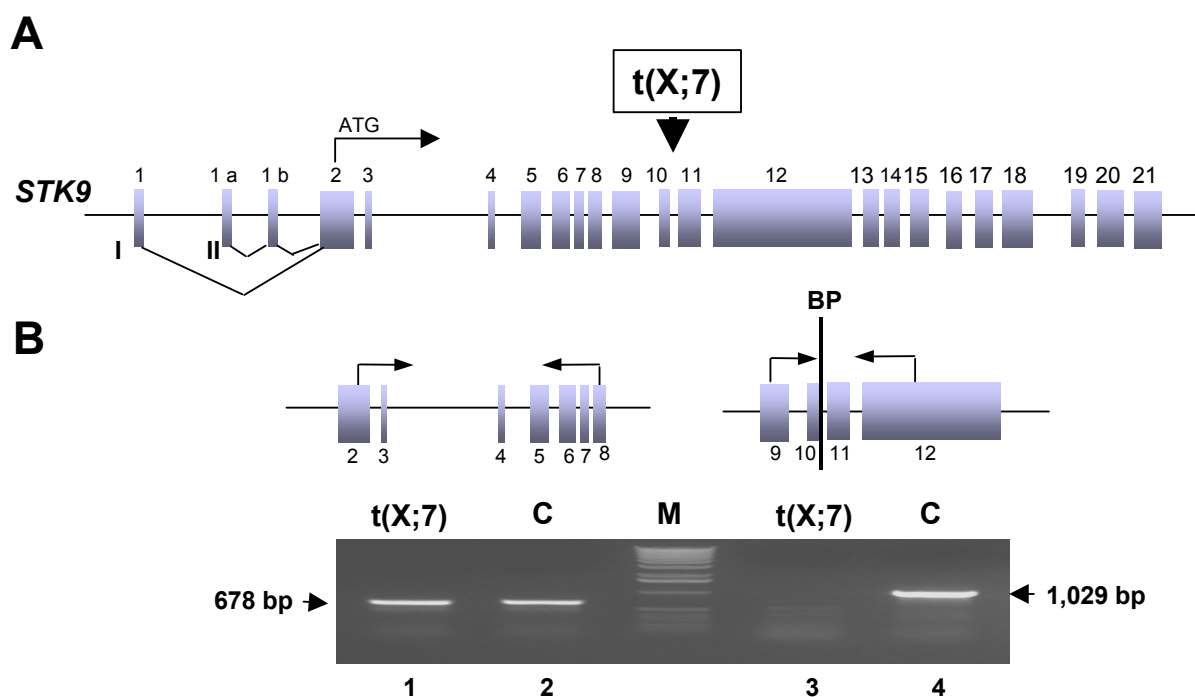


Figure 10. Expression of *STK9* in patient 1. A, Diagram depicting the two *STK9* isoforms, which are different in their 5'UTR. Isoform I contains exon 1, and isoform II contains exons 1a and 1b. The relative location of the X-chromosomal breakpoint is indicated on top. B, RT-PCR for *STK9* expression analysis in the patient-derived fibroblast cell line. The relative position of the primers and the breakpoint are depicted on top. In lanes 1 and 2, RT-PCR with the primer pair upstream of the breakpoint (primers STK9-96for and STK9-773rev, see Table 15) resulted in a specific RT-PCR product of 678 bp in both the patient [t(X;7)] and a control (C). In lanes 3 and 4, RT-PCR with the primer pair spanning the breakpoint primers (STK9-811for and STK9-1839rev, see Table 15) resulted in a specific RT-PCR product of 1029 bp in the control but not in the patient (M = marker).

ARX, the human ortholog of the drosophila aristaless-related homeobox gene, has recently been found to be implicated in X-linked infantile spasms families, too (Stromme et al. 2002). This gene is separated from *STK9* by ~ 6 Mb of genomic sequence, as determined from the UCSC Genome Browser (*STK9* is at position ~18.4 Mb and *ARX* at position ~24.3 Mb). To evaluate the expression status of the *ARX* gene in patient 1, RNA from the patient-derived fibroblast cell was reverse-transcribed and amplified with *ARX* gene specific primers. Semi-nested PCR with primer pair ARX-1274for and ARX-1752rev in the first round of PCR, and primer pair ARX-1274for and ARX-1696rev in the second round of PCR amplified a specific PCR product of 208 bp in both the patient and a control (for primer sequences, see Table 15). Therefore, a position effect of the breakpoint on the expression of *ARX* was considered as being unlikely.

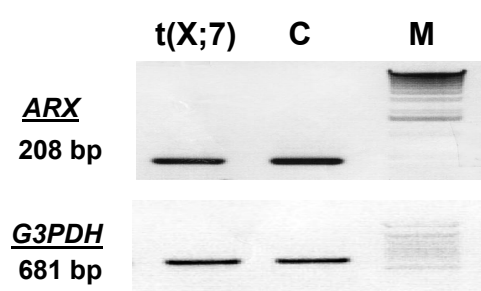


Figure 11. *ARX* expression analysis in patient 1 with RNAs from the patient-derived fibroblast cell line. RT-PCR with the *ARX* gene specific primers (see section 2.2.8) obtained a specific PCR product of 208 bp in both the patient [t(X;7)] and a control (C). Amplification of the *G3PDH* gene served as a control for the amount of cDNA template (M = marker).

3.2 *De novo* mutations in *STK9* are associated with a severe form of atypical Rett syndrome

The disruption of *STK9* in patient 1 with a *de novo* balanced X;autosomal translocation strongly suggests that the severe phenotype present in this patient was caused by altered *STK9* expression. Therefore we further investigated the possible role of *STK9* in MR and related disorders. Based on neurological features of patient 1, including early-onset infantile spasms, global developmental arrest, and profound mental retardation, three cohorts of patients with related neurological symptoms were selected for *STK9* mutation analysis. The first panel included 96 male patients with idiopathic infantile spasms, in whom no mutation had been identified in the *ARX* gene. The second group contained index patients from 150 families with XLMR, in which linkage data were not available due to small family size or where a linkage interval of Xp22 could not be excluded.

The third panel included 32 index patients (7 males and 25 females) with Rett syndrome-like features. Rett syndrome (RTT, MIM 312750) is a progressive neurodevelopmental disorder affecting almost exclusively girls. The classic form of RTT is characterized by apparently normal development until age 6 to 18 months, followed by neurological developmental arrest and regression (Hagberg et al. 1983). Affected girls gradually lose their acquired skills such as speech and purposeful hand use, display decelerating head growth and autistic features, and develop irregular breathing patterns, seizures, ataxia, and stereotypical hand wringing. The increase in cognitive and motor impairments may continue for many years before reaching a plateau; this progression typically leads to profound mental retardation. In addition to classic RTT, atypical cases of milder or more severe forms have been delineated (Hanefeld 1985; Goutieres and Aicardi 1986; Hagberg and Skjeldal 1994). Patients with a milder variant may retain some speech and motor functions, whereas those with more severe forms develop the disease shortly after birth, and often have congenital hypotonia and infantile spasms. In approximately 80% of typical RTT patients, the disease is caused by mutations in the methyl-CpG-binding protein 2 gene (*MECP2*), but only 20-40% of atypical RTT syndrome patients have been shown to carry a mutation in *MECP2* (Buyse et al. 2000; Cheadle et al. 2000; Bourdon et al. 2001). These findings indicate the

possible presence of another, yet undetected gene on the X chromosome that may play a role in both forms. As the phenotype exhibited in patient 1 is reminiscent of the neonatal onset encephalopathy present in several patients with a severe form of atypical RTT (Schanen et al. 1998; Villard et al. 2000b; Zeev et al. 2002), a panel of RTT-like patients with no mutation in *MECP2* was included in the *STK9* mutation screening.

3.2.1 Mutation screening in the coding region of *STK9*

Results of mutation screening in the three cohorts of patients are shown in Table 20. We identified seven novel nucleotide exchanges; four of them were shown to be polymorphisms. The c.2372A>C change was present in eight patients with infantile spasms, three patients with XLMR,

Table 20 Summary of *STK9* sequence alterations in three panels of patients with MR

Exon	Nucleotide exchange ^a	Amino acid exchange ^b	No. of patients with exchange	No. of control X chromosomes
4	IVS4+17A>G ^c	N/A	3 patients with XLMR 1 patient with RTT-like features	2/267
7	c.455G>T	p.C152F	1 patient with RTT-like features	0/427
8	c.525A>T	p.R175S	1 patient with RTT-like features	0/427
12	c.1330C>T	p.R444C	1 patient with XLMR	0/405
16	c.2372A>C	p.Q791P	8 patients with IS 3 patients with XLMR 5 patients with RTT-like features	3/96
21	c.3003C>T ^c	p.H1001H	3 patients with XLMR 1 patient with RTT-like features	2/267
21	c.3084G>A ^c	p.T1028T	3 patients with XLMR 1 patient with RTT-like features	2/267

Note— Potentially disease-causing mutations are highlighted in boldface.

a GenBank accession number NM_003159

b GenBank accession number NP_003150

c Nucleotide changes that segregated in a rare conserved haplotype

N/A= not applicable

five patients with RTT-like features, and three out of 96 control X chromosomes. The other three nucleotide exchanges, IVS4+17A>G, c.3003C>T and c.3084G>A, forming a rare conserved haplotype, were found in three patients with XLMR, one patient with RTT-like features, and two out of 267 control X chromosomes. Of particular importance, we found three sequence variants that were not present in over 400 control X chromosomes. A c.1330C>T nucleotide change was identified in the index patient of a family with XLMR. However, DNAs from other members in this family were not available for performing co-segregation studies. c.455G>T and c.525A>T nucleotide exchanges were found in index patients with RTT-like features. DNAs from the nuclear family members allowed us to further characterize these sequence variants.

3.2.2 Patient 2 with p.C152F missense mutation

In patient 2 (Fig. 12B), a c.455G>T nucleotide exchange (GenBank accession number NM_003159) was found in exon 7, resulting in a cysteine-to-phenylalanine substitution at position 152 (p.C152F) of the STK9 protein (GenBank accession number NP_003150) (Fig. 12C). The corresponding sequence of the parents' DNA did not show this change (Fig. 12C), strongly suggesting that the missense variant present in the patient is a new mutation.

Patient 2 is a female born by spontaneous delivery after an uneventful pregnancy. Her parents are healthy and non-consanguineous, and she has a healthy sister. Her birth weight was 3500 g and length was 53 cm. The neonatal period was normal. At five weeks of age she had blitz-nick-salaam-like seizures. At three months of age her EEG was normal. Therapies with vigabatrin, phenobarbital, and carbamacepin had no effect. Following implantation of a vagus nerve stimulator at the age of 4.5 years, the parents reported that seizures occurred less frequently. At re-evaluation at 5 years of age, the patient weighed 13.9 kg (3rd centile), her length was 115 cm (75th centile), and her head circumference was 48.8 cm (10th centile). EEG showed abnormal and generalized theta rhythm, but neither focal disturbances nor any patterns typical for epilepsy was observed. She was very hypotonic, was unable to crawl, and could not sit without support. She understood simple words but could not speak.

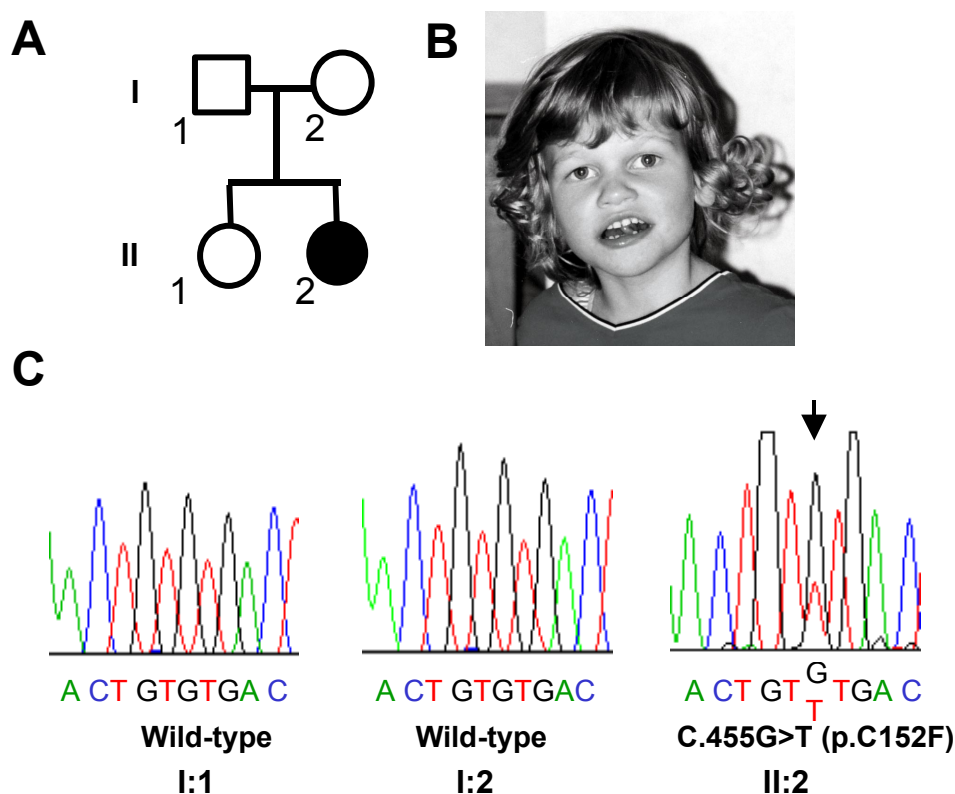


Figure 12. *STK9* mutation c.455G>T (p.C152F) in patient 2. A, Family pedigree of patient 2. B, Patient 2 at the age of 6.5 years. C, Sequence chromatograms from family members I:1, I:2, and the proband (II:1). The affected nucleotide is indicated by an arrow.

3.2.3 Patients 3 and 4 with p.R175S missense mutation

In patient 3 (Fig.13B), a c.525A>T nucleotide change was found in exon 8, changing an arginine to serine at position 175 (p.R175S) of the *STK9* protein. The patient is one of the monozygotic twins born to healthy unrelated parents. Her birth weight was 3420 g, and the pregnancy was normal. The mother was on treatment for hypothyroidism and had had two previous miscarriages. The patient developed IS at two months of age, which disappeared at 6 months of age, but later in life absence seizures were repeatedly observed. During infancy, severe psychomotor retardation was noticed (mental scale of Bayley: 2 months at the age of 12 years). She was able to sit without support at 3 years of age, and at age 10 she was able to walk a few steps with support. She never developed speech. There was general hypotonia, mild ataxia and stereotypic movements of the hands. Intentional activity or eye contact was absent. Mood swings were noticed with alternating

bursts of crying and laughter, as well as episodes of hyperventilation. On further follow-up she developed progressive sinistro-convex thoraco-lumbar kyphoscoliosis and hypertonia leading to flexion contractures of the arms. Growth parameters for height, length and head circumference are within the 5th to 25th centile. Her adult head circumference is 54.5 cm. Now aged 41 years, she is wheelchair-bound and still presents with stereotypic hand movements, mood swings and episodes of hyperventilation. Additional examinations including brain scan, ophthalmological and hearing tests, routine blood analyses, thyroid hormone tests, metabolic screening, and karyotype analysis were normal. Repeated EEG analyses exhibited diffuse slow theta activity but typical epileptiform abnormalities were not observed.

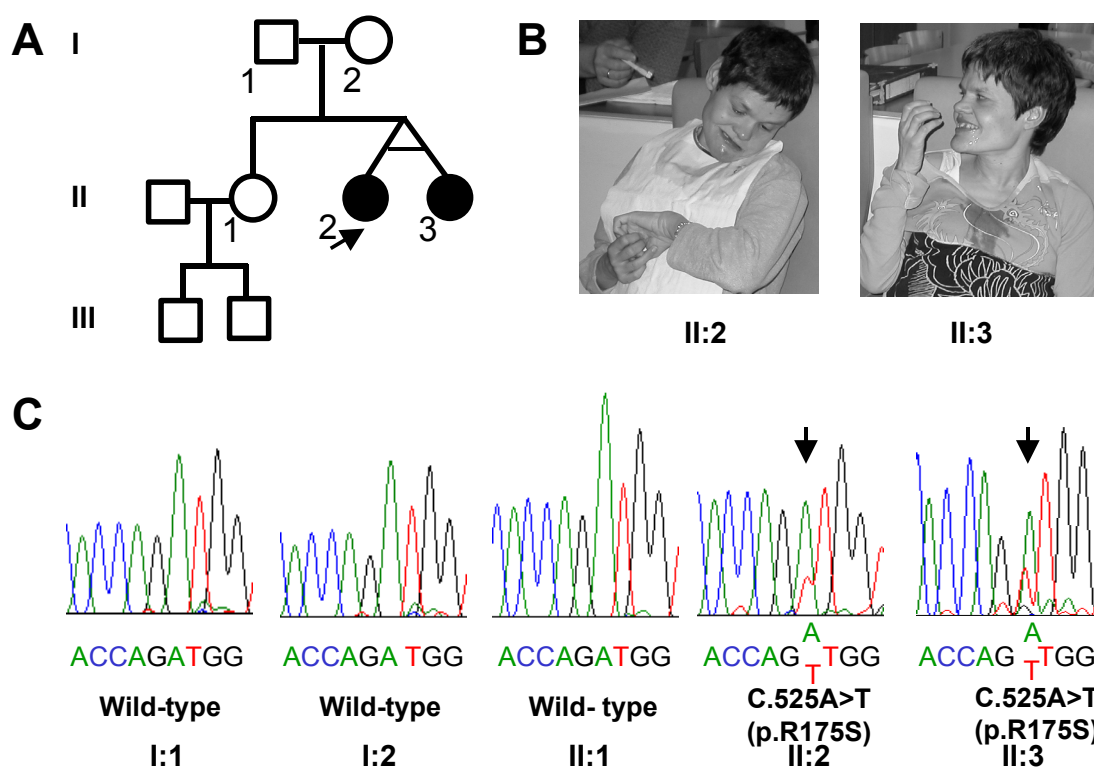


Figure 13. *STK9* mutation c.525A>T (p.R175S) in patient 3 and 4. A, Family pedigree of the affected twin sisters. The proband, patient 3 (II:2), is indicated by an arrow. B, The affected twin sisters at the age of 41 years. Note stereotype hand movements in patient 3 (II:2). C, Sequence results from the family members. From left to right: father (I:1), mother (I:2), unaffected sister (II:1), patient 3 (II:2), and patient 4 (II:3). Affected nucleotide is indicated by an arrow.

Patient 4, the monozygotic twin sister of patient 3, exhibits a similar phenotype (Fig. 13B); PCR amplification and sequence analysis of exon 8 confirmed the presence of the same mutation (Fig. 13C). Like her twin sister, she developed IS at ten weeks of age, which disappeared at 6 months of age. During infancy, severe psychomotor retardation was noticed, although the impairment of her motor development was less severe than that in her sister. Her walk is characterized by atactic movements and impaired coordination, but at 8 years of age she was able to walk alone. Like her sister, she exhibited stereotypic movements of the hands, and made little eye contact, and demonstrated essentially no interaction with her environment. Mood swings and hyperventilation episodes were also present. On further follow-up she presented with an S-shaped dorso-lumbar scoliosis and hypertonia, as well as flexion contractures of the arms, knees and achilles tendons. Growth parameters for height, length and head circumference are within the normal range (5th to 15th centile), and her adult head circumference is 54 cm. Now at the age of 41 years, she is still able to walk some steps with support. Both sisters also exhibit abdominal distention because of excessive air-swallowing.

The mutation identified in the twin sisters was neither present in their healthy parents nor in an unaffected sister (Fig. 13C), suggesting that it occurred *de novo*.

3.2.4 Sequence analysis of p.C152F and p.R175S missense mutations

The predicted STK9 protein contains a conserved serine/threonine kinase domain at the N-terminus. Database searches in the GenBank showed that STK9 vertebrate orthologs are present in mouse (GenBank accession number XP_356367) and in Fugu (Brunner et al. 1999) (GenBank accession number AAD28798), sharing an overall sequence identity of 95.8% and 51.7% with human STK9, respectively. The serine/threonine kinase domain is identical in human and mouse and highly similar (82%) between human and Fugu (Fig. 14A). In addition, the conserved serine/threonine kinase domain of STK9 shares sequence homology with a number of protein kinases of the CMGC group (Hanks and Hunter 1995). Among them a subgroup of cdc2-related protein kinases, including p53 KKIAMRE (CDKL2) (Taglienti et al. 1996), p42 KKIALRE (CDKL1) (Yen et al. 1995) and NKIAMRE (CDKL3) (Midmer et al. 1999), is more closely

related to STK9 than the others, with an overall sequence identity from 49% to 43%. Members of the CDK family and MAPK family in the CMGC group show slightly lower homologies to STK9, with an overall sequence identity from 41% to 33% (Fig.14A).

The C152F and R175S missense mutations identified in the patients with RTT-like features are located within the protein kinase domain. Both are conserved in mouse and Fugu STK9 orthologs, and are also present in the closely related subgroup of cdc2-related protein kinases (Fig. 14B). Of significant importance, the mutated amino acids both lie in critical protein regions that are important for proper kinase function. The Cys152 amino acid in kinase subdomain VII lies immediately N-terminal to the conserved Asp-Phe-Gly motif (Fig. 14B), one of the kinase signatures involved in phosphotransfer (Hanks and Hunter 1995). Although in other unrelated protein kinases, other small amino acids, such as alanine, glycine, serine or threonine may be found at this position, none of the protein kinases present in the GenBank database contains a phenylalanine residue here. The substitution of a cysteine with a phenylalanine residue would likely alter the proper orientation of the adjacent Asp-Phe-Gly motif and thus impair the catalytic activity of the protein. The other mutated amino acid, Arg175, lies within kinase subdomain VIII (Fig. 15), which is important for substrate recognition (Hanks and Hunter 1995). The sequence context of this amino acid (YVATRWYR) is highly conserved in proline-directed protein kinase subfamilies such as MAPKs and CDKs, and is required for the selectivity towards substrates containing a proline at the P+1 position relative to the phosphate acceptor (Russo et al. 1996; Canagarajah et al. 1997). Exchange of a positively charged arginine to an uncharged serine would likely influence substrate binding specificity.

3.3 Generation of a polyclonal antibody against STK9 protein

Results from positional cloning and mutation analysis demonstrated that alterations in *STK9* cause a wide range of clinical features, varying from early-onset encephalopathy to atypical RTT syndrome with early-onset seizures. To explore the molecular and cellular function of STK9, which will ultimately shed light on the pathogenic process in these associated diseases, we generated a polyclonal antibody that specifically recognizes STK9 protein. Recombinant STK9 peptides for immunizing animals were prepared in a bacterial expression system, and were then purified with immobilized-metal affinity chromatography.

3.3.1 Expression of 6×His tagged STK9 peptides in *E. coli*

To avoid cross-reaction with other protein kinases, a fragment outside the serine/threonine kinase domain corresponding to amino acids 520-830 of the STK9 protein was chosen for expression in *E. coli* (Fig. 15A upper panel). The respective coding sequence was amplified and subcloned into the bacterial expression vector pQE-30 (Qiagen), which harbors a 6 × His tag in 5' to the cloning site, and a promoter-operator element consisting of a phage T5 promoter and two lac operators (Fig. 15A lower panel). The resulting bacterial expression construct pQE-STK9AB was transformed into M15 *E. coli* host cells, and expression of the 6×His tagged STK9 peptides was induced by addition of isopropyl-β-D-thiogalactoside (IPTG). To evaluate protein expression, bacterial cells were harvested 3 hr after induction with IPTG, and total cell lysates were examined on Western blots using an anti- 6×His antibody. As shown in Fig. 15B, the antibody detected two strong bands at around 35 kDa and two weak bands around 25 kDa in the lysates of the cells that were transformed with the pQE-STK9AB construct, but not with the control pQE-30 vector. Among the four detected bands, the highest one corresponds to the molecular mass predicted from the sequence (ca. 35 kDa). The three lower bands were most likely proteolytic degradation forms of the 6 × His tagged recombinant peptides (see below). This result indicated that the 6 × His tagged STK9 peptides were expressed in the bacterial expression system.

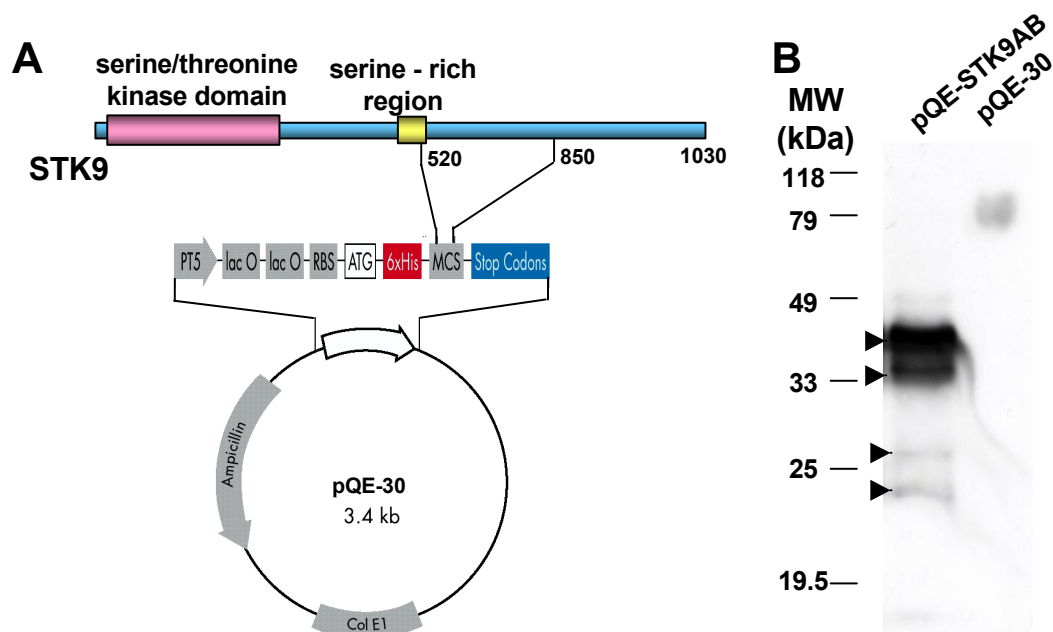


Figure 15. Expression of recombinant STK9 peptides in *E. coli*. A, Diagram depicting the construction of pQE-STK9AB. The upper panel shows the predicted STK9 protein structure, containing a serine/threonine kinase domain (pink) in the N-terminus and a serine-rich region (yellow) in the middle. A fragment following the serine-rich region and corresponding to a.a. 520-850 was chosen for expression in *E. coli*. The respective coding sequence was cloned into the bacterial expression vector pQE-30. The lower panel shows the map of the pQE-30 vector, which harbors a T5-lacO promoter-operator element and a 6 × His tag 5' to the cloning site (RBS = ribosome binding site, MCS = multiple cloning site). B, Western blot analysis of recombinant STK9 peptides expressed in *E. coli*. M 15 *E. coli* cells were transformed with either the pQE-STK9AB construct or the control pQE-30 vector. Cells were harvested three hours after induction with IPTG. Cell pellets (20 μg) were lysed in 1 × electrophoresis buffer and analyzed by SDS-PAGE and Western blot. Specific bands of around 35 kDa and 25 kDa recognized by the anti-6 × His antibody are indicated by arrowheads (MW = molecular weight).

3.3.2 Purification and concentration of 6 × His tagged STK9 peptides

For purification of the 6 × His tagged STK9 peptides, proteins were first extracted under native conditions. Bacterial cell pellets were resuspended in native condition buffer containing no denaturants and lysed by sonication. However, even with the presence of protease inhibitors, a large proportion of the 6 × His tagged STK9 peptides were degraded into the two small fragments of around 25 kDa during the process of cell lysis (Fig. 16). Therefore, a denaturing condition containing 8 M urea was used to inhibit protein degradation.

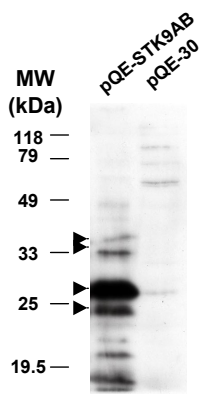


Figure 16. Degradation of 6 × His tagged STK9 peptides in native extraction condition. M 15 *E. coli* cells were transformed with either the pQE-STK9AB construct or the pQE-30 vector. Cells were harvested three hours after induction with IPTG. Cell pellets (20 μg) were suspended in native condition buffer (50 mM NaH₂PO₄, pH8.0, 300 mM NaCl, 10 mM imidazole), proteins were extracted by sonication followed by centrifugation. The protein extracts were analyzed by Western blot using an anti- 6 × His antibody. Note the decreased intensity of the bands around 35 kD and the increased intensity of the bands around 25 kD (arrowheads) compared to that in Fig. 16. (MW = molecular weight)

Under denaturing condition, protein extractions containing the 6 × His tagged STK9 peptides were purified by nickel-nitrilotriacetic acid (Ni-NTA) metal-affinity chromatography (Qiagen) (for principle, see Fig. 17A). Two factors were found to be crucial for protein purification. First, inclusion of 20 mM imidazole, a chemical having a similar structure as histidine, in the binding and washing steps resulted in decreased nonspecific binding without interfering with the binding of the 6 × His tagged STK9 peptides to Ni-NTA matrices. Second, a two-step pH gradient of washing, one at pH 8.0 and the other at pH 6.5, effectively removed contaminating proteins without significant loss of the 6 × His tagged proteins. The bound proteins were finally eluted under a condition of combined low pH (pH 5.0) and high concentration of imidazole (100 mM). Samples of each purification fraction were analyzed by SDS-PAGE and the proteins were detected by Coomassie blue staining (Fig. 17B). A prominent band of approximately 35 kDa was detected in the elution fraction. This fraction was essentially free of contaminating proteins. To evaluate the protein property, the same set of samples was also analyzed by Western blot using an anti- 6 × His antibody. The antibody detected the predicted 35 kDa band in all fractions, but only the total lysates and the elution fractions showed strong signals, while other washing fractions showed very weak signals (Fig. 17C). This result suggested that the prominent band of 35 kDa eluted from Ni-NTA matrices represented the 6 × His tagged STK9 peptides. The elution fraction containing the purified proteins was ultrafiltered through an anisotropic membrane for further concentration. The enriched proteins were used as immunogens for immunizing animals.

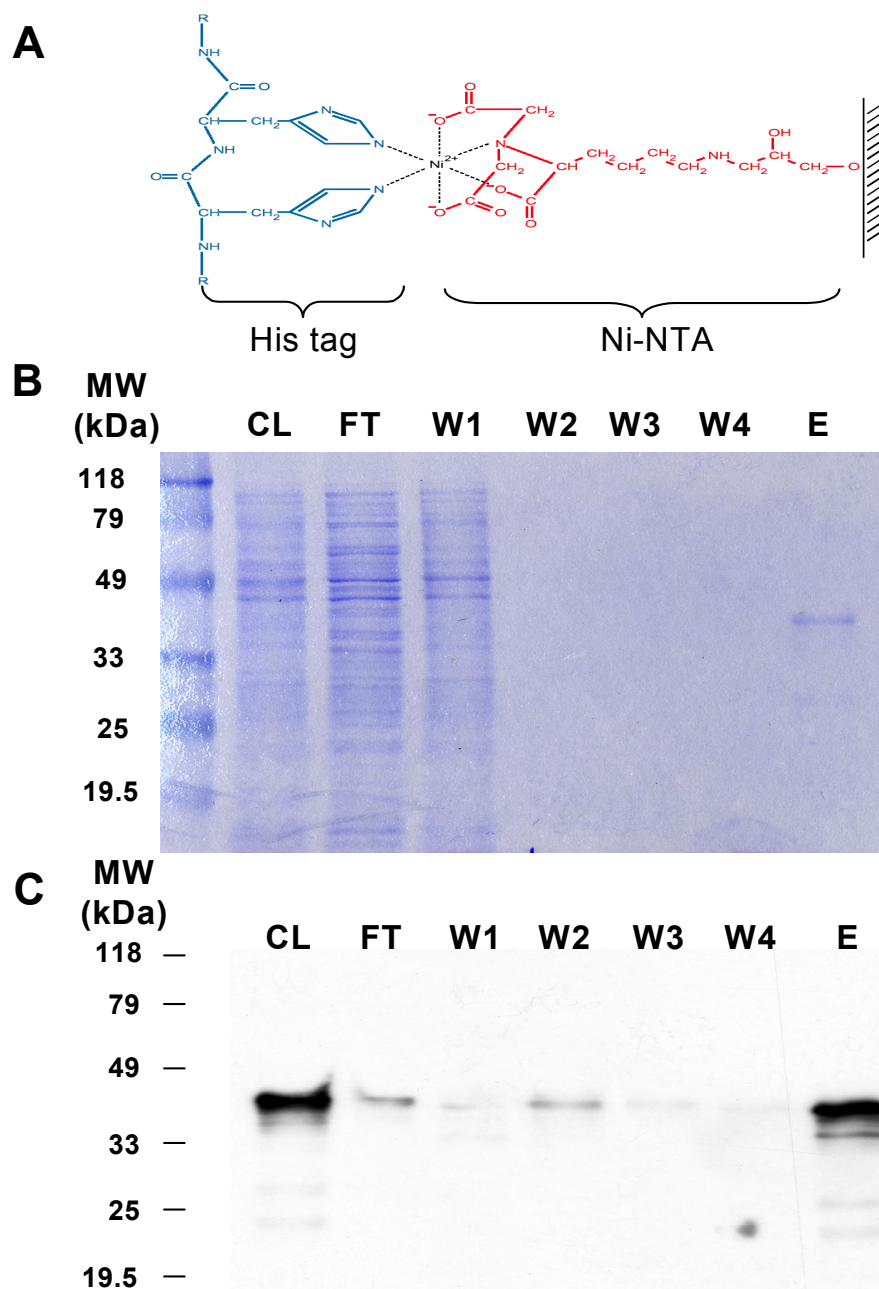


Figure 17. Purification of the 6×His tagged STK9 peptides by Ni-NTA affinity chromatography under denaturing condition. A, Diagram depicting the principle of Ni-NTA affinity chromatography (adopted from the QIAexpressionist user manual, Qiagen). A nickel ion that is immobilized by a NTA molecule can bind two histidine residues through two free chelating sites. B and C, Analysis of the samples from each purification fraction. CL: cell lysate; FT: flow-through; W1&W2: imidazole 20 mM, pH 8.0, wash; W3&W4: imidazole 20 mM, pH5.0 wash; E: imidazole 100 mM, pH 5.0 elution. MW: molecular weight. B, SDS-PAGE analysis. Samples (10 μ l) were analyzed on 10% gel and proteins were stained with Coomassie blue. A band of approximate 35 kD was detected in the elution fraction, which was free of contaminating proteins. C, Western blot analysis. The same set of samples used for B were analyzed by Western blot with an anti-6 \times His antibody, with the exception of the samples from CL and E, which were 1:10 diluted. The antibody detected a band of approximate 35 kD in all fractions, with strong signal intensity in fractions CL and E.

3.3.3 Evaluation of immunoreactivity of the anti- STK9 antiserum

After immunization, the resulting antiserum was tested for immunoreactivity towards ectopically expressed STK9 protein. To express STK9 protein in mammalian cells, the coding sequence of full-length STK9 was cloned into the mammalian expression vector pCMV-Tag 3B (Stratagene),

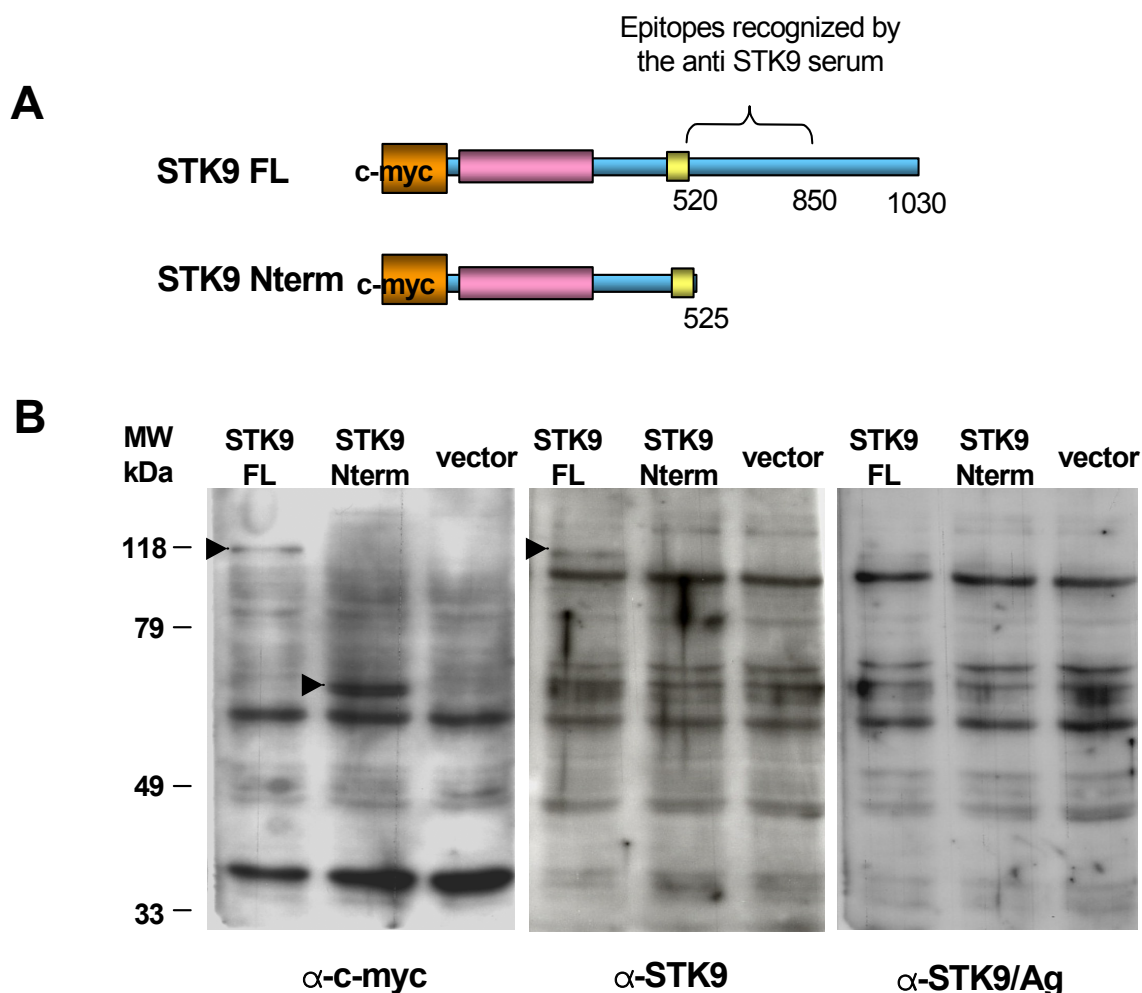


Figure 18. Expression of c-myc tagged STK9 proteins in mammalian cells. A, Diagram of c-myc tagged full-length STK9 (STK9FL) and truncated STK9 (STK9Nterm) proteins. B, Western blot analysis of c-myc tagged STK9 expressed in COS-7 cells. COS-7 cells were transiently transfected with the pCMV-STK9 FL, the pCMV-STK9Nterm or the control pCMV-Tag 3B vector. Cells were harvested 24 hr after transfection, and were analyzed by Western blot with an anti- c-myc antibody (left panel), the anti- STK9 antiserum (middle panel) or the anti- STK9 antiserum pre-incubated with the purified 6 × His tagged STK9 peptides (right panel). Specific signals recognized by the antibodies are indicated by arrowheads. MW= molecular weight.

which contains a c-myc epitope (EQKLISEEDL) 5' to the cloning site (Fig. 18A upper panel). As a control, the coding sequence for the first 525 amino acids of the STK9 protein, which does not contain the epitopes recognized by the anti- STK9 antiserum, was similarly cloned into the pCMV-Tag 3B vector (Fig. 18A lower panel). The resulting full-length (pCMV-STK9FL) and C-terminal deleted (pCMV-STK9Nterm) constructs were transiently expressed in COS-7 cells. Expression of the c-myc tagged proteins was examined with an anti- c-myc antibody and the anti- STK9 serum by Western blot analysis. As expected, the anti- c-myc antibody specifically detected a band of 115 kDa in the cells transfected with the pCMV-STK9FL construct, and a band of 60 kDa in the cells transfected with the pCMV-STK9Nterm construct. Neither of the bands was detected in the cells transfected with the control pCMV-Tag 3B vector (Fig. 18B left panel). The anti- STK9 antiserum recognized the same 115 kDa band of the full-length STK9, but not the 60 kDa band of the truncated STK9Nterm proteins (Fig. 18B middle panel). Moreover, the 115 kDa band of the full-length STK9 was absent when the anti- STK9 antiserum was pre-absorbed with the antigen (purified 6×His tagged STK9 peptides) (Fig. 18B right panel). These results indicated that the anti- STK9 antiserum is able to detect ectopically expressed STK9 proteins upon Western blot analysis.

The anti- STK9 antiserum was also tested in immunocytochemical analysis. COS-7 cells transiently transfected with either pCMV-STK9FL or pCMV-STK9Nterm construct were fixed with paraformaldehyde. The subcellular distribution of the c-myc tagged proteins was examined by double immunostaining with an anti- c-myc antibody and the anti- STK9 serum. In the cells transfected with the pCMV-STK9FL construct, the signals of the anti- c-myc antibody were predominant in the cytoplasm, in a punctuated pattern (Fig. 19A and D). The anti- STK9 antiserum gave an essentially identical pattern of signals as the anti- c-myc antibody (Fig. 19B and C). The specific signals produced by the anti- STK9 antiserum were abolished by pre-absorption with the antigen (purified 6×His tagged STK9 peptides) (Fig. 19E). Interestingly, a fraction of signals detected by both the anti- c-myc antibody and the anti- STK9 antiserum formed a distinct dot-like structure in the perinucleus, which is reminiscent of the centrosome. To investigate this further, an anti- γ -tubulin antibody, which specifically detects the centrosome component γ -tubulin, was used in a separate experiment. Double immunostaining with an anti- c-myc and an anti- γ -tubulin

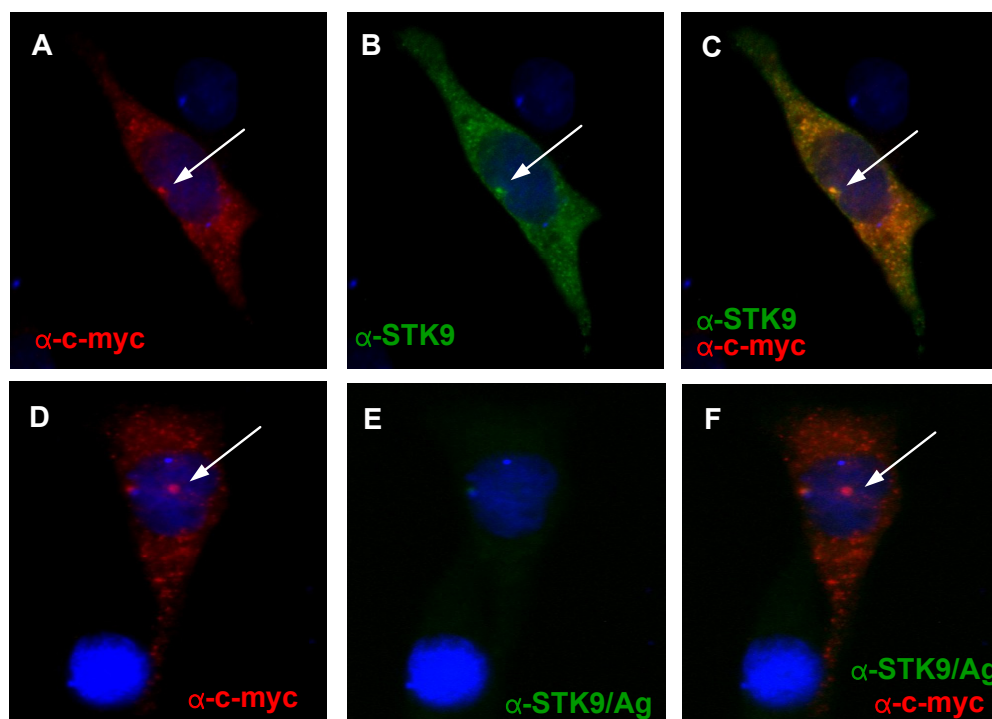


Figure 19. Immunoreactivity of the anti- STK9 antiserum in immunocytochemical analysis. COS-7 cells transiently transfected with the pCMV-STK9FL construct were co-immunostained with an anti- c-myc antibody and the anti- STK9 antiserum (A-C), or with an anti- c-myc antibody and the antigen pre-absorbed anti- STK9 antiserum (D-E). The immunoreactivity of the anti- c-myc antibody was detected in red (A and D), the immunoreactivity of the anti- STK9 antiserum was detected in green (B and E), and the nuclei were labeled with DAPI in blue. C is the merged image of A and B. The anti- STK9 antiserum gave an essentially identical pattern of immunofluorescence signals as the anti- c-myc antibody (overlapping signals are shown in yellow). F is the merged image of D and E. The specific signals detected by the anti- STK9 antiserum was absent after pre-incubation with the antigen (E). The dot-like signals detected by both the anti- c-myc antibody and the anti- STK9 antiserum are indicated by arrows.

antibody revealed extensive co-localization of the dot-like structure with the centrosome marker γ -tubulin (Fig. 20). These data suggest that the anti- STK9 antiserum is able to detect STK9 proteins in immunocytochemical analysis. The ectopically expressed full-length STK9 proteins were predominantly located in the cytoplasm, and a fraction of STK9 proteins was specifically targeted to the centrosome.

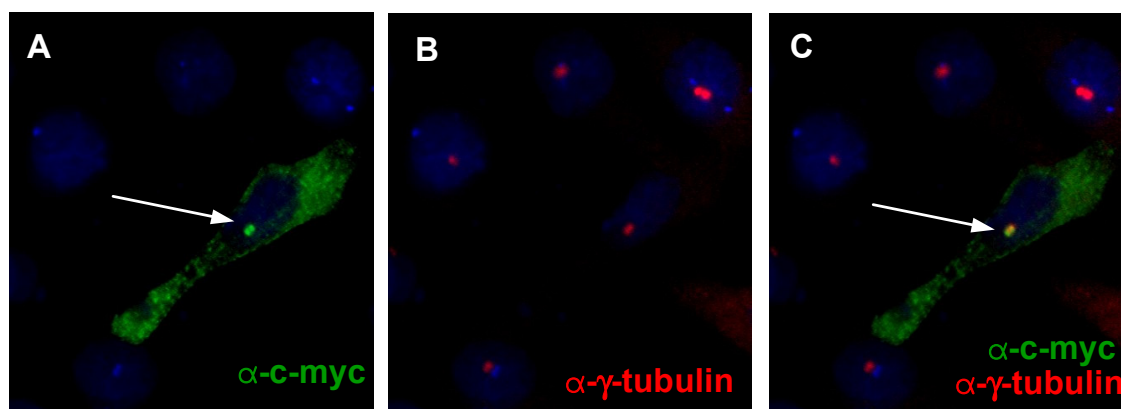


Figure 20. Localization of full-length STK9 in the centrosome. COS-7 cells were transiently transfected with the pCMV-STK9FL construct. STK9 proteins were detected with an anti- c-myc antibody in green (A), centrosomes were labeled with an anti- γ -tubulin antibody in red (B), and nuclei were labeled with DAPI in blue. C is the merged image of A and B. Note the dot-like signals detected by the anti- c-myc antibody (arrow) overlap extensively with the centrosome signals (overlapping signals are shown in yellow).

In the cells transfected with the STK9Nterm construct, immunoreactivity signals of the anti-c-myc antibody were distributed throughout the cell, uniformly in the cytoplasm and the nucleus (Fig. 21). This result indicated that the truncated STK9Nterm without the C-terminal 505 amino acids lost the specific subcellular distribution pattern as seen in the full-length STK9.

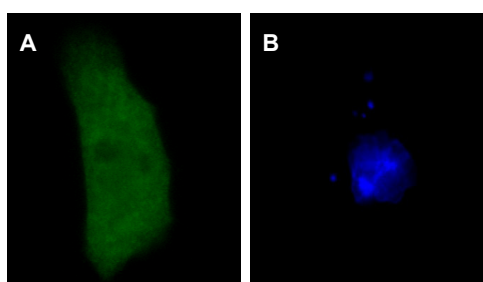


Figure 21. Subcellular localization of the truncated STK9Nterm proteins. COS-7 cells were transiently transfected with the pCMV-STK9Nterm construct. The truncated STK9Nterm proteins were detected with an anti- c-myc antibody in green (A), and nuclei were labeled with DAPI in blue (B). The signals detected by the antibody were diffused all over the cell.

3.4 Screening for STK9 interaction partners

The presence of an N-terminal serine/threonine kinase domain in the STK9 protein suggests its potential function as a protein kinase, phosphorylating specific downstream substrates in response to distinct upstream signals. To identify proteins that interact with STK9, and to obtain insights into the biochemical function of the STK9 signaling network, we performed a yeast two-hybrid library screening.

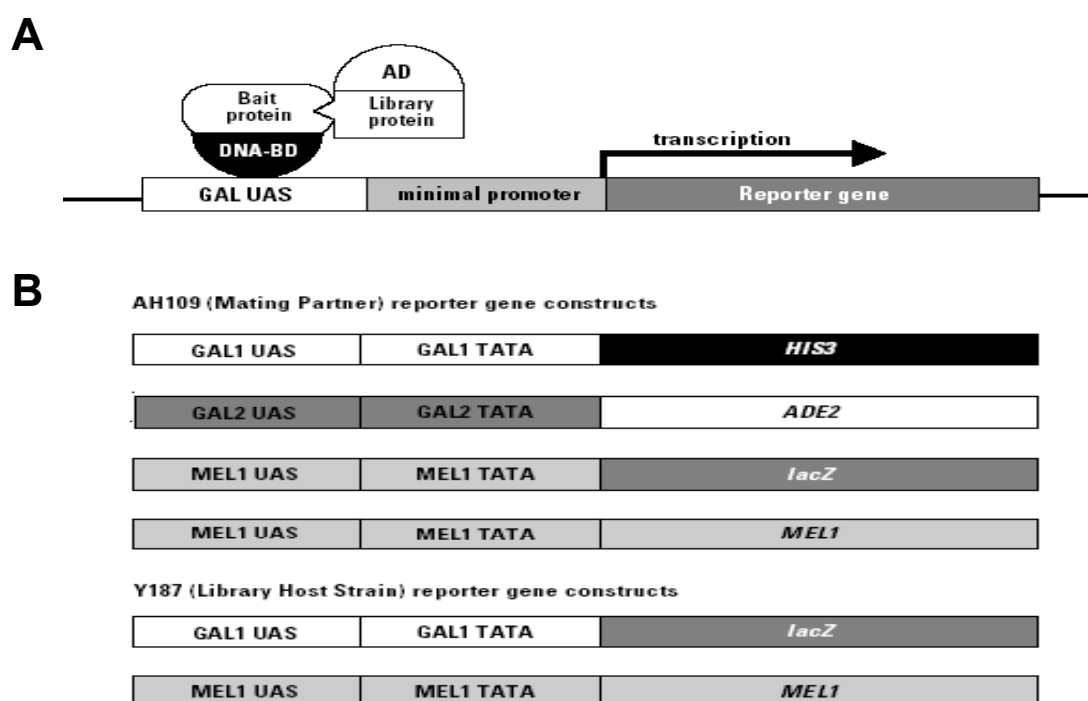


Figure 22. Diagram depicting the yeast two-hybrid system 3 (adopted from the MATCHMAKER Gal4 Two-hybrid system 3 user manual, BD Biosciences). A, Principle of the yeast two-hybrid assay. The yeast transcription factor Gal4 can be physically and functionally separated into a DNA binding domain (BD) and a transcription activating domain (AD). BD is fused to a target protein (bait), and AD is fused to a library of proteins. When a protein in the library interacts with the bait, the two domains are brought in close proximity to reconstitute the transcriptional activity of Gal4. B, The reporter genes used in system 3. GAL1 UAS, GAL2 UAS and MEL1 UAS are DNA consensus sequences that specifically bind the BD of GAL4. *HIS3* and *ADE2* are nutrition reporters allowing positive clones to grow on the selective medium without the respective amino acid. *MEL1* and *lacZ* encode α -galactosidase and β -galactosidase, respectively, allowing white/blue selection in the presence of the respective substrate (X- α -Gal for *MEL1* and X-Gal for *lacZ*).

The yeast two-hybrid system 3 purchased from BD Biosciences was used in the screening. This system is based on the properties of the yeast transcription factor Gal4, which can be physically and functionally separated into a DNA binding domain (BD) and a transcription activating domain (AD). Each domain alone is non-functional as a transcription factor but, when in very close proximity to each other, can reconstitute transcriptional activity (Fig. 22A). In the experiment, STK9 was fused to BD (designated bait), and proteins from a fetal brain library were fused to AD (designated prey). The bait and prey fusion proteins were expressed in two haploid yeast strains of opposite mating type (MATa and MAT α) and were brought together in diploid cells through mating. Induction of the reporter genes will only occur when a prey protein from the library interacts with STK9, resulting in spatial association of the two domains. The system uses three different reporters, ADE2, HIS3 and MEL1/LacZ (Fig. 22B). Each of them is under the control of a distinct GAL4 upstream activating sequence (UAS) and a TATA box. GAL1::HIS3 reporter is assayed by growth on media lacking histidine; GAL2::ADE2 reporter is assayed by growth on media lacking adenine; MEL1::MEL1 and MEL1::LacZ are assayed by colorimetric detection of α - and β - galactosidase, respectively.

3.4.1 Construction of a kinase-deficient mutant STK9-K42R

To stabilize kinase–substrate interactions for a higher chance of identifying specific substrates, a kinase-deficient mutant was created in addition to the wild-type STK9 (Fig. 23B). The mutant protein carries a lysine to arginine substitution at position 42 of the STK9 protein (K42R). This lysine corresponds to the invariant lysine in kinase subdomain II of all known protein kinases (Fig. 23A), and has been shown to be crucial for contact with α and β phosphate groups of ATP, positioning them for proper phosphoryl transfer reactions (Carrera et al. 1993; Hanks and Hunter 1995). Replacement of this conserved lysine by alanine or arginine in several protein kinases dramatically decreased the protein kinase activities, but did not perturb the binding to ATP or their substrates (Li et al. 1995; Robinson et al. 1996).

Mutant STK9 was first examined for its subcellular localization. Like its wild-type counterpart, the coding sequence of STK9-K42R was cloned into the mammalian expression

seen for the wild-type, including punctated distribution throughout the cytoplasm, and co-localization with the centrosome in the perinucleus (Fig. 23C). This finding suggested that the K42R substitution in the mutant does not affect overall subcellular targeting.

To express wild-type and mutant BD-STK9 fusion proteins in yeast, the respective coding sequences were cloned into the yeast two-hybrid bait vector pGBKT7 (BD Biosciences), which contains coding sequences for the Gal4 BD and a c-myc epitope 5' to the cloning site. The resulting wild-type (pGBKT7-STK9-WT) and mutant (pGBKT7-STK9-K42R) bait constructs were transformed into yeast MATa strain AH109, and expression of the c-myc BD fusion proteins was examined by Western blot analysis. Both the anti- c-myc antibody and the anti- STK9 antiserum detected a band at the expected molecular weight (approximately 130 kDa) in the yeast cells harboring the wild-type or the mutant bait construct (Fig. 24). This result suggested that wild-type and mutant BD-STK9 proteins were expressed in yeast, and both could be recognized by the anti- STK9 antiserum. Subsequently, potential auto-activation activity of the two bait

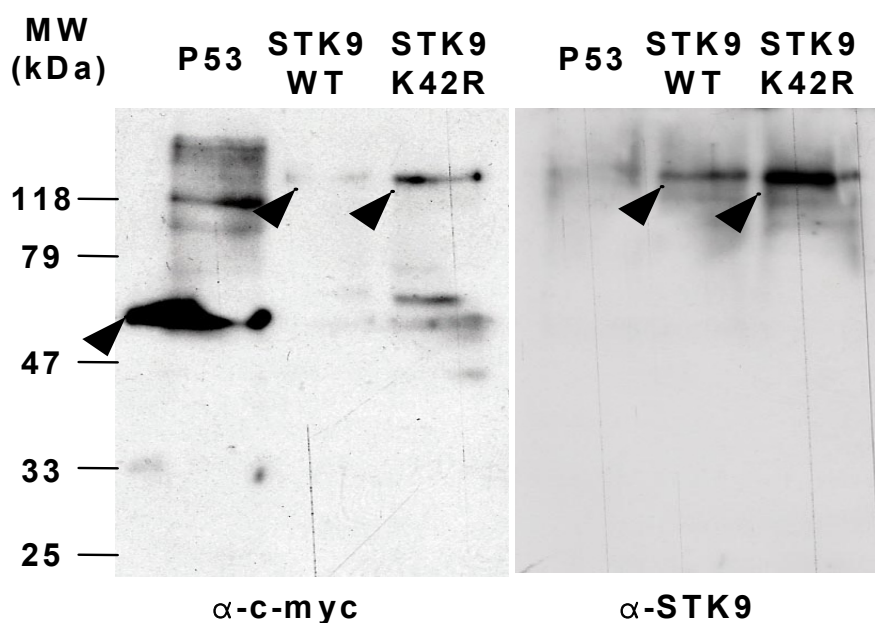


Figure 24. Expression of c-myc tagged STK9 proteins in yeast cells. Yeast strain AH109 was transformed with the positive control pGBKT-53, the pGBKT-STK9-WT or the pGBKT-STK9-K42R construct. Cells were harvested at OD₆₀₀ of 0.6. Cell pellets were lysed in cracking buffer, and the protein extracts were analyzed by Western blot using an anti-c-myc antibody (left panel) or the anti- STK9 antiserum (right panel). Specific signals recognized by the antibodies are indicated by arrowheads

constructs was examined. Yeast AH109 cells harboring the wild-type or the mutant bait construct were plated on the selective medium; neither of the constructs showed auto-activation activity of the reporter genes. However, yeast cells harboring the wild-type bait construct grew more slowly than those harboring the mutant one or the control pGBKT7 vector, indicating that over-expression of wild-type STK9 protein is toxic to the yeast host strain. Therefore, only the mutant bait construct pGBKT7-STK9-K42R was chosen for further library screening.

3.4.2 Yeast two-hybrid library screening

To co-express the bait and prey proteins, MAT α yeast strain Y187 pretransformed with fetal brain cDNA library prey constructs (BD Biosciences) was mated with MATa yeast strain AH109 containing the bait construct pGBKT7-STK9- K42R. A modified mating protocol was employed, including a pre-incubation step on acidic media (YCM, pH 3.5 and pH 4.5, see section 2.2.15) before mating, and an optimized cell ratio of 3:1 between MATa and MAT α yeast cells. With this protocol, a total number of $\sim 8.8 \times 10^6$ diploids were obtained, 2.5 times fold over the complexity of the original fetal brain cDNA library (3.5×10^6 of independent clones in the library).

Using nutrition and colorimetric selection markers, 109 yeast clones expressing His, Ade and MEL1 reporter genes were isolated. The prey identity of each positive clone was retrieved by PCR amplification combined with direct sequencing. After removal of genomic and redundant sequences, the prey cDNAs in those positive clones represented a total of 68 independent genes.

Due to technical limitations, yeast two-hybrid library assays usually generate a number of false-positive interactions. Several approaches were introduced to facilitate the identification of true positives. First, sequence of prey cDNAs in the positive clones were examined, only 19 out of 68 genes were found to be fused in-frame with the AD coding sequence. Subsequently, the prey plasmids were examined for auto-activation activity. Each of these 19 prey plasmids was transformed into yeast AH109 cells and the transformed yeast cells were plated on the nutrition selective medium; additional two prey plasmids were removed due to their auto activation of the reporter genes without presence of the bait construct pGBKT7-STK9-K42R. Finally, the bait-prey interactions were retested. Each of the remaining 17 prey plasmids was isolated and co-transformed with the freshly prepared bait construct pGBKT7-STK9-K42R in yeast AH109

cells. Only three of the preys showed interaction in the retested yeast two–hybrid assay. The three prey plasmids isolated from the yeast two-hybrid library screening contained sequence fragments of the promyelocytic leukemia zinc finger protein gene (*PLZF*), the transporter associated with antigen processing 1 gene (*TAPI*) and the clathrin heavy chain gene (*CTLC*)(Table 21).

Table 21 Potential interaction partners of STK9 identified in the yeast two-hybrid library screening

Prey identity	Reference nucleotide sequence	Fragment in prey plasmid (encoding functional domain)	Protein function
<i>PLZF</i>	NM_006006	1150-2374 (zinc finger domain)	transcription factor, associated with acute promyelocytic leukaemia
<i>TAPI</i>	NM_000593	2076-2960 (nucleotide binding domain)	ATP binding cassette transporters, involved in the pumping of degraded cytosolic peptides across the endoplasmic reticulum for binding onto class I molecules.
<i>CLTC</i>	NM_004859	4672-6541	protein component of clathrin coated vesicles, involved in intracellular protein trafficking

4 DISCUSSION

4.1 Positional cloning identified *STK9* as a candidate gene for XLMR

In the course of a systematic search for new XLMR genes, we studied a mentally retarded female patient with a 46,X,t(X;7)(p22.3;p15) *de novo* balanced translocation (patient 1). The patient presented with a severe phenotype of neonatal onset encephalopathy, comprising infantile spasms, global developmental arrest and profound mental retardation. Positional cloning localized the translocation breakpoints on both chromosomes. The autosomal breakpoint did not disrupt any obvious transcripts. However, the X chromosomal breakpoint interrupted the *STK9* gene in intron 10. *STK9* transcripts were disrupted by the X-chromosomal breakpoint, as shown by RT-PCR with RNAs from the patient-derived fibroblast cell line. The truncated transcripts, if translated, would encode a protein of 275 amino acids, which may retain some functional properties.

Independently, a clinically and cytogenetically matching translocation case has been identified (Kalscheuer et al. 2003). The patient carried a 46,X,t(X;6)(p22.3;q14) *de novo* balanced translocation, and exhibited clinical features very similar to patient 1, such as early-onset infantile spasms, global developmental arrest and profound mental retardation. The X chromosomal breakpoint in that patient was mapped to intron 1 of the *STK9* gene, close to the 5' end of the gene and upstream of the ATG start codon. RT-PCR with RNAs from the patient-derived lymphoblastoid cell line showed that *STK9* isoform I was completely absent in the patient. Expression of isoform II, which is likely to be transcribed from a different promoter ~12 kb downstream of the breakpoint, could not be examined as it is not transcribed in lymphocytes. However, because of the separation of the coding part of the gene from the isoform II promoter, it is likely that the expression of isoform II was compromised as well.

Disruption of the *STK9* gene in two unrelated female patients strongly suggested that their similar phenotypes were the result of aberrant *STK9* expression. Complete absence of normal *STK9* transcripts in the patient-derived cell lines indicated that *STK9* was subjected to X

chromosome inactivation (XCI), and that in both translocation patients, transcription of *STK9* from the normal X chromosome was completely lacking due to skewed XCI, which is the rule in females with reciprocal X;autosomal translocations. The autosomal breakpoints in these patients were most likely not involved in the disease phenotype, as they were on different chromosomes. Very likely, the *ARX* gene, mutated in a subset of families with X-linked infantile spasms, did not contribute to the disease phenotype either. In patient 1, *ARX* expression was identical to that of controls. In the matching translocation case with 46,X,t(X;6)(p22.3;q14), expression of *ARX* could not be evaluated in lymphocytes, but mutations in the *ARX* coding sequence could be excluded (Kalscheuer et al. 2003).

4.2 Mutation analysis confirmed the causative role of *STK9* in MR

To further investigate the possible role of *STK9* in MR, mutation screening of its entire coding sequence was performed in three cohorts of mentally retarded patients. Three sequence variants that were not present in controls were identified in *STK9* mutation analysis. One of them was a c.1330C>T nucleotide change, found in the index patient from a family with XLMR, resulting in an arginine-to-cysteine substitution at position 444 of the STK9 protein. Arg 444 is located outside the serine/threonine kinase domain. It is conserved in mouse, but not in Fugu. The biochemical effect of this sequence variant is not clear at present.

Of particular interest are the other two variants found in the panel of patients with RTT-like features. The c.455G>T exchange, resulting in a cysteine to phenylalanine substitution at position 152 of the STK9 protein, was present in a female patient presenting with early-onset seizures, psychomotor development delay and absence of speech (patient 2). The c.525A>T nucleotide exchange, changing an arginine to serine at position 175, was found in monozygotic twin sisters exhibiting almost identical clinical features of classical RTT, with a history of early-onset seizures (patients 3 and 4). Several lines of evidence argue for the pathogenic nature of these missense mutations. First, both mutations most likely occurred *de novo*. Secondly, they both lie within critical regions of the serine/threonine kinase domain and therefore most likely have deleterious

effects on STK9 kinase activity. Thirdly, the mutated amino acids are conserved in mouse and Fugu STK9 orthologs, and are also present in a group of closely related Cdc2-related protein kinases, including CDKL1, CDKL2 and CDKL3. Finally, none of these missense mutations was found in 427 control X chromosomes.

Additional evidence implicating STK9 in atypical RTT comes from the recent work of J. Gécz's group (Adelaide), where truncating frameshift mutations were identified in two unrelated families (Weaving et al., submitted). In the first family, a c.183delT mutation creating a premature stop codon at amino acid 75 of the STK9 protein was found in female homozygotic twins with discordant phenotypes. One sister had classical RTT with a history of early-onset seizures, while the other had mild mental retardation with autistic features. A hemizygous brother who carried the same mutation presented with a more severe neonatal onset encephalopathy. In the second family, an IVS13-1G>A mutation affecting splicing led to a premature stop codon at amino acid 783. The affected female exhibited atypical RTT features with a history of early-onset seizures.

4.3 STK9 alterations are likely to affect its kinase activities

The spectrum of identified STK9 defects, including the mutations reported by the Australian group (Kalscheuer et al. 2003; Weaving et al. submitted), now encompasses two chromosome translocations, two frameshift mutations, and two missense mutations (Fig. 25). The chromosome translocations and frameshift mutations resulted in premature stop of translation of the STK9 gene, whereas the missense mutations caused substitutions of the critical amino acids in the functional serine/threonine kinase domain. All defects, except for the splice site mutation IVS13-1G>A, are located within the protein kinase domain and are likely to inactivate the protein kinase activity. The IVS13-1G>A splicing mutation is predicted to result in a truncated protein that retains the intact protein kinase domain. Given that ectopically expressed truncated STK9 proteins containing only the first 525 amino acids showed altered intracellular distribution, it is likely that the C-terminus of STK9 is required for correct subcellular targeting. Whether the truncated protein of

783 amino acids resulting from the IVS13-1G>A mutation would affect target specificity remains to be investigated.

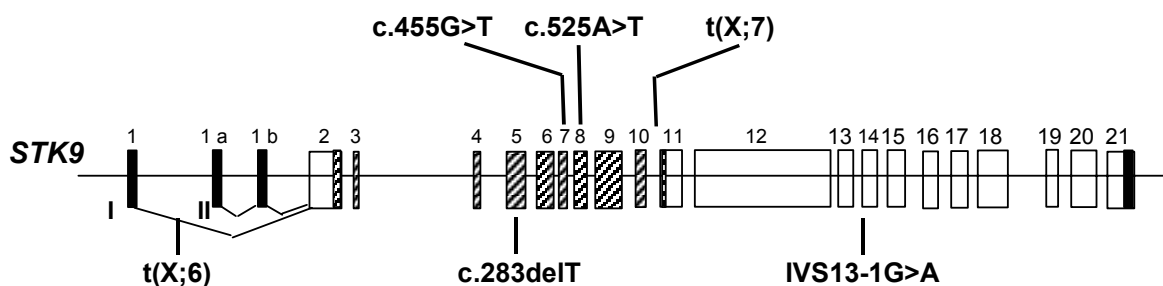


Figure 25. Schematic representation of the pathogenic alterations found in *STK9*. Exons are shown in boxes, noncoding regions in black, and the serine/threonine kinase domain in hatched form. The alternative splicing patterns are indicated below the gene for the known isoforms I and II. The pathogenic alterations found in this study are shown above the gene; alterations identified by the collaboration group in Australian are shown below the gene.

4.4 *STK9* alterations are associated with a wide range of clinical features

Our studies, together with the work of the collaborating Australian group suggest that *STK9* is a new XLMR gene, and that alterations in *STK9* are associated with a wide range of clinical features. The associated disorder may be severe, with early-onset encephalopathy, as documented by both translocation patients and one male patient with a frameshift mutation (Weaving et al. submitted). These patients presented with infantile spasms, severe global developmental arrest and profound intellectual impairment; they never learned to speak, sit or walk, and they never developed visual or social response. At the other end of the spectrum is the mild mental retardation with autistic features in one female twin with a frameshift mutation in *STK9* (Weaving et al. submitted). She retains reasonable verbal skills and has no obvious motor deficiencies. The variable RTT-like features in the female patients described in this study and in one female patient reported by Weaving et al. lie between these extreme examples. All of them have had an apparently normal pre-and perinatal period, but developed severe epileptic activity between 5 weeks and 3 months of age, followed by psychomotor and behavioral developmental delay with or without a period of

Table 22 Diagnostic criteria for atypical RTT fulfilled by the patients with *STK9* alterations

Case	This study				Kalscheuer et al	Weaving et al			
	Patient 1	Patient 2	Patient 3	Patient 4	Patient 2	III:3	Family 1 III:1	III:2	Family 2
Genotype	t(X;7)	c.455G>T	c.525A>T	c.525A>T	t(X;6)	183delT	183delT	183delT	IVS13-1G>A
Gender	F	F	F	F	F	M	F	F	F
Normal pre- and perinatal period	+	+	+	+	+	+	+	+	+
Normal early psychomotor development (0-6 mos)	– (ES)	– (ES)	– (ES)	– (ES)	– (ES)	– (ES)	+(ES)	+	– (ES)
Normal head circumference at birth	+	+	+	+	+	+	+	+	NA
Microcephaly and/ or deceleration of head growth	+	–	–	–	–	+	–	–	+
Developmental and psychomotor delay/regression	+	+	+	+	+	+	+	–	+
Mental retardation at examination	+	+	+	+	+	+	+	+	+
Autism-communication dysfunction	+	+	+	+	+	+	+	+	+
Initial normal use of hands	NA	NA	NA	NA	NA	NA	+	+	+
Absence of purposeful use of hand at examination	+	+	+	+	+	+	+	–	+
Hand stereotypes	–	–	+	+	–	–	+	–	+
Gait apraxia/ ataxia	– (N)	– (N)	+	+	– (N)	– (N)	+	–	+

Abbreviation: F= Female; M= Male; ES= early onset seizures; N= never able to walk; NA= Not available

regression. Upon examination, all of these affected girls exhibited motor deficiency, autistic features, and mental retardation, as well as absence of speech and purposeful hand use. These clinical features meet most of the criteria for atypical forms of RTT suggested by Goutieres and Aicardi (1986) (Table 22).

As *STK9* is subjected to X-inactivation, the phenotypic heterogeneity observed in female patients with a mutation in this gene might be explained by variable X-inactivation (XCI) patterns. In line with this hypothesis, the most severe phenotype, with early-onset encephalopathy, was present in the females carrying an X;autosome translocation, where we could show that the normal X chromosome was completely inactivated. Likewise, the hemizygous male with a frameshift mutation was severely affected. In females with an incompletely skewed XCI pattern, expression of the wild-type allele in at least a portion of the cells could mitigate the clinical manifestations. Indeed, a balanced XCI pattern was found in the monozygotic twins investigated in this study (patient 3 and 4, M. Raynaud, personal communication), and a slightly skewed XCI pattern in favor of the normal allele was found in one female patient reported by Weaving et al., 2004. However, there was not always a good correlation between phenotypic severity and the ratio of XCI in peripheral blood leukocytes, e.g. the twin sisters described by Weaving et al. exhibited completely different clinical features but had a similar XCI pattern. In this case, the XCI pattern in blood leukocytes presumably does not reflect the XCI in the brain, which is the primarily affected tissue.

It is interesting to note that mutation screening in 96 patients with idiopathic infantile spasms did not yield any disease-causing mutations, although infantile spasms is the initial clinical feature linked to *STK9* defects. This observation suggests that the etiology of infantile spasms is heterogeneous. However, as patients in this panel were males, we cannot exclude that *STK9* is more frequently mutated in female patients with infantile spasms.

4.5 The phenotypic spectrum associated with *STK9* alterations overlaps with that of *MECP2* mutation

The finding that alterations in *STK9* were associated with variable RTT-like features is intriguing, since RTT has been considered as a monogenic disorder that is caused by defects in the *MECP2* gene (Amir et al. 1999; Renieri et al. 2003). Mutations in *MECP2* have been reported in up to 90% of classic RTT cases and 20-40% of atypical cases (Buyse et al. 2000; Cheadle et al. 2000; Bourdon et al. 2001). The failure of mutation detection in *MECP2*-negative cases has been attributed to the different stringencies of the diagnostic criteria, and to limitations of the current mutation detection system (Buyse et al. 2000; Miltenberger-Miltenyi and Laccone 2003). Indeed, in a small percentage of *MECP2*-negative cases, large deletions or rearrangements that disrupt the structure of *MECP2* but escape from the routine PCR-based screening strategy were identified (Bourdon et al. 2001; Schollen et al. 2003; Laccone et al. 2004). More recently, two mutations in the new coding sequence of the previously unknown *MECP2* isoform were described (Mnatzakanian et al. 2004). Interestingly, in these newly identified cases with novel *MECP2* defects, 17 out of 20 cases are typical RTT; and for the three remaining cases, their phenotypes could not be classified due to insufficient clinical data (Bourdon et al. 2001; Schollen et al. 2003; Laccone et al. 2004). The lower frequency of *MECP2* mutations in atypical RTT cases suggests the existence of locus heterogeneity, but so far, no other gene defect has been associated with this group. On reviewing clinical features, the individuals with *STK9* defects presented with a continuous phenotypic profile, including severe neonatal onset encephalopathy, congenital RTT variant, RTT with early-onset seizures and mild mental retardation with autistic features, which largely overlaps with the phenotypic spectrum of patients who have a mutation in *MECP2*. Could *STK9* be a second gene on the X chromosome contributing to RTT, especially atypical RTT variants with early-onset seizures? Mutation screening of *STK9* in a large cohort of patients with *MECP2*-negative RTT-like features may answer this question.

The phenotypic overlap caused by mutations in *MECP2* and *STK9* suggests that the two genes act in a common pathogenic pathway. MeCP2 protein is known to preferentially bind to

methylated CpG dinucleotides through its methyl-CpG binding domain and to silence downstream target genes (Lewis et al. 1992; Nan et al. 1998). Thus, *MECP2* mutations disrupting the normal developmental program of gene silencing in the central nervous system may underlie the pathology of RTT. Recent studies demonstrated a dynamic association of MeCP2 with the methylated promoter region of two neuronal specific genes, *BDNF* and *Hairy2a* (Chen et al. 2003; Stancheva et al. 2003). In both cases, MeCP2 is released from the promoter upon specific signaling stimulation, thereby facilitating transcription of target genes. In the case of *BDNF*, a time-dependent increase in phosphorylation of MeCP2 was observed upon stimulation. Phosphorylation modification in response to extracellular stimulation was suggested to regulate the binding affinity of MeCP2 for its target promoter. It is therefore tempting to hypothesize that STK9 and its signaling components may function to mediate processes that influence MeCP2 phosphorylation. Further characterization of the STK9 signaling pathway, including its upstream activators and downstream substrates, will help to elucidate the potential link between STK9 and MeCP2.

4.6 Primary sequence analysis suggests that STK9 functions in a similar way as ERKs in activity-dependent synaptic plasticity

Given that most of the pathogenic sequence variants are found clustered in the conserved region of the serine/threonine kinase domain, it is likely that STK9 kinase activity and the involved signaling pathway are indispensable for normal brain development. The sequence of the conserved serine/threonine kinase domain in STK9 is most closely related to a subgroup of Cdc2-related protein kinases, including CDKL2, CDKL1, and CDKL3, with sequence identity ranging from 49% to 43%. Sequences of these kinases contain two putative dual phosphorylation sites that are classically found in CDKs and MAPKs (Fig. 26). The first one is Ser14Tyr15 (CDKL2 numbering) located within the glycine-rich loop in kinase subdomain I, corresponding to the regulatory site that is critical in CDKs (Morgan 1995). The second one is the Thr-Asp-Tyr triplet in subdomain

VIII, corresponding to the Thr-Xaa-Tyr activating motif that is unique in MAPKs (Canagarajah et al. 1997). The sequence of these characteristic regulatory sites, however, is not conserved in STK9. In fact, STK9 does not contain the CDK-like dual phosphorylation site in subdomain I, instead, a putative single phosphorylation site of Ala14Tyr15 is found at this position. Moreover, STK9 contains a Thr-Glu-Tyr triplet in subdomain VIII, which is different from the Thr-Asp-Tyr triplet in the sequence of CDKL1, CDKL2 and CDKL3. Interestingly, in these putative regulatory sites, the sequence of STK9 is identical to that of ERKs (Fig. 26), a subset of MAPKs in the CMGC group. Even more interestingly, STK9 and ERKs share remarkably high homology in the kinase subdomains VIII and IX, despite a relatively low homology in the overall sequences (38% of sequence identity) (Fig. 26). It is noteworthy that the sequence of ERKs in these subdomains forms a distinct hydrophobic pocket, which is responsible for interacting with the substrates that contain the specific docking motif with the Phe-X-Phe-Pro consensus sequence (Lee et al. 2004). The high homology between STK9 and ERKs in the sequence determinant for specificity of substrate recognition suggests that STK9 may function in a similar way as ERKs in controlling a common subset of downstream effectors.

ERKs, including ERK1 and ERK2 isoforms, are the prototype of the MAPK family that also includes the JNK and p38 members. ERKs are evolutionarily conserved signaling transducers that play a pivotal role in the response of many cell types to growth factors and other mitogens, mediating their effects on cell proliferation and differentiation (Chang and Karin 2001). ERKs are highly expressed in post-mitotic mature neurons (Boulton et al. 1991). Studies with ERK signaling inhibitors have demonstrated that ERK signaling is essential for synaptic plasticity *in vitro* (English and Sweatt 1997), an activity-dependent remodeling of synaptic strength in response to electrical, chemical or behavior stimuli. As synaptic plasticity is a widely proposed cellular mechanism underlying learning and long-term memory, the role of ERK activation in learning *in vivo* has also been evaluated. ERK signaling inhibitors greatly impaired long-term memory in tested animals (Atkins et al. 1998; Sweatt 2001; Valjent et al. 2001). It is clear that the activity of neuronal ERKs is regulated by extracellular neurotrophins and neurotransmitters via the conserved Ras-Raf-MEK-ERK cascade as in non-neuronal cells, whereas the downstream targets of ERKs that regulate these neuronal processes are mostly unidentified (Sweatt 2001; Valjent et al.

2001; Thomas and Huganir 2004). However, given a universal requirement for transcription and translation in long-term memory (Davis and Squire 1984; McGaugh 2000), nuclear proteins such as transcription factors are important targets of ERK signaling in the regulation of synaptic plasticity (Sweatt 2001; Valjent et al. 2001; Thomas and Huganir 2004). In support of this idea, CREB, the most extensively studied transcription factor in the field of learning and memory (Lonze and Ginty 2002; West et al. 2002), can be phosphorylated *in vitro* by RSK2 and MSKs—two sets of kinases that are downstream of ERKs (Frodin and Gammeltoft 1999; Wiggin et al. 2002). In addition to nuclear proteins, synaptic and/ or cytoplasmic targets phosphorylated by ERKs during learning have also been reported (Bailey et al. 1997; Angers et al. 2002), which may contribute to early synaptic changes during learning process (Thomas and Huganir 2004).

In light of the primary sequence of STK9 which provides a structural basis for it to function in a similar way as ERKs, it is reasonable to hypothesize that STK9 would also likely play a role in synaptic plasticity. It is noteworthy that the patients with STK9 alterations appeared apparently normal in the pre- and perinatal period but developed severe neurological symptoms during early infancy. The timing of disease onset coincides with the timing for a wide range of shaping and refining of the developing brain structure, which is required for the immature brain to adapt itself to its environment and to establish functional neuronal connectivity. The developmental synaptic plasticity, of which the cellular process is thought similar to those occurring during learning in the adult nervous system, has been hypothesized to participate in the refinement of the immature neuronal network (Goodman and Shatz 1993; Katz and Shatz 1996). Thus, clinical observations in the patients with STK9 alterations, together with the results from primary sequence analysis, suggest that STK9 could controls a same subset of ERK-induced downstream events for regulating the activity-dependent synaptic changes in the immature brain, as ERKs do for the adult brain.

4.7 Function of the putative interaction partners of the STK9 mutant suggests a role of STK9 signaling in synaptic plasticity

A yeast two-hybrid assay was performed with the aim of identifying proteins that interact with STK9. In the experiment, two steps were modified from the standard protocol to ensure a complete coverage of the library complexity, which is the critical point for a successful library screening. In the step of bait selection, a kinase-deficient mutant STK9 was chosen instead of the wild-type STK9. This replacement was based on several considerations. First, the STK9 mutant that carries the K42R substitution in the ATP binding region is assumed to stabilize kinase-substrate interactions. Therefore the chance of finding specific substrates is higher with the bait of STK9 mutant than with the wild-type STK9. Secondly, the STK9 mutant shows lower toxicity than the wild-type protein, which makes it more suitable for yeast two-hybrid screening. Thirdly, the ectopically expressed STK9 mutant has a cellular distribution pattern indistinguishable from its wild-type counterpart, suggesting that mutant STK9 retains the overall cellular targeting property of the wild-type counterpart, and therefore is an ideal substitution. In the step of mating, an improved protocol described by Soellick and Uhrig (2001) was adopted. This optimized protocol gave a higher mating efficiency than the standard method, increasing the value from 2-3% to 10%. With these modifications, approximately 8.8×10^6 bait-prey double transformants were screened, which was 2.5 times fold higher than the complexity of the original fetal brain cDNA library. In the further steps of selection, three additional selection approaches were applied in addition to the conventional nutrition and colorimetric selections. Three potential interaction partners for STK9 were finally isolated from the yeast two-hybrid library screening, namely, promyelocytic leukemia zinc finger protein (PLZF), clathrin heavy chain (CLTC), and transporter associated with antigen processing 1 (TAP1). These proteins may serve as substrates, activators, signaling scaffolds or regulators of intracellular localization of the STK9 molecules. Although the biological significance of these interactions has not been evaluated, the functions of these well-characterized interaction partners may give insights into the biochemical function of the STK9 signaling network.

PLZF, also called ZNF 145, was identified by virtue of its involvement in chromosomal translocations associated with acute promyelocytic leukemia (Chen et al. 1993). At the C terminus, PLZF contains nine Kruppel-type zinc finger domains, which recognize specific DNA sequences (Li et al. 1997). At the N terminus, PLZF contains a BTB/POZ domain, which mediates protein-protein interaction (Dong et al. 1996). Like MeCP2 which is the main player in RTT, PLZF is a nuclear protein and functions as a transcriptional repressor (Hong et al. 1997; He et al. 1998). It has been shown that PLZF binds to the regulatory elements of HoxB and HoxD and regulates transcription of these target genes (Barna et al. 2002; Ivins et al. 2003). Of particular relevance, expression of PLZF is prominent in the developing CNS. *In situ* analysis in mouse embryos between 7.0 and 10.5 days of development revealed that expression of mPLZF mRNAs and proteins correlates with the development of the rhombomeres in hindbrain, in a spatially restricted and temporally dynamic pattern (Cook et al. 1995). More recently, *eor-1*— the *C.elegans* ortholog of PLZF— has been shown to act downstream of ERK signaling and to regulate ERK-dependent gene transcription (Howard and Sundaram 2002). Given the high homology between ERKs and STK9 in the sequence for substrate recognition, it is possible that PLZF may serve as a downstream target of STK9 in regulating gene transcription in the developing brain.

CLTC, another putative STK9 interaction partner, is a protein component of clathrin-coated vesicles. These specialized organelles are involved in intracellular trafficking and endocytosis. In neurons, clathrin mediated endocytosis participates in recycling of synaptic vesicles in pre-synapses and in regulating the level of transmitter receptors and transmitter transporters on the post-synaptic cell surface (Man et al. 2000a; Galli and Haucke 2001; Sheng and Kim 2002). For instance, in cultured cerebellar neurons and hippocampal CA1 neurons, clathrin-dependent endocytosis is an important mechanism regulating the redistribution of the AMPA (α -amino-3-hydroxy-5-methylisoxazole-4-propionic acid)-subtype glutamate receptors in synaptic regions (Man et al. 2000b; Wang and Linden 2000). The AMPA receptor is the principal receptor mediating fast synaptic transmission in most of the CNS excitatory synapses (Hollmann and Heinemann 1994). The rapid changes in the number of functional AMPA receptors in the post-synaptic membrane have been proposed as an important means of controlling synaptic

transmission efficacy, which is one of the critical events in the activity-dependent synaptic plasticity (Man et al. 2000b). Although the significance of the interaction between CLTC and STK9 is presently unknown, STK9 could be involved in the control of AMPA receptor trafficking via regulation of clathrin-mediated endocytosis, thereby mediating synaptic plasticity. Furthermore, Malinow and colleagues recently showed a direct link between Ras/ERK activation and AMPA receptor insertion into synapses (Zhu et al. 2002), but the molecular events linking ERK signaling and AMPA receptor trafficking were not investigated in that study. It would be intriguing to determine whether the ERK-regulated clathrin-dependent endocytosis may underline the missing process, if ERKs could function in a similar way as suggested for STK9.

TAP1, a third potential STK9 interaction partner, is a member of the superfamily of ATP-binding cassette (ABC) transporter. It contains an N-terminal transmembrane domain (TMD) and a C-terminal cytosolic nucleotide-binding domain (NBD). The TMD is involved in substrate interaction and transport, whereas the NBD energizes the transport by ATP hydrolysis (Higgins 1992). TAP1 heterodimerizes with another functionally related protein TAP2 to form the TAP complex, which functions to deliver degraded peptides into the lumen of the endoplasmic reticulum for binding onto major histocompatibility complex (MHC) class I molecules (Pamer and Cresswell 1998). Inactivation of TAP1 by deletion or mutation resulted in a defective expression of class I molecules at the cell surface (Spies et al. 1990; Trowsdale et al. 1990). Class I MHC molecules, although known to be important for immune responses to antigens, are also expressed by specific sets of neurons that undergo activity-dependent, long-term synaptic modifications (Corriveau et al. 1998). Shatz and colleagues showed that in mice genetically deficient for class I MHC signaling (by deletion of TAP1, beta-2-microglobulin— a co-subunit of class I MHC or CD3 ζ — the class I MHC receptor component), precise connections between retina and central targets during eye development were affected; the area occupied by projections from retina was significantly expanded in central eye-specific layer. Moreover, upon examining synaptic plasticity in the adult hippocampus, long-term potentiation (LTP) was enhanced, and long-term depression (LTD) was absent in all mutant mice (Huh et al. 2000). As the refinement of neural structure is thought to follow changes in synaptic plasticity, with LTD preceding withdrawal of connections, and LTP preceding stabilization of connections, the authors suggested that class I MHC

signaling-mediated LTD might be necessary for the removal of inappropriate connections, and the observed inaccurate projections in central targets could arise from the lack of synaptic depression in mice deficient for class I MHC signaling (Huh et al. 2000). Of particular relevance, the patients with STK9 alterations presented with extensive epileptic activity in early infancy, which is a clinical sign of aberrant synaptic connections during the time of establishing functional neuronal connectivity (Shields 2000). Therefore, it will be critical to determine whether the neurological phenotype in these patients can be attributed to the dysfunction of class I MHC signaling, which is likely a downstream target of STK9 through the interaction with TAP1.

4.8 Localization of STK9 in the centrosome suggests its potential association with the microtubule network

In addition to the yeast two-hybrid library screening, a polyclonal antibody that specifically detects STK9 in Western blot and immunocytochemical analysis was generated in this study, which will be a useful tool for further investigations into the function of STK9. In the process of evaluating immunoreactivity of the anti- STK9 antibody, epitope tagged STK9 was constructed and the subcellular localization of ectopically expressed STK9 proteins was studied in COS-7 cells. Full-length STK9 was localized predominantly in the cytoplasm in a punctated manner, whereas the truncated protein containing the intact serine/threonine kinase domain was diffusely distributed throughout the cell. Loss of the specific subcellular distribution of the truncated protein suggests that the C-terminus of STK9 contains sequences important for its specific subcellular targeting. Predominant localization of full-length STK9 in the cytoplasm is consistent with its potential role as a signal transducer mediating extracellular stimuli to specific targets in the cell. Of particular interest, a fraction of full-length STK9 proteins was localized in the centrosome, which was confirmed by co-localization with the centrosome marker, γ -tubulin. The centrosome is the primary microtubule-organization center in the cell, contributing to assembly and function of the spindle, as well as to the G1 to S transition in mitotic cells (Doxsey 2001). In postmitotic neuronal

cells, proteins implicated in neuronal migration such as LIS1, FAK, Nudel and dynein were found to be associated with the centrosome (Xie et al. 2003). Although the subcellular distribution in neuronal cells was not examined in this study, centrosome targeting in COS-7 cells suggests a link between STK9 and the microtubule network. Recently, Tsien and colleagues have shown that activation of ERK is required for morphological changes in dendritic spines following electric stimulated depolarization of cultured neurons (Wu et al. 2001). This result suggested that the signaling pathway operating in synaptic plasticity could be involved in the control of cytoskeletal dynamics. The potential association of STK9 with the microtubule network is consistent with its putative role as a signaling transducer implicated in synaptic plasticity.

4.9 Abnormal synaptic plasticity may be a common cause for some MR

The primary data from the yeast two-hybrid library screening and immunocytochemistry, together with the information obtained from the sequence analysis, indicate that STK9 signaling may be involved in synaptic plasticity, and that the phenotypes in the patients with STK9 alterations may be caused by deficiency in developmental synaptic plasticity that is critical for construction of functional neural connectivity. In support of this idea, mutations in cascade enzymes of the ERK signaling pathway that has an established role in synaptic plasticity have been linked to MR. A well-known example is the ribosomal protein S6 kinase, RSK2, which is directly phosphorylated and activated by ERKs both *in vitro* and *in vivo*. Mutations in the X-linked *RSK2* gene cause Coffin-Lowry syndrome (CLS, MIM 303600), which is characterized by severe psychomotor retardation, facial and digital dysmorphisms, and progressive skeletal deformations. Analysis of cells from patients with CLS showed that cognitive impairment correlated with reduced capacity for RSK2 activation (Harum et al. 2001). Another example is the neurofibromatosis-1 protein (NF1), which is a Ras-GTPase-activating protein serving as an upstream negative regulator of Ras/ERK signaling. Mutations in the *NF1* gene are associated with learning deficits in humans and mice (Silva et al. 1997; North 2000). Analysis of *NF1*^{+/-} heterozygous knock-out mice indicated

that Ras was excessively activated in these animals, and their learning deficits could be rescued by manipulations that decrease Ras activity (Costa et al. 2002). In addition to these well-characterized ERK cascade enzymes, a subgroup of XLMR genes products that potentially function as transcription factors might be implicated in synaptic plasticity as well. As is the case for many transcription factors, the target genes that are regulated by this group of genetic factors and their associated downstream cellular events have not been identified. However, given a universal requirement for transcription and translation in synaptic plasticity (Davis and Squire 1984; McGaugh 2000) and especially, a potentially functional link between STK9 and MeCP2, it is reasonable to speculate that a proportion of these XLMR gene products may contribute to the activity-dependent synaptic plasticity in response to signaling such as STK9 or ERKs.

Taking these genetic studies into account, it seems that synaptic plasticity represents an emerging theme other than cytoskeletal dynamics (see section 1.1.4.2), subserving as a second cellular basis that are commonly deficient in MR. These basic cellular events correlate well with the two developmental processes that are required for construction of functional neuronal circuits (Goodman and Shatz 1993). The initial morphological neural connectivity of the CNS is assembled through multiple interactions among extending axons and surface molecules on the target tissue, and the formation of synaptic connections between hundreds of thousands of neurons. After the initial patterning, synapses are extensively remodeled in an activity-dependent manner to establish precise functional neural connections. The XLMR genes encoding cell surface proteins, Rho GTPase signaling cascade and cytoskeleton-associated proteins that are involved in the regulation of cytoskeletal dynamics could be important molecules in the formation of structural circuits; whereas those encoding molecules of signaling cascades that operate in activity-dependent synaptic plasticity may be critical for construction of functional circuits.

4.10 The future

Identification of *STK9* as a new gene for syndromic XLMR provides a molecular bridge that could bring us closer to understanding the mechanisms underlying various forms of XLMR. Future studies on *STK9* will no doubt focus on two aspects. On one side, mutation screening in mentally retarded patients, especially in those with postnatal early-onset neurological symptoms, e.g. epilepsy, will give us a clearer picture of the associated disease spectrum. On the other side, identification of *STK9* signaling components, especially the upstream activators and downstream substrates, as well as neuroelectrophysiological and behavioral studies in genetically manipulated animal models, should enable us to better understand the role of *STK9* signaling in brain development. Further characterization of the cellular and developmental role of *STK9* will not only shed light onto the molecular mechanisms by which the immature brain establishes its functional connectivity, but may also elucidate molecular targets for future therapeutic interventions using pharmaceutical approaches.

5 SUMMARY

Mental retardation (MR) is one of the most frequent causes of serious handicap in children and young adults, with an incidence of 1-3% in the general population. However, as the pathogenesis of MR is not clear, early diagnosis, prevention or treatment is not possible in most cases; therefore, MR still remains one of the major unsolved problems in medicine. Epidemiological studies in cohorts of mentally retarded patients suggest that about 10% of all MR cases can be attributed to the defects in genes on the X chromosome (designated X-linked mental retardation or XLMR). Concerted clinical and molecular investigations have led to significant progress in the search of the genetic factors underlying XLMR. This has greatly improved our insights into the etiology of the associated disease conditions, and advanced our understanding of the molecular basis of cognitive function.

In a systematic search for new causative genes for XLMR, we investigated a mentally retarded female with a 46,X,t(X;7)(p22.3;p15) *de novo* translocation (patient 1). The patient presented with a severe phenotype, including early-onset infantile spasms, global developmental arrest and profound mental retardation. The breakpoints on both chromosomes were mapped and cloned using a series of cytogenetic and molecular approaches. On chromosome X, the serine/threonine kinase 9 gene (*STK9*) was found to be truncated. Expression studies in the patient-derived fibroblast cells revealed complete absence of normal *STK9* transcripts, due to disruption of the *STK9* gene on the rearranged X chromosome, and to preferential inactivation of the normal X chromosome. These results were corroborated by similar observations of a collaborating Australian group in another female patient with an X;autosome translocation truncating the *STK9* gene.

To further investigate the involvement of *STK9* in XLMR, mutation screening in the whole coding sequence of *STK9* was performed in three cohorts of mentally retarded patients, including 96 patients with idiopathic infantile spasms, index patients from 150 families with XLMR, and 32 index patients with RTT-like features. Three sequence variants were identified that were not found in over 400 control X chromosomes. Two of these, a c.455G>T and a c.525A>T nucleotide

exchange, were identified in patients with RTT-like features and analyzed in detail. The c.455G>T exchange, which results in a cysteine-to-phenylalanine substitution at position 152, was found in a girl who presented with early-onset seizures, psychomotor developmental delay and absence of speech (patient 2). The c.525A>T nucleotide exchange, replacing an arginine by serine at position 175 was found in monozygotic twin sisters who exhibited almost identical clinical features of classical RTT, with a history of early-onset seizures (patient 3 and 4). Neither of the nucleotide changes was found in the patients' healthy parents, suggesting that they occurred *de novo*. Furthermore, both mutations are located within the protein kinase domain and affect highly conserved amino acids that are critical for kinase activities. Therefore, these sequence variants are most likely disease-causing mutations.

To explore the function of STK9, an STK9-specific polyclonal antiserum was prepared, using recombinant STK9 peptides obtained from a bacterial expression system. Immunocytochemistry studies in transfected COS-7 cells revealed that a fraction of the ectopically expressed STK9 proteins was specifically targeted to the centrosome. Upon yeast two-hybrid library screening using an STK9 kinase-deficient mutant as bait, three potential interaction partners of STK9 were isolated, namely promyelocytic leukemia zinc finger protein (PLZF), clathrin heavy chain (CTLC), and transporter associated with antigen processing 1 (TAP1).

As judged from the function of these proteins, STK9 may play a role in the regulation of activity-dependent synaptic plasticity. In the substrate-binding domain, STK9 shows a high degree of sequence similarity with the MAP kinases, ERKs. Since ERKs are known to be involved in signaling in synaptic plasticity and long-term memory in the adult brain, these findings indicate that STK9 may have a similar role. As a cellular mechanism underlying the fine-tuning of the immature brain structure, activity-dependent synaptic plasticity may be critical in the construction of functional neuronal connectivity which, together with regulation of cytoskeletal dynamics that is important for construction of the morphological neuronal connectivity, represent two basic cellular processes that are commonly affected in MR.

Taken together, we identified a truncation and two *de novo* missense mutations in *STK9* in four patients with MR and variable neurological features. Our findings clearly demonstrate that *STK9* is a new genetic locus for syndromic XLMR, and that defects in *STK9* are associated with a

group of neurodevelopmental disorders, including a severe form of neonatal onset encephalopathy, and a relative milder form of classical or atypical RTT with a history of early-onset seizures. Further characterization of the cellular and developmental role of STK9 will not only shed light on the molecular mechanisms by which the immature brain establishes its functional connectivity, but also will elucidate molecular targets for future therapeutic intervention.

6 ELECTRONIC DATABASE INFORMATION

BLAST, <http://www.ncbi.nlm.nih.gov/BLAST/>

ClustalW, <http://www.ebi.ac.uk/clustalw/>

GenBank, <http://www.ncbi.nlm.nih.gov/Genbank/>

Integrated X chromosome database, <http://ixdb.molgen.mpg.de/>

Online Mendelian Inheritance in Man (OMIM), <http://www.ncbi.nlm.nih.gov/Omim/>

The Sanger Institute human X chromosome project, <http://www.sanger.ac.uk/HGP/ChrX/>

UCSC golden path, <http://genome.ucsc.edu/cgi-bin/hgGateway/>

Whitehead Institute YAC and RH map, http://www.broad.mit.edu/cgi-bin/contig/phys_map

XLMR update, <http://www.rm.unicatt.it/xlmr>

XLMR update (Greenwood Genetic Center), <http://www.ggc.org/xlmr.htm>

7 REFERENCES

- Allen KM, Gleeson JG, Bagrodia S, Partington MW, MacMillan JC, Cerione RA, Mulley JC, Walsh CA (1998) PAK3 mutation in nonsyndromic X-linked mental retardation. *Nat Genet* 20:25-30
- Amir RE, Van den Veyver IB, Wan M, Tran CQ, Francke U, Zoghbi HY (1999) Rett syndrome is caused by mutations in X-linked MECP2, encoding methyl-CpG-binding protein 2. *Nat Genet* 23:185-8
- Angers A, Fioravante D, Chin J, Cleary LJ, Bean AJ, Byrne JH (2002) Serotonin stimulates phosphorylation of Aplysia synapsin and alters its subcellular distribution in sensory neurons. *J Neurosci* 22:5412-22
- Atkins CM, Selcher JC, Petraitis JJ, Trzaskos JM, Sweatt JD (1998) The MAPK cascade is required for mammalian associative learning. *Nat Neurosci* 1:602-9
- Bagrodia S, Taylor SJ, Creasy CL, Chernoff J, Cerione RA (1995) Identification of a mouse p21Cdc42/Rac activated kinase. *J Biol Chem* 270:22731-7
- Bahi N, Friocourt G, Carrie A, Graham ME, Weiss JL, Chafey P, Fauchereau F, Burgoyne RD, Chelly J (2003) IL1 receptor accessory protein like, a protein involved in X-linked mental retardation, interacts with Neuronal Calcium Sensor-1 and regulates exocytosis. *Hum Mol Genet* 12:1415-25
- Bailey CH, Kaang BK, Chen M, Martin KC, Lim CS, Casadio A, Kandel ER (1997) Mutation in the phosphorylation sites of MAP kinase blocks learning-related internalization of apCAM in Aplysia sensory neurons. *Neuron* 18:913-24
- Barna M, Merghoub T, Costoya JA, Ruggero D, Branford M, Bergia A, Samori B, Pandolfi PP (2002) Plzf mediates transcriptional repression of HoxD gene expression through chromatin remodeling. *Dev Cell* 3:499-510
- Bergmann C, Zerres K, Senderek J, Rudnik-Schoneborn S, Eggermann T, Hausler M, Mull M, Ramaekers VT (2003) Oligophrenin 1 (OPHN1) gene mutation causes syndromic X-linked mental retardation with epilepsy, rostral ventricular enlargement and cerebellar hypoplasia. *Brain* 126:1537-44
- Biancalana V, Briard ML, David A, Gilgenkrantz S, Kaplan J, Mathieu M, Piussan C, Poncin J, Schinzel A, Oudet C, et al. (1992) Confirmation and refinement of the genetic localization of the Coffin-Lowry syndrome locus in Xp22.1-p22.2. *Am J Hum Genet* 50:981-7

- Bienvenu T, Poirier K, Friocourt G, Bahi N, Beaumont D, Fauchereau F, Ben Jeema L, Zemni R, Vinet MC, Francis F, Couvert P, Gomot M, Moraine C, van Bokhoven H, Kalscheuer V, Frints S, Gecz J, Ohzaki K, Chaabouni H, Fryns JP, Desportes V, Beldjord C, Chelly J (2002) ARX, a novel Prd-class-homeobox gene highly expressed in the telencephalon, is mutated in X-linked mental retardation. *Hum Mol Genet* 11:981-91
- Billuart P, Bienvenu T, Ronce N, des Portes V, Vinet MC, Zemni R, Roest Crollius H, Carrie A, Fauchereau F, Cherry M, Briault S, Hamel B, Fryns JP, Beldjord C, Kahn A, Moraine C, Chelly J (1998) Oligophrenin-1 encodes a rhoGAP protein involved in X-linked mental retardation. *Nature* 392:923-6
- Bishop AL, Hall A (2000) Rho GTPases and their effector proteins. *Biochem J* 348 Pt 2:241-55
- Boulton TG, Nye SH, Robbins DJ, Ip NY, Radziejewska E, Morgenbesser SD, DePinho RA, Panayotatos N, Cobb MH, Yancopoulos GD (1991) ERKs: a family of protein-serine/threonine kinases that are activated and tyrosine phosphorylated in response to insulin and NGF. *Cell* 65:663-75
- Bourdon V, Philippe C, Labrune O, Amsallem D, Arnould C, Jonveaux P (2001) A detailed analysis of the MECP2 gene: prevalence of recurrent mutations and gross DNA rearrangements in Rett syndrome patients. *Hum Genet* 108:43-50
- Brunner B, Todt T, Lenzner S, Stout K, Schulz U, Ropers HH, Kalscheuer VM (1999) Genomic structure and comparative analysis of nine Fugu genes: conservation of synteny with human chromosome Xp22.2-p22.1. *Genome Res* 9:437-48
- Bugge M, Bruun-Petersen G, Brondum-Nielsen K, Friedrich U, Hansen J, Jensen G, Jensen PK, Kristoffersson U, Lundsteen C, Niebuhr E, Rasmussen KR, Rasmussen K, Tommerup N (2000) Disease associated balanced chromosome rearrangements: a resource for large scale genotype-phenotype delineation in man. *J Med Genet* 37:858-65
- Buyse IM, Fang P, Hoon KT, Amir RE, Zoghbi HY, Roa BB (2000) Diagnostic testing for Rett syndrome by DHPLC and direct sequencing analysis of the MECP2 gene: identification of several novel mutations and polymorphisms. *Am J Hum Genet* 67:1428-36
- Cainarca S, Messali S, Ballabio A, Meroni G (1999) Functional characterization of the Opitz syndrome gene product (midin): evidence for homodimerization and association with microtubules throughout the cell cycle. *Hum Mol Genet* 8:1387-96
- Canagarajah BJ, Khokhlatchev A, Cobb MH, Goldsmith EJ (1997) Activation mechanism of the MAP kinase ERK2 by dual phosphorylation. *Cell* 90:859-69
- Carrera AC, Alexandrov K, Roberts TM (1993) The conserved lysine of the catalytic domain of

- protein kinases is actively involved in the phosphotransfer reaction and not required for anchoring ATP. *Proc Natl Acad Sci U S A* 90:442-6
- Carrie A, Jun L, Bienvenu T, Vinet MC, McDonnell N, Couvert P, Zemni R, Cardona A, Van Buggenhout G, Frints S, Hamel B, Moraine C, Ropers HH, Strom T, Howell GR, Whittaker A, Ross MT, Kahn A, Fryns JP, Beldjord C, Marynen P, Chelly J (1999) A new member of the IL-1 receptor family highly expressed in hippocampus and involved in X-linked mental retardation. *Nat Genet* 23:25-31
- Chang L, Karin M (2001) Mammalian MAP kinase signalling cascades. *Nature* 410:37-40
- Cheadle JP, Gill H, Fleming N, Maynard J, Kerr A, Leonard H, Krawczak M, Cooper DN, Lynch S, Thomas N, Hughes H, Hulten M, Ravine D, Sampson JR, Clarke A (2000) Long-read sequence analysis of the MECP2 gene in Rett syndrome patients: correlation of disease severity with mutation type and location. *Hum Mol Genet* 9:1119-29
- Chechlacz M, Gleeson JG (2003) Is mental retardation a defect of synapse structure and function? *Pediatr Neurol* 29:11-7
- Chelly J, Mandel JL (2001) Monogenic causes of X-linked mental retardation. *Nat Rev Genet* 2:669-80
- Chen WG, Chang Q, Lin Y, Meissner A, West AE, Griffith EC, Jaenisch R, Greenberg ME (2003) Derepression of BDNF transcription involves calcium-dependent phosphorylation of MeCP2. *Science* 302:885-9
- Chen Z, Brand NJ, Chen A, Chen SJ, Tong JH, Wang ZY, Waxman S, Zelent A (1993) Fusion between a novel Kruppel-like zinc finger gene and the retinoic acid receptor-alpha locus due to a variant t(11;17) translocation associated with acute promyelocytic leukaemia. *Embo J* 12:1161-7
- Cook M, Gould A, Brand N, Davies J, Strutt P, Shaknovich R, Licht J, Waxman S, Chen Z, Gluecksohn-Waelsch S, et al. (1995) Expression of the zinc-finger gene PLZF at rhombomere boundaries in the vertebrate hindbrain. *Proc Natl Acad Sci U S A* 92:2249-53
- Corriveau RA, Huh GS, Shatz CJ (1998) Regulation of class I MHC gene expression in the developing and mature CNS by neural activity. *Neuron* 21:505-20
- Costa RM, Federov NB, Kogan JH, Murphy GG, Stern J, Ohno M, Kucherlapati R, Jacks T, Silva AJ (2002) Mechanism for the learning deficits in a mouse model of neurofibromatosis type 1. *Nature* 415:526-30
- Crow YJ, Tolmie JL (1998) Recurrence risks in mental retardation. *J Med Genet* 35:177-82
- D'Adamo P, Menegon A, Lo Nigro C, Grasso M, Gulisano M, Tamanini F, Bienvenu T, Gedeon

- AK, Oostra B, Wu SK, Tandon A, Valtorta F, Balch WE, Chelly J, Toniolo D (1998) Mutations in *GDI1* are responsible for X-linked non-specific mental retardation. *Nat Genet* 19:134-9
- D'Adamo P, Welzl H, Papadimitriou S, Raffaele di Barletta M, Tiveron C, Tatangelo L, Pozzi L, Chapman PF, Knevett SG, Ramsay MF, Valtorta F, Leoni C, Menegon A, Wolfer DP, Lipp HP, Toniolo D (2002) Deletion of the mental retardation gene *Gdi1* impairs associative memory and alters social behavior in mice. *Hum Mol Genet* 11:2567-80
- Davis HP, Squire LR (1984) Protein synthesis and memory: a review. *Psychol Bull* 96:518-59
- DeMali KA, Wennerberg K, Burridge K (2003) Integrin signaling to the actin cytoskeleton. *Curr Opin Cell Biol* 15:572-82
- des Portes V, Pinard JM, Billuart P, Vinet MC, Koulakoff A, Carrie A, Gelot A, Dupuis E, Motte J, Berwald-Netter Y, Catala M, Kahn A, Beldjord C, Chelly J (1998) A novel CNS gene required for neuronal migration and involved in X-linked subcortical laminar heterotopia and lissencephaly syndrome. *Cell* 92:51-61
- Dong S, Zhu J, Reid A, Strutt P, Guidez F, Zhong HJ, Wang ZY, Licht J, Waxman S, Chomienne C, et al. (1996) Amino-terminal protein-protein interaction motif (POZ-domain) is responsible for activities of the promyelocytic leukemia zinc finger-retinoic acid receptor-alpha fusion protein. *Proc Natl Acad Sci U S A* 93:3624-9
- Doxsey S (2001) Re-evaluating centrosome function. *Nat Rev Mol Cell Biol* 2:688-98
- Emes RD, Ponting CP (2001) A new sequence motif linking lissencephaly, Treacher Collins and oral-facial-digital type 1 syndromes, microtubule dynamics and cell migration. *Hum Mol Genet* 10:2813-20
- English JD, Sweatt JD (1997) A requirement for the mitogen-activated protein kinase cascade in hippocampal long term potentiation. *J Biol Chem* 272:19103-6
- Etienne-Manneville S, Hall A (2002) Rho GTPases in cell biology. *Nature* 420:629-35
- Farag TI, al-Awadi SA, el-Badramary MH, Aref MA, Kasrawi B, Krishna Murthy DS, el-Khalifa MY, Yadav G, Marafie MJ, Bastaki L, et al. (1993) Disease profile of 400 institutionalized mentally retarded patients in Kuwait. *Clin Genet* 44:329-34
- Fox JW, Lamperti ED, Eksioglu YZ, Hong SE, Feng Y, Graham DA, Scheffer IE, Dobyns WB, Hirsch BA, Radtke RA, Berkovic SF, Huttenlocher PR, Walsh CA (1998) Mutations in *filamin 1* prevent migration of cerebral cortical neurons in human periventricular heterotopia. *Neuron* 21:1315-25
- Fransen E, Van Camp G, Vits L, Willems PJ (1997) L1-associated diseases: clinical geneticists

- divide, molecular geneticists unite. *Hum Mol Genet* 6:1625-32
- Frodin M, Gammeltoft S (1999) Role and regulation of 90 kDa ribosomal S6 kinase (RSK) in signal transduction. *Mol Cell Endocrinol* 151:65-77
- Galli T, Haucke V (2001) Cycling of synaptic vesicles: how far? How fast! *Sci STKE* 2001:RE1
- Gdalyahu A, Ghosh I, Levy T, Sapir T, Sapoznik S, Fishler Y, Azoulay D, Reiner O (2004) DCX, a new mediator of the JNK pathway. *Embo J* 23:823-32
- Geppert M, Sudhof TC (1998) RAB3 and synaptotagmin: the yin and yang of synaptic membrane fusion. *Annu Rev Neurosci* 21:75-95
- Gibbons RJ, Picketts DJ, Villard L, Higgs DR (1995) Mutations in a putative global transcriptional regulator cause X-linked mental retardation with alpha-thalassemia (ATR-X syndrome). *Cell* 80:837-45
- Gibbons RJ, Suthers GK, Wilkie AO, Buckle VJ, Higgs DR (1992) X-linked alpha-thalassemia/mental retardation (ATR-X) syndrome: localization to Xq12-q21.31 by X inactivation and linkage analysis. *Am J Hum Genet* 51:1136-49
- Gil OD, Sakurai T, Bradley AE, Fink MY, Cassella MR, Kuo JA, Felsenfeld DP (2003) Ankyrin binding mediates L1CAM interactions with static components of the cytoskeleton and inhibits retrograde movement of L1CAM on the cell surface. *J Cell Biol* 162:719-30
- Gleeson JG, Allen KM, Fox JW, Lamperti ED, Berkovic S, Scheffer I, Cooper EC, Dobyns WB, Minnerath SR, Ross ME, Walsh CA (1998) Doublecortin, a brain-specific gene mutated in human X-linked lissencephaly and double cortex syndrome, encodes a putative signaling protein. *Cell* 92:63-72
- Gleeson JG, Lin PT, Flanagan LA, Walsh CA (1999) Doublecortin is a microtubule-associated protein and is expressed widely by migrating neurons. *Neuron* 23:257-71
- Goodman CS, Shatz CJ (1993) Developmental mechanisms that generate precise patterns of neuronal connectivity. *Cell* 72 Suppl:77-98
- Goutieres F, Aicardi J (1986) Atypical forms of Rett syndrome. *Am J Med Genet Suppl* 1:183-94
- Hagberg B, Aicardi J, Dias K, Ramos O (1983) A progressive syndrome of autism, dementia, ataxia, and loss of purposeful hand use in girls: Rett's syndrome: report of 35 cases. *Ann Neurol* 14:471-9
- Hagberg BA, Skjeldal OH (1994) Rett variants: a suggested model for inclusion criteria. *Pediatr Neurol* 11:5-11
- Hanefeld F (1985) The clinical pattern of the Rett syndrome. *Brain Dev* 7:320-5
- Hanks SK, Hunter T (1995) Protein kinases 6. The eukaryotic protein kinase superfamily: kinase

- (catalytic) domain structure and classification. *Faseb J* 9:576-96
- Harum KH, Alemi L, Johnston MV (2001) Cognitive impairment in Coffin-Lowry syndrome correlates with reduced RSK2 activation. *Neurology* 56:207-14
- He LZ, Guidez F, Tribioli C, Peruzzi D, Ruthardt M, Zelent A, Pandolfi PP (1998) Distinct interactions of PML-RARalpha and PLZF-RARalpha with co-repressors determine differential responses to RA in APL. *Nat Genet* 18:126-35
- Hemler ME (2001) Specific tetraspanin functions. *J Cell Biol* 155:1103-7
- Higgins CF (1992) ABC transporters: from microorganisms to man. *Annu Rev Cell Biol* 8:67-113
- Hollmann M, Heinemann S (1994) Cloned glutamate receptors. *Annu Rev Neurosci* 17:31-108
- Holmes LB, Gang DL (1984) Brief clinical report: an X-linked mental retardation syndrome with craniofacial abnormalities, microcephaly and club foot. *Am J Med Genet* 17:375-82
- Hong SH, David G, Wong CW, Dejean A, Privalsky ML (1997) SMRT corepressor interacts with PLZF and with the PML-retinoic acid receptor alpha (RARalpha) and PLZF-RARalpha oncoproteins associated with acute promyelocytic leukemia. *Proc Natl Acad Sci U S A* 94:9028-33
- Howard RM, Sundaram MV (2002) *C. elegans* EOR-1/PLZF and EOR-2 positively regulate Ras and Wnt signaling and function redundantly with LIN-25 and the SUR-2 Mediator component. *Genes Dev* 16:1815-27
- Huh GS, Boulanger LM, Du H, Riquelme PA, Brotz TM, Shatz CJ (2000) Functional requirement for class I MHC in CNS development and plasticity. *Science* 290:2155-9
- Hunter AG, Evans JA, Thompson DR, Ramsay S (1980) A study of institutionalized mentally retarded patients in Manitoba. I: Classification and preventability. *Dev Med Child Neurol* 22:145-62
- Ivins S, Pemberton K, Guidez F, Howell L, Krumlauf R, Zelent A (2003) Regulation of Hoxb2 by APL-associated PLZF protein. *Oncogene* 22:3685-97
- Jouet M, Rosenthal A, Armstrong G, MacFarlane J, Stevenson R, Paterson J, Metzberg A, Ionasescu V, Temple K, Kenwrick S (1994) X-linked spastic paraplegia (SPG1), MASA syndrome and X-linked hydrocephalus result from mutations in the L1 gene. *Nat Genet* 7:402-7
- Kalscheuer VM, Tao J, Donnelly A, Hollway G, Schwinger E, Kubart S, Menzel C, Hoeltzenbein M, Tommerup N, Eyre H, Harbord M, Haan E, Sutherland GR, Ropers HH, Gecz J (2003) Disruption of the serine/threonine kinase 9 gene causes severe X-linked infantile spasms and mental retardation. *Am J Hum Genet* 72:1401-11

- Katz LC, Shatz CJ (1996) Synaptic activity and the construction of cortical circuits. *Science* 274:1133-8
- Kiely M (1987) The prevalence of mental retardation. *Epidemiol Rev* 9:194-218
- Kitamura K, Yanazawa M, Sugiyama N, Miura H, Iizuka-Kogo A, Kusaka M, Omichi K, Suzuki R, Kato-Fukui Y, Kamiirisa K, Matsuo M, Kamiyo S, Kasahara M, Yoshioka H, Ogata T, Fukuda T, Kondo I, Kato M, Dobyns WB, Yokoyama M, Morohashi K (2002) Mutation of ARX causes abnormal development of forebrain and testes in mice and X-linked lissencephaly with abnormal genitalia in humans. *Nat Genet* 32:359-69
- Koehn MA, Duchowny M (2002) Infantile spasms: unique syndrome or general age-dependent manifestation of a diffuse encephalopathy? *Int Rev Neurobiol* 49:57-62
- Kremer EJ, Pritchard M, Lynch M, Yu S, Holman K, Baker E, Warren ST, Schlessinger D, Sutherland GR, Richards RI (1991) Mapping of DNA instability at the fragile X to a trinucleotide repeat sequence p(CCG)_n. *Science* 252:1711-4
- Kutsche K, Yntema H, Brandt A, Jantke I, Nothwang HG, Orth U, Boavida MG, David D, Chelly J, Fryns JP, Moraine C, Ropers HH, Hamel BC, van Bokhoven H, Gal A (2000) Mutations in ARHGEF6, encoding a guanine nucleotide exchange factor for Rho GTPases, in patients with X-linked mental retardation. *Nat Genet* 26:247-50
- Laccone F, Junemann I, Whatley S, Morgan R, Butler R, Huppke P, Ravine D (2004) Large deletions of the MECP2 gene detected by gene dosage analysis in patients with Rett syndrome. *Hum Mutat* 23:234-44
- Laxova R, Ridler MA, Bowen-Bravery M (1977) An etiological survey of the severely retarded Hertfordshire children who were born between January 1, 1965 and December 31, 1967. *Am J Med Genet* 1:75-86
- Lee T, Hoofnagle AN, Kabuyama Y, Stroud J, Min X, Goldsmith EJ, Chen L, Resing KA, Ahn NG (2004) Docking motif interactions in MAP kinases revealed by hydrogen exchange mass spectrometry. *Mol Cell* 14:43-55
- Lehrke R (1972a) Theory of X-linkage of major intellectual traits. *Am J Ment Defic* 76:611-9
- Lehrke R (1972b) A theory of X-linkage of major intellectual traits. Response to Dr. Anastasi and to the Drs. Nance and Engel. *Am J Ment Defic* 76:626-31
- Leonard H, Wen X (2002) The epidemiology of mental retardation: challenges and opportunities in the new millennium. *Ment Retard Dev Disabil Res Rev* 8:117-34
- Lewis JD, Meehan RR, Henzel WJ, Maurer-Fogy I, Jeppesen P, Klein F, Bird A (1992) Purification, sequence, and cellular localization of a novel chromosomal protein that binds

- to methylated DNA. *Cell* 69:905-14
- Li JY, English MA, Ball HJ, Yeyati PL, Waxman S, Licht JD (1997) Sequence-specific DNA binding and transcriptional regulation by the promyelocytic leukemia zinc finger protein. *J Biol Chem* 272:22447-55
- Li W, Yu JC, Shin DY, Pierce JH (1995) Characterization of a protein kinase C-delta (PKC-delta) ATP binding mutant. An inactive enzyme that competitively inhibits wild type PKC-delta enzymatic activity. *J Biol Chem* 270:8311-8
- Lonze BE, Ginty DD (2002) Function and regulation of CREB family transcription factors in the nervous system. *Neuron* 35:605-23
- Lossi AM, Millan JM, Villard L, Orellana C, Cardoso C, Prieto F, Fontes M, Martinez F (1999) Mutation of the XNP/ATR-X gene in a family with severe mental retardation, spastic paraplegia and skewed pattern of X inactivation: demonstration that the mutation is involved in the inactivation bias. *Am J Hum Genet* 65:558-62
- Luckasson R, Coulter DL, Pollway EA (1992) Mental retardation: Definition, classification, and systems of supports. Washington DC: American association on Mental Retardation
- Luo L (2000) Rho GTPases in neuronal morphogenesis. *Nat Rev Neurosci* 1:173-80
- Man HY, Ju W, Ahmadian G, Wang YT (2000a) Intracellular trafficking of AMPA receptors in synaptic plasticity. *Cell Mol Life Sci* 57:1526-34
- Man HY, Lin JW, Ju WH, Ahmadian G, Liu L, Becker LE, Sheng M, Wang YT (2000b) Regulation of AMPA receptor-mediated synaptic transmission by clathrin-dependent receptor internalization. *Neuron* 25:649-62
- Manser E, Chong C, Zhao ZS, Leung T, Michael G, Hall C, Lim L (1995) Molecular cloning of a new member of the p21-Cdc42/Rac-activated kinase (PAK) family. *J Biol Chem* 270:25070-8
- Manser E, Loo TH, Koh CG, Zhao ZS, Chen XQ, Tan L, Tan I, Leung T, Lim L (1998) PAK kinases are directly coupled to the PIX family of nucleotide exchange factors. *Mol Cell* 1:183-92
- McGaugh JL (2000) Memory--a century of consolidation. *Science* 287:248-51
- Midmer M, Haq R, Squire JA, Zanke BW (1999) Identification of NKIAMRE, the human homologue to the mitogen-activated protein kinase-/cyclin-dependent kinase-related protein kinase NKIATRE, and its loss in leukemic blasts with chromosome arm 5q deletion. *Cancer Res* 59:4069-74
- Miltenberger-Miltenyi G, Laccone F (2003) Mutations and polymorphisms in the human methyl

- CpG-binding protein MECP2. *Hum Mutat* 22:107-15
- Mnatzakanian GN, Lohi H, Munteanu I, Alfred SE, Yamada T, MacLeod PJ, Jones JR, Scherer SW, Schanen NC, Friez MJ, Vincent JB, Minassian BA (2004) A previously unidentified MECP2 open reading frame defines a new protein isoform relevant to Rett syndrome. *Nat Genet* 36:339-41
- Montini E, Andolfi G, Caruso A, Buchner G, Walpole SM, Mariani M, Consalez G, Trump D, Ballabio A, Franco B (1998) Identification and characterization of a novel serine-threonine kinase gene from the Xp22 region. *Genomics* 51:427-33
- Morgan DO (1995) Principles of CDK regulation. *Nature* 374:131-4
- Nan X, Ng HH, Johnson CA, Laherty CD, Turner BM, Eisenman RN, Bird A (1998) Transcriptional repression by the methyl-CpG-binding protein MeCP2 involves a histone deacetylase complex. *Nature* 393:386-9
- Nishimura K, Yoshihara F, Tojima T, Ooashi N, Yoon W, Mikoshiba K, Bennett V, Kamiguchi H (2003) L1-dependent neuritogenesis involves ankyrinB that mediates L1-CAM coupling with retrograde actin flow. *J Cell Biol* 163:1077-88
- North K (2000) Neurofibromatosis type 1. *Am J Med Genet* 97:119-27
- Oberle I, Rousseau F, Heitz D, Kretz C, Devys D, Hanauer A, Boue J, Bertheas MF, Mandel JL (1991) Instability of a 550-base pair DNA segment and abnormal methylation in fragile X syndrome. *Science* 252:1097-102
- Pamer E, Cresswell P (1998) Mechanisms of MHC class I--restricted antigen processing. *Annu Rev Immunol* 16:323-58
- Pasteris NG, Cadle A, Logie LJ, Porteous ME, Schwartz CE, Stevenson RE, Glover TW, Wilroy RS, Gorski JL (1994) Isolation and characterization of the faciogenital dysplasia (Aarskog-Scott syndrome) gene: a putative Rho/Rac guanine nucleotide exchange factor. *Cell* 79:669-78
- Quaderi NA, Schweiger S, Gaudenz K, Franco B, Rugarli EI, Berger W, Feldman GJ, Volta M, Andolfi G, Gilgenkrantz S, Marion RW, Hennekam RC, Opitz JM, Muenke M, Ropers HH, Ballabio A (1997) Opitz G/BBB syndrome, a defect of midline development, is due to mutations in a new RING finger gene on Xp22. *Nat Genet* 17:285-91
- Ramakers GJ (2002) Rho proteins, mental retardation and the cellular basis of cognition. *Trends Neurosci* 25:191-9
- Renieri A, Meloni I, Longo I, Ariani F, Mari F, Pescucci C, Cambi F (2003) Rett syndrome: the complex nature of a monogenic disease. *J Mol Med* 81:346-54

- Robertson SP, Twigg SR, Sutherland-Smith AJ, Biancalana V, Gorlin RJ, Horn D, Kenwrick SJ, Kim CA, Morava E, Newbury-Ecob R, Orstavik KH, Quarrell OW, Schwartz CE, Shears DJ, Suri M, Kendrick-Jones J, Wilkie AO (2003) Localized mutations in the gene encoding the cytoskeletal protein filamin A cause diverse malformations in humans. *Nat Genet* 33:487-91
- Robinson MJ, Harkins PC, Zhang J, Baer R, Haycock JW, Cobb MH, Goldsmith EJ (1996) Mutation of position 52 in ERK2 creates a nonproductive binding mode for adenosine 5'-triphosphate. *Biochemistry* 35:5641-6
- Roeleveld N, Zielhuis GA, Gabreels F (1997) The prevalence of mental retardation: a critical review of recent literature. *Dev Med Child Neurol* 39:125-32
- Ropers HH, Hoeltzenbein M, Kalscheuer V, Yntema H, Hamel B, Fryns JP, Chelly J, Partington M, Geetz J, Moraine C (2003) Nonsyndromic X-linked mental retardation: where are the missing mutations? *Trends Genet* 19:316-20
- Russo AA, Jeffrey PD, Pavletich NP (1996) Structural basis of cyclin-dependent kinase activation by phosphorylation. *Nat Struct Biol* 3:696-700
- Sambrook J, Fritsch EF, Maniatis T (1989) *Molecular Cloning : A Laboratory Manual*. Cold Spring Harbor Laboratory Press
- Saugier-veber P, Munnich A, Bonneau D, Rozet JM, Le Merrer M, Gil R, Boespflug-Tanguy O (1994) X-linked spastic paraplegia and Pelizaeus-Merzbacher disease are allelic disorders at the proteolipid protein locus. *Nat Genet* 6:257-62
- Schaar BT, Kinoshita K, McConnell SK (2004) Doublecortin microtubule affinity is regulated by a balance of kinase and phosphatase activity at the leading edge of migrating neurons. *Neuron* 41:203-13
- Schanen NC, Kurczynski TW, Brunelle D, Woodcock MM, Dure LSt, Percy AK (1998) Neonatal encephalopathy in two boys in families with recurrent Rett syndrome. *J Child Neurol* 13:229-31
- Schollen E, Smeets E, Deflem E, Fryns JP, Matthijs G (2003) Gross rearrangements in the MECP2 gene in three patients with Rett syndrome: implications for routine diagnosis of Rett syndrome. *Hum Mutat* 22:116-20
- Schweiger S, Foerster J, Lehmann T, Suckow V, Muller YA, Walter G, Davies T, Porter H, van Bokhoven H, Lunt PW, Traub P, Ropers HH (1999) The Opitz syndrome gene product, MID1, associates with microtubules. *Proc Natl Acad Sci U S A* 96:2794-9
- Schweiger S, Schneider R (2003) The MID1/PP2A complex: a key to the pathogenesis of Opitz

- BBB/G syndrome. *Bioessays* 25:356-66
- Sheng M, Kim MJ (2002) Postsynaptic signaling and plasticity mechanisms. *Science* 298:776-80
- Shields WD (2000) Catastrophic epilepsy in childhood. *Epilepsia* 41 Suppl 2:S2-6
- Siebert PD, Chenchik A, Kellogg DE, Lukyanov KA, Lukyanov SA (1995) An improved PCR method for walking in uncloned genomic DNA *Nucleic Acids Res.* Vol. 23, pp 1087-8
- Silva AJ, Frankland PW, Marowitz Z, Friedman E, Laszlo GS, Cioffi D, Jacks T, Bourtchuladze R, Lazlo G (1997) A mouse model for the learning and memory deficits associated with neurofibromatosis type I. *Nat Genet* 15:281-4
- Soellick TR, Uhrig JF (2001) Development of an optimized interaction-mating protocol for large-scale yeast two-hybrid analyses. *Genome Biol* 2:RESEARCH0052
- Spies T, Bresnahan M, Bahram S, Arnold D, Blanck G, Mellins E, Pious D, DeMars R (1990) A gene in the human major histocompatibility complex class II region controlling the class I antigen presentation pathway. *Nature* 348:744-7
- Stancheva I, Collins AL, Van den Veyver IB, Zoghbi H, Meehan RR (2003) A mutant form of MeCP2 protein associated with human Rett syndrome cannot be displaced from methylated DNA by notch in *Xenopus* embryos. *Mol Cell* 12:425-35
- Stevenson RE (2000) Splitting and lumping in the nosology of XLMR. *Am J Med Genet* 97:174-82
- Stevenson RE, Abidi F, Schwartz CE, Lubs HA, Holmes LB (2000a) Holmes-Gang syndrome is allelic with XLMR-hypotonic face syndrome. *Am J Med Genet* 94:383-5
- Stevenson RE, Schwartz CE, Schroer RJ (2000b) X-Linked Mental Retardation. Oxford University Press, New York
- Stossel TP, Condeelis J, Cooley L, Hartwig JH, Noegel A, Schleicher M, Shapiro SS (2001) Filamins as integrators of cell mechanics and signalling. *Nat Rev Mol Cell Biol* 2:138-45
- Stromme P, Mangelsdorf ME, Shaw MA, Lower KM, Lewis SM, Bruyere H, Lutchera V, Gedeon AK, Wallace RH, Scheffer IE, Turner G, Partington M, Frints SG, Fryns JP, Sutherland GR, Mulley JC, Gecz J (2002) Mutations in the human ortholog of *Aristaless* cause X-linked mental retardation and epilepsy. *Nat Genet* 30:441-5
- Sutherland GR (1977) Fragile sites on human chromosomes: demonstration of their dependence on the type of tissue culture medium. *Science* 197:265-6
- Sweatt JD (2001) The neuronal MAP kinase cascade: a biochemical signal integration system subserving synaptic plasticity and memory. *J Neurochem* 76:1-10
- Taglienti CA, Wusk M, Davis RJ (1996) Molecular cloning of the epidermal growth

- factor-stimulated protein kinase p56 KKIAMRE. *Oncogene* 13:2563-74
- Tanaka T, Serneo FF, Tseng HC, Kulkarni AB, Tsai LH, Gleeson JG (2004) Cdk5 phosphorylation of doublecortin ser297 regulates its effect on neuronal migration. *Neuron* 41:215-27
- Thomas GM, Huganir RL (2004) MAPK cascade signalling and synaptic plasticity. *Nat Rev Neurosci* 5:173-83
- Tigges U, Koch B, Wissing J, Jockusch BM, Ziegler WH (2003) The F-actin cross-linking and focal adhesion protein filamin A is a ligand and in vivo substrate for protein kinase C alpha. *J Biol Chem* 278:23561-9
- Trowsdale J, Hanson I, Mockridge I, Beck S, Townsend A, Kelly A (1990) Sequences encoded in the class II region of the MHC related to the 'ABC' superfamily of transporters. *Nature* 348:741-4
- Ueda K, Ohta Y, Hosoya H (2003) The carboxy-terminal pleckstrin homology domain of ROCK interacts with filamin-A. *Biochem Biophys Res Commun* 301:886-90
- Vadlamudi RK, Li F, Adam L, Nguyen D, Ohta Y, Stossel TP, Kumar R (2002) Filamin is essential in actin cytoskeletal assembly mediated by p21-activated kinase 1. *Nat Cell Biol* 4:681-90
- Valjent E, Caboche J, Vanhoutte P (2001) Mitogen-activated protein kinase/extracellular signal-regulated kinase induced gene regulation in brain: a molecular substrate for learning and memory? *Mol Neurobiol* 23:83-99
- Verkerk AJ, Pieretti M, Sutcliffe JS, Fu YH, Kuhl DP, Pizzuti A, Reiner O, Richards S, Victoria MF, Zhang FP, et al. (1991) Identification of a gene (FMR-1) containing a CGG repeat coincident with a breakpoint cluster region exhibiting length variation in fragile X syndrome. *Cell* 65:905-14
- Villard L, Fontes M, Ades LC, Gecz J (2000a) Identification of a mutation in the XNP/ATR-X gene in a family reported as Smith-Fineman-Myers syndrome. *Am J Med Genet* 91:83-5
- Villard L, Gecz J, Mattei JF, Fontes M, Saugier-veber P, Munnich A, Lyonnet S (1996) XNP mutation in a large family with Juberg-Marsidi syndrome. *Nat Genet* 12:359-60
- Villard L, Kpebe A, Cardoso C, Chelly PJ, Tardieu PM, Fontes M (2000b) Two affected boys in a Rett syndrome family: clinical and molecular findings. *Neurology* 55:1188-93
- Wang YT, Linden DJ (2000) Expression of cerebellar long-term depression requires postsynaptic clathrin-mediated endocytosis. *Neuron* 25:635-47
- Weaving LS, Christodoulou J, Williamson SL, Friend KL, Mckenzie OL, Archer H, Evans J, Clarke A, Pelka GJ, Tam PPL, Watson C, Lahooti H, Ellaway CJ, Bennetts B, Leonard H, Gecz J (submitted) Mutations of *STK9* Cause Infantile Spasms, Mental Retardation and a

- Rett Syndrome-like Phenotype *Am J Hum Genet*
- Weller S, Gartner J (2001) Genetic and clinical aspects of X-linked hydrocephalus (L1 disease): Mutations in the L1CAM gene. *Hum Mutat* 18:1-12
- West AE, Griffith EC, Greenberg ME (2002) Regulation of transcription factors by neuronal activity. *Nat Rev Neurosci* 3:921-31
- Wiggin GR, Soloaga A, Foster JM, Murray-Tait V, Cohen P, Arthur JS (2002) MSK1 and MSK2 are required for the mitogen- and stress-induced phosphorylation of CREB and ATF1 in fibroblasts. *Mol Cell Biol* 22:2871-81
- Wirth J, Nothwang HG, van der Maarel S, Menzel C, Borck G, Lopez-Pajares I, Brondum-Nielsen K, Tommerup N, Bugge M, Ropers HH, Haaf T (1999) Systematic characterisation of disease associated balanced chromosome rearrangements by FISH: cytogenetically and genetically anchored YACs identify microdeletions and candidate regions for mental retardation genes. *J Med Genet* 36:271-8
- Wong M, Trevathan E (2001) Infantile spasms. *Pediatr Neurol* 24:89-98
- Wu GY, Deisseroth K, Tsien RW (2001) Spaced stimuli stabilize MAPK pathway activation and its effects on dendritic morphology. *Nat Neurosci* 4:151-8
- Xie Z, Sanada K, Samuels BA, Shih H, Tsai LH (2003) Serine 732 phosphorylation of FAK by Cdk5 is important for microtubule organization, nuclear movement, and neuronal migration. *Cell* 114:469-82
- Yauch RL, Hemler ME (2000) Specific interactions among transmembrane 4 superfamily (TM4SF) proteins and phosphoinositide 4-kinase. *Biochem J* 351 Pt 3:629-37
- Yen SH, Kenessey A, Lee SC, Dickson DW (1995) The distribution and biochemical properties of a Cdc2-related kinase, KKIALRE, in normal and Alzheimer brains. *J Neurochem* 65:2577-84
- Yntema HG, Oudakker AR, Kleefstra T, Hamel BC, van Bokhoven H, Chelly J, Kalscheuer VM, Fryns JP, Raynaud M, Moizard MP, Moraine C (2002) In-frame deletion in MECP2 causes mild nonspecific mental retardation. *Am J Med Genet* 107:81-3
- Yu S, Pritchard M, Kremer E, Lynch M, Nancarrow J, Baker E, Holman K, Mulley JC, Warren ST, Schlessinger D, et al. (1991) Fragile X genotype characterized by an unstable region of DNA. *Science* 252:1179-81
- Zeev BB, Yaron Y, Schanen NC, Wolf H, Brandt N, Ginot N, Shomrat R, Orr-Urtreger A (2002) Rett syndrome: clinical manifestations in males with MECP2 mutations. *J Child Neurol* 17:20-4

REFERENCES

- Zemni R, Bienvenu T, Vinet MC, Sefiani A, Carrie A, Billuart P, McDonell N, et al. (2000) A new gene involved in X-linked mental retardation identified by analysis of an X;2 balanced translocation. *Nat Genet* 24:167-70
- Zheng Y, Fischer DJ, Santos MF, Tigyi G, Pasteris NG, Gorski JL, Xu Y (1996) The faciogenital dysplasia gene product FGD1 functions as a Cdc42Hs-specific guanine-nucleotide exchange factor. *J Biol Chem* 271:33169-72

8 ACKNOWLEDGEMENT

I would first like to thank Prof. Dr. Hans-Hilger Ropers and Dr. Vera Kalscheuer, for guiding me into the studies of X-linked mental retardation, the most fascinating research field of human genetics, and for their supervision throughout this project.

I am particular grateful to Sabine Kübart for stimulating discussions and valuable suggestions, which helped in solving problems in many molecular experiments, and for encouragement during the hard times when experiments were not going well.

I would additionally like to thank Kirsten Hoffmann and Bettina Moser for their technical assistance with DHPLC analysis, Corinna Menzel and Petra Viertel for assistance in FISH analysis, Susanne Freier and Hannelore Madle for assistance in cell culture, Jens Ruschmann and Stella Kunde for assistance in sequence analysis, and Marion Klein and Dietmar Vogt for assistance in plasmid preparation.

I would also like to thank Dr. Maria Hoeltzenbein, Prof. Eberhard Schwinger, Dr. Hilde Van Esch, for participation in collection of clinical data used in this project, Dr. Jozef Gécz for sharing scientific data, which helped in formulating the selection criteria for mutation screening. I also thank the patients and their families for their willingness to participate in this research.

I would like to thank Dr. Susann Schweiger and Vanessa Suckow for their helpful suggestions in the aspects of protein experiments, Dr. Harry Scherthan, Dr. Edgar Trelles-Sticken and Bodo Liebe for their help in cytochemical experiments.

I would like to acknowledge my colleagues, Dr. Lars Riff Jensen, Dr. Luciana Musante, Dr. Sarah Shoichet, Barbara Dlugaszewska, Olivier Hagens, and Kristine Freude, who have created a pleasant working atmosphere.

I want to thank Dr. Constance Scharff for taking time from her busy schedule to read all sections of my thesis, and her critical comments on this manuscript.

Finally, I am deeply grateful to my husband and my parents, for their understanding and continuous support to my professional development.

9 CURRICULUM VITAE

Personal information

Name Jiong Tao
Date of birth May 9, 1970
Nationality P. R. China
Current address Hans-Böhm-Zeile 30
14165, Berlin, Germany
Tel: 0049-30-84131250 (lab)
E-mail: jjong@molgen.mpg.de; taojiong@hotmail.com
Permanent address Rm. 42, 1522 Nanjing Xi Lu
200030 Shanghai, P. R. China
Tel: 0086-21-62892237

Education and Academic Awards

Oct. 2000-present Max-Planck Institute for Molecular Genetics, Berlin (Germany)
Ph.D candidate enrolled in Charité – Universitätsmedizin Berlin
(Germany)
Theme: Identification and characterization of serine/threonine kinase 9
as a causative gene for X-linked mental retardation.

Sep. 1997-Jul. 2000 Institute of Hematology, Shanghai Second Medical University (P.R.China)
Master degree in Genetics (2000)
Theme: Preliminary study on the role of cAMP-PKA pathway in
retinoic acid induced differentiation of APL cells
SSMU Scholarship for Outstanding Personality and Studies (1998 and
1999)
Medical Education Scholarship of United Laboratories (2000)

Sep. 1987-Jul. 1993 Department of Clinical Medicine, Shanghai Medical University (P.R.China)
Bachelor degree in Medicine (1993)
People's Scholarship for Outstanding Personality and Studies
(1988,1989,1990,1991).
Guang Hua Memorial Scholarship for Outstanding Personality and
Studies (1992)

Work Experience

- Aug.1993-Dec.1997 Lab of Immunology, Shanghai Institute of Cell Biology, Chinese Academy of Sciences (P.R.China)
Research assistant
Theme: establish an ELISA kit for detecting soluble interleukine-2 receptor
- Jan.1995-Dec.1995 Lab of Monoclonal antibody, National Institute of Cancer Research, Genoa (Italy)
Visiting Investigator of World Laboratory
Theme: screening phage display library for human recombinant antibody against DNase I
- Apr.1993-Jul. 1993 Lab of Immunology, Shanghai Medical University (P.R. China)
Internship, participated in studies of the effect of Astragalus Polyacchrid (a Chinese herb extraction) in immune system, measured the activity of LAK and NK cells
- Jul.1991-Apr.1993 Affiliated hospitals of Shanghai Medical University (P.R. China)
Internship, practised in internal medicine, surgery, gynaecology, paediatrics, ophthalmology and otolaryngology

Professional development

- Oct. 2003 4th Annual Meeting German Society of Human Genetics, Marburg (Germany)
Poster: Identification of interaction partners of serine-threonine kinase 9 (STK9), which was functionally absent in two female patients with severe infantile spasms
- Aug. 2003 11th International Workshop on Fragile X Syndrome and X-Linked Mental Retardation (Cyprus)
Scientific talk: Identification of interaction partners of serine-threonine kinase 9 (STK9), which was functionally absent in two female patients with severe infantile spasms
- Oct. 2002 13th Annual Meeting German Society of Human Genetics, Leipzig (Germany)
Poster: Disruption of the serine/threonine kinase 9 gene as the cause of severe X-linked infantile spasms
- Apr. 2002 15th Course in Medical Genetics, European School of Genetic Medicine, Bertinoro (Italy)
- Apr. 2002 1st Course in Comparative and Functional Genomics, European School of Genetic Medicine, Bertinoro (Italy)

Aug 1999

8th International Symposium of Society of Chinese Bioscientists in American, HongKong (P. R. China)

Poster: Gene Expression patterns in ATRA resistant promyelocytic NB4-R1 cells: dissection of cAMP pathway in retinoic acid-induced differentiation.

10 PUBLICATIONS

Tao J, Van Esch H, Hagedorn-Greiwe M, Hoffmann K, Moser B, Raynaud M, Sperner J, Fryns JP, Schwinger E, Gécz J, Ropers HH, Kalscheuer VM (2004) De novo mutations in the X-linked serine/threonine kinase 9 gene (*STK9*) are associated with a severe variant of Rett syndrome. *Am J Hum Genet.* (Submitted)

Zhao Q, **Tao J**, Zhu Q, Jia PM, Dou AX, Li X, Cheng F, Waxman S, Chen GQ, Chen SJ, Lanotte M, Chen Z, Tong JH (2004) Rapid induction of cAMP/PKA pathway during retinoic acid-induced acute promyelocytic leukemia cell differentiation. *Leukemia.* 18: 285-92

Kalscheuer V.M, **Tao J**, Donnelly A, Hollway G, Schwinger E, Kübart S, Menzel C, Hoeltzenbein M, Tommerup N, Eyre H, Harbord M, Haan E, Sutherland G.R, Ropers H.H., Gécz J (2003) Disruption of the Serine/Threonine Kinase 9 gene causes severe X-linked infantile spasms and mental retardation. *Am J Hum Genet.*72:1401-11

Kalscheuer VM, Freude K, Musante L, Jensen LR, Yntema HG, Gecz J, Sefiani A, Hoffmann K, Moser B, Haas S, Gurok U, Haesler S, Aranda B, Nshedjan A, Tzschach A, Hartmann N, Roloff TC, Shoichet S, Hagens O, **Tao J**, Van Bokhoven H, Turner G, Chelly J, Moraine C, Fryns JP, Nuber U, Hoeltzenbein M, Scharff C, Scherthan H, Lenzner S, Hamel BC, Schweiger S, Ropers HH (2003) Mutations in the polyglutamine binding protein 1 gene cause X-linked mental retardation. *Nat Genet* 35:313-5

Liu TX, Zhang JW, **Tao J**, Zhang RB, Zhang QH, Zhao CJ, Tong JH, Lanotte M, Waxman S, Chen SJ, Mao M, Hu GX, Zhu L, Chen Z (2000) Gene expression networks underlying retinoic acid-induced differentiation of acute promyelocytic leukemia cells. *Blood.* 2000. 96:1496-504 (co-first author)

Zhang QH, Ye M, Wu XY, Ren SX, Zhao M, Zhao CJ, Fu G, Shen Y, Fan HY, Lu G, Zhong M, Xu XR, Han ZG, Zhang JW, **Tao J**, Huang QH, Zhou J, Hu GX, Gu J, Chen SJ, Chen Z (2000) Cloning and functional analysis of cDNAs with open reading frames for 300 previously undefined genes expressed in CD34+ hematopoietic stem/progenitor cells. *Genome Res* 10:1546-60

Tao J, Liu TX, Chen Z (1999) The role of cAMP-PKA pathway in retinoic acid-induced differentiation of acute promyelocytic leukemia cells, *Nature Magazine* 21:264-266 (review article, Chinese)

Zhao LL, **Tao J**, Ge XR (1995) Dynamic changes of soluble interleukin 2 Receptor in the patients with malignant tumors and infectious diseases. *Journal of Shanghai Immunology* 15: 305-308 (Chinese)

ERKLÄRUNG

Hiermit erkläre ich, die vorliegende Arbeit selbständig und ohne unerlaubte Hilfe angefertigt zu haben. Sämtliche Hilfsmittel und Inhalte aus anderen Quellen wurden als solche kenntlich gemacht. Ich versichere, daß diese Arbeit in dieser oder anderer Form noch keiner anderen Prüfungsbehörde vorgelegt wurde. Der Inhalt der Promotionsordnung der Medizinische Fakultät Charité der Humboldt-Universität zu Berlin in der Fassung vom 12. Dezember 2000 ist mir bekannt.

Berlin, im Juli 2004

Jiong Tao